Intervention in Hepatic Lipid Metabolism:

Implications for Atherosclerosis Progression and Regression

PROEFSCHRIFT

ter verkrijging van
de graad van Doctor aan de Universiteit Leiden,
op gezag van de Rector Magnificus Prof. Mr. P.F. van der Heijden,
volgens besluit van het College voor Promoties
te verdedigen op dinsdag 27 september 2011
klokke 11.15 uur

door

Zhaosha Li
geboren te Changsha, China
in 1983

PROMOTIECOMMISSIE

Promotor:	Prof. Dr. Th.J.C. van Berkel	
Co-promotor:	Dr. M. Hoekstra	
Overige leden:	Prof.Dr.M.Danhof	(LACDR, Leiden University)
	Prof.Dr.A.IJzerman	(LACDR, Leiden University)
	Dr.M.Smit	(MSD Oss)
	Prof.Dr.B. Staels	(Université Lille Nord de France)

The studies presented in this thesis were supported by Top Institute Pharma (TI Pharma) project T2-110-1 and were performed at the Division of Biopharmaceutics, Leiden/Amsterdam Center for Drug Research (LACDR), Leiden University, Leiden, The Netherlands.

Time will tell.

To my parents
For my love Tristan

Intervention in Hepatic Lipid Metabolism: Implications for Atherosclerosis Progression and Regression

Author: Zhaosha Li
Lay-out: Zhaosha Li
Cover design: Mai Chen; Zhaosha Li
Venetian mask

Print: Wöhrmann Print Service

ISBN: 978-90-8570-855-1

Academic thesis, Leiden University, Leiden, The Netherlands

© Z. Li, Leiden 2011
All rights reserved. No part of this publication may be reproduced, stored, or transmitted in any form or by any means, without permission of the author.

Printing of this thesis was financially supported by:
- LACDR
- Leiden University

TABLE OF CONTENTS

Chapter 1

General introduction

Zhaosha Li

Division of Biopharmaceutics, Leiden/Amsterdam Center for Drug Research, Leiden University, The Netherlands

TABLE OF CONTENTS

1. LIPID METABOLISM

Hypercholesterolemia holds a key role in the development and progression of atherosclerosis and is a causative factor for coronary artery disease [1]. Hyperlipidemia is a metabolic disorder defined by either elevated levels of plasma concentrations of low-density lipoprotein (LDL) cholesterol and triglycerides, or decreased levels of the athero-protective lipid biomarker high-density lipoprotein (HDL) cholesterol[2]. Lowering of very-low-density lipoprotein- (VLDL-) and low-density lipoprotein- (LDL-) cholesterol levels leads to a reduction in cardiovascular morbidity and mortality[2]. In contrast, high levels of HDL cholesterol are associated with a decreased risk of cardiovascular disease[3].

1.1 Lipoproteins

Lipoproteins are spherical macromolecular complexes in which hydrophobic molecules, in particular triglyceride and cholesteryl ester, are enveloped within a monolayer of amphipathic molecules of phospholipids, free cholesterol, and apoproteins [4]. The major lipoprotein classes include intestinally derived chylomicrons that transport dietary fats and cholesterol, hepatic-derived VLDL, intermediate-density lipoprotein (IDL), and LDL that are considered to be pro-atherogenic, and hepatic- and intestinally derived HDL that are considered to be anti-atherogenic. Figure 1 illustrates the major lipoprotein classes and their compositions.

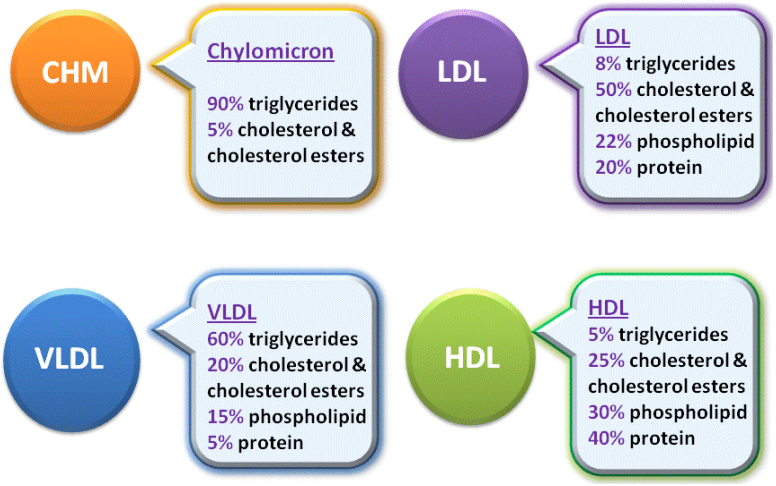

Figure 1. Illustration of the composition of four major classes of lipoproteins[5]. See text for explanation.

1.1.1 Chylomicron, VLDL, and LDL

Apolipoprotein B (apoB) is necessary for the assembly and secretion of chylomicrons by the intestine while it is also an essential component for VLDL, IDL, and LDL[6]. As shown in Figure 2, the liver secretes VLDL particles, which contain triglycerides and cholesterol esters. Capillaries in muscle and adipose tissue remove the triglycerides, and the lipid particle is modified into LDL, with its

cholesteryl ester core and apoB-100 coat. LDLs circulate in the plasma and the apoB-100 component binds to LDL receptors on the surface of hepatocytes. Through receptor-mediated endocytosis, receptor-bound LDLs enter hepatocytes and undergo degradation in lysosomes, and the cholesterol remnants enter a cellular cholesterol pool[7]. Plasma levels of apoB containing lipoproteins are regulated by both environmental effects on lipid metabolism and by genetic factors affecting the surface of the lipoproteins and enzymes in plasma[8].

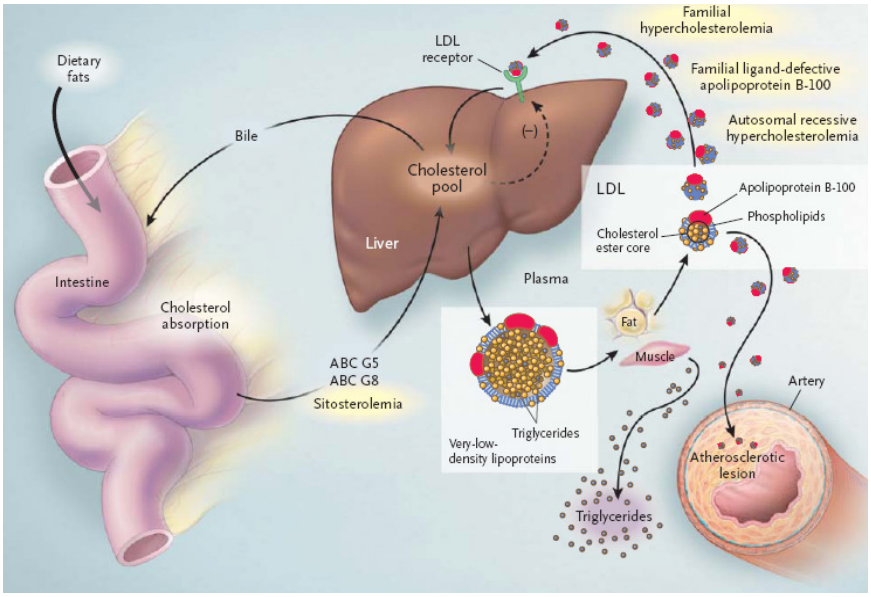

Figure 2. The basic pathways of cholesterol synthesis and excretion[7]. See text for explanation.

1.1.2 HDL and reverse cholesterol transport

The major protein of HDL is apolipoprotein A-I (apoA-I), which is synthesized in the liver and intestine. HDL metabolism consists of five main processes: (1) apoA-I synthesis and secretion into plasma as nascent HDL; (2) uptake of free cholesterol from the periphery; (3) maturation into large spherical particles with cholesterol esterification; (4) delivery of cholesteryl ester to the liver, steroidogenic organs, and apoB-containing lipoproteins; and (5) catabolism of apoA-I[9]. HDL serves an anti-atherogenic function because of its ability to mediate reverse cholesterol transport (RCT), which is a major protective system against atherosclerosis[10,11]. HDL can remove cholesterol from the periphery, allowing it to be cleared by the liver and then excreted into the bile[12]. Cholesterol efflux from macrophages to HDL is a crucial step in RCT and it occurs at all stages of atherosclerosis[13]. As shown in Figure 3, the liver secretes lipid-poor apoA-I, which quickly acquires cholesterol via the hepatocyte ABCA1 transporter. Lipid-poor apoA-I also promotes the efflux of free cholesterol from macrophages via ABCA1. LCAT esterifies free cholesterol to cholesteryl esters to form mature HDL, which promotes cholesterol efflux from macrophages via the ABCG1 transporter. In macrophages, both ABCA1 and ABCG1 are regulated by nuclear receptor LXR. Mature HDL can transfer its cholesterol to the liver directly via SR-BI or indirectly via CETP-mediated transfer to

apoB-containing lipoproteins, with subsequent uptake by the liver via the LDL-receptor[14]. Modulation of major macrophage mediators in RCT, such as ABCA1, ABCG1, and SR-B1 has been considered as promising strategies for the development of drugs aimed at the prevention of atherosclerosis[15,16,17].

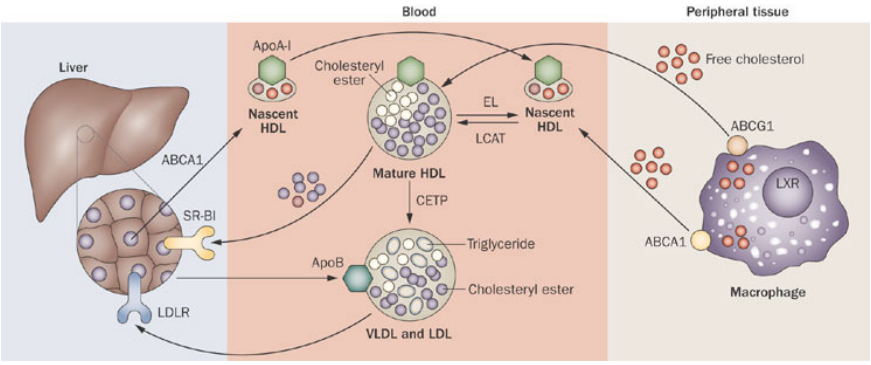

Figure 3. HDL metabolism and reverse cholesterol transport14. See text for explanation.

1.2 Hepatic lipid metabolism

Atherosclerosis is a liver disease of the heart[18]. Liver is considered as the major organ with significant therapeutic importance for the maintenance of metabolic homeostasis[19]. A common associated clinical feature of patients with non-alcoholic fatty liver disease (NAFLD) is atherogenic dyslipidaemia, i.e. high triacylglycerol, low HDL-cholesterol, and increased LDL-cholesterol levels[20]. Liver fat is highly significantly and linearly correlated with all components of the metabolic syndrome independent of obesity[21]. NAFLD is not merely a marker of atherosclerosis, but may also be actively involved in the pathogenesis of atherosclerosis[22,23].

The liver consists of different types of cells, including parenchymal cells, namely hepatocytes, and a variety of non-parenchymal cells (Figure 4). Non-parenchymal cells are comprised of mainly liver sinusoidal endothelial cells and Kupffer cells. Liver endothelial cells form a continuous but fenestrated lining of the hepatic sinusoids, while Kupffer cells are found in the sinusoidal lumen on top of or between endothelial cells[24]. Liver endothelial cells free the bloodstream from a variety of macromolecular waste products during inflammation[25]. Kupffer cells are a population of hepatic resident macrophages. They constitute 80-90% of the tissue macrophages present in the body[26]. Although non-parenchymal cells count for only 6.5% of the liver volume, they contain 55% of the lipid droplets in the liver and 43% of the lysosomes, and specific activities of enzymes are generally higher in non-parenchymal cells than in parenchymal cells [27, 28]. Parenchymal and non-parenchymal cells synchronize crucial roles in liver metabolic homeostasis as well as inflammation. The majority of studies upon liver has focused on the array of target genes and metabolic pathways within parenchymal cells[29,30]. However, non-parenchymal cells are also intimately involved in the pathogenesis of various liver metabolic diseases including steatohepatitis, non-alcoholic fatty liver, and liver fibrosis[31]. Previous studies have shown that diet-induced hypercholesterolemia results in marked changes in the hepatic distribution of LDL and significant accumulation of cholesteryl ester/lipid droplets in liver endothelial and Kupffer cells, suggesting a prominent role of liver non-parenchymal cells in removing modified

LDL from blood[32,33,34]. It has also been shown that cross-talk between Kupffer cells and hepatocytes regulates hepatic lipid storage[35].

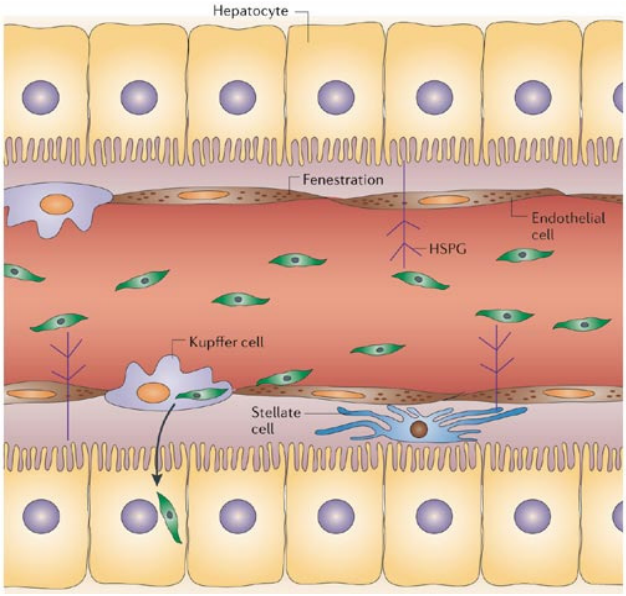

Figure 4. Cell composition of liver[36].

2. ATHEROSCLEROSIS

Cardiovascular diseases are the leading cause of morbidity and mortality in industrialized countries [37] . Atherosclerosis is the underlying cause of most cardiovascular diseases. Lipid accumulation leads to an inflammatory condition clinically causing occlusive vascular disease, myocardial infarction and stroke[38]. The atherosclerotic process is initiated when cholesterol-containing low-density lipoproteins accumulate in the intima and activate the endothelium.

2.1 Lesion progression

Macrophages contribute to the pathogenesis of atherosclerosis through their accumulation of cholesterol and development into foam cells[39]. Foam cells arise either from resident macrophages in the arterial wall or from blood monocytes that enter the wall at sites of endothelial damage[40]. Figure 5 illustrates the infiltration and inflammation of macrophages in arterial wall. Leukocyte adhesion molecules and chemokines promote recruitment of monocytes which differentiate into macrophages and up-regulate pattern recognition receptors on these cells, including scavenger receptors. Scavenger receptors mediate lipoprotein internalization, leading to foam-cell formation, inflammation, and, ultimately, to tissue damage[41,42]. Accumulation of cholesterol-loaded “foam cells” is the hallmark of the early atherosclerotic lesion[43].

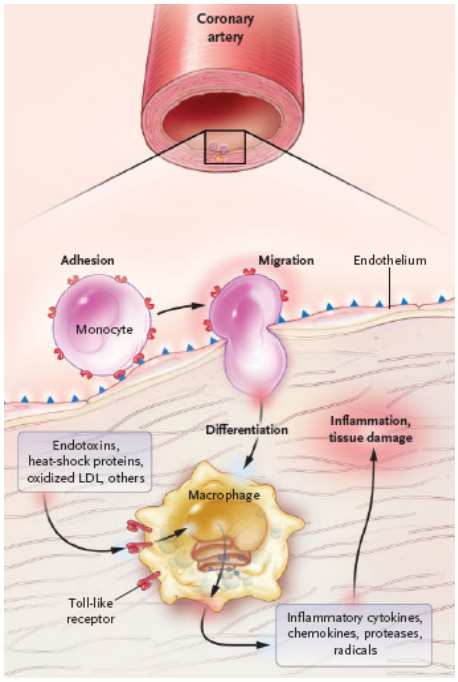

Figure 5. Illustration of macrophage infiltration and inflammation in arterial wall41. See text for explanation.

The atherosclerotic plaque is a dynamic tissue, where increases in cell number (driven by cell proliferation and migration) and decreases in cell number (driven by cell death and possibly emigration) are continuous processes [44]. Initial atherosclerotic lesions are primarily composed of lipid-loaded macrophages. Stable advanced lesion contains a macrophage core, a small necrotic core, if present at all, extracellular matrix and a firm fibrous cap of smooth muscle cells (SMCs)[45]. Instable advanced atherosclerotic lesions are characterized by a thin fibrous cap containing few SMCs and overlying a large necrotic core composed of dead cells, lipid deposits, and cellular debris[46].

2.2 Lesion regression

While numerous studies have been dedicated to inhibit the development and progression of atherosclerosis, recent attention has been drawn to the goal of reversing atherosclerosis, meaning regressing pre-existing atherosclerotic plaques. The first evidence of dramatic atherosclerotic regression in mice was achieved via robust surgical measures to rapidly improve plaque environment[47]. That study suggested that the essential prerequisite for promoting regression of atherosclerotic lesions is robust improvement of plasma lipoprotein profiles and plaque milieu, including large plasma reductions in atherogenic apoB-lipoproteins and brisk enhancements in efflux of cholesterol from plaques to the blood circulation and subsequently into the liver. Recently, the same group showed that the LXR agonist T0901317 promotes egress of monocyte-derived cells from mouse aortic plaques, indicating that LXR is required for maximal effects on plaque

macrophage egression during atherosclerosis regression in mice[48]. In another mouse model, apoE*3Leiden mice, LXR agonist was also shown to promote regression of moderate lesions[49]. Raffai *et al* for the first time addressed the apoE-mediated mechanisms of atherosclerosis regression[50]. They demonstrate that apoE promotes the regression of atherosclerosis independently of lowering plasma cholesterol levels. Potteaux *et al* also achieved regression of atherosclerosis after apoE complementation in ApoE$^{-/-}$ mice, suggesting that therapies to inhibit monocyte recruitment to plaques may constitute a viable strategy to reduce plaque macrophage burden than attempts to promote migratory egress[51].

3. ANIMAL MODELS IN ATHEROSCLEROSIS

Atherosclerosis is a complex and chronic inflammatory disease in which multiple modulating factors may play a role. Its chronicity and complexity make it very difficult to study the detailed mechanisms of atherogenesis in unregulated human populations. Therefore, animal models with a homogenous genetic background are useful for the study of the mechanism of this process[52]. With the development of genetic models of atherosclerosis the mouse has become a very accessible model, especially with the very large genetic data base about this species in relation to human biology that has become available[53].

3.1 C57BL/6 mice

The C57BL/6 mouse strain is used as a model for studies of diet-induced atherosclerosis[54, 55, 56]. C57BL/6 mice fed with a high-fat cholate-containing atherogenic diet have a hyperlipidemic response, develop fatty streak lesions, and form atheromatous plaques in the aorta and coronary arteries[57]. This murine model of atherogenesis represents an alternative to the use of genetically modified mice with impaired lipoprotein clearance, thus it may prove beneficial for the evaluation of new classes of anti-hyperlipidemic agents[58].

3.2 LDLr$^{-/-}$ mice

LDLr$^{-/-}$ mice are among the most widely used mouse models for characterization of atherosclerosis. Due to the absence of hepatic LDL receptors, LDLr$^{-/-}$ mice exhibit prolonged half life of plasma VLDL and LDL[59]. These mice display a modestly elevated plasma cholesterol level when maintained on a regular chow diet, whilst on potent cholesterol-rich diet, LDLr$^{-/-}$ mice show strongly elevated plasma cholesterol levels (hypercholesterolemic) and rapid development of atherosclerosis[60].

3.3 ApoE$^{-/-}$ mice

ApoE$^{-/-}$ mice with targeted deletion of the apoE gene show severe hypercholesterolemia. Therefore, ApoE$^{-/-}$ mice form one of the most common animal models to study atherogenesis. The most obvious phenotype of ApoE$^{-/-}$ mice is the spontaneous development of atherosclerotic lesions, even on a standard chow diet which is low in fat content and does not contain cholesterol. Lesions of ApoE$^{-/-}$ mice develop over time from initial fatty streaks to complex lesions, and this process can be strongly accelerated by a high-fat, high-cholesterol diet[61].

4. DRUG TARGETS AND PHARMACEUTICAL INTERVENTIONS

Lipid-lowering is established as a proven intervention to reduce atherosclerosis and its complications. The development of the HMG-CoA reductase inhibitors (statins) has lead to important advances in the management of cardiovascular disease[62]. However, statins reduce cardiovascular events by only about 20%-40%, and non-statin therapies (either as monotherapy or in addition to statins) to reduce LDL-cholesterol by mechanisms that do not involve inhibition of HMG-CoA reductase are also likely to be useful for patients in need of LDL reduction[63]. These therapies include drug targets such as squalene synthase, microsomal transfer protein (MTP), acyl-cholesterol acyl transferase (ACAT), cholesterol ester transfer protein (CETP), and peroxosimal proliferator activating receptors (PPARs)[64].

4.1 Nuclear receptor

The nuclear receptor (NR) superfamily describes a related but diverse array of ligand-activated transcription factors. NR binds DNA and translates physiological signals into gene regulation involved in biological processes. Figure 6 shows a higher-order network tying nuclear receptor function to reproduction, development, central, and basal metabolic functions, dietary-lipid metabolism, and energy homeostasis[65]. Several receptors including the peroxisome proliferator activated receptors (PPARs), the liver X receptors (LXRs), the farnesoid X receptor (FXR) and the retinoid-related orphan receptors (RORs) are called “metabolic receptors” and poised to sense and respond to small changes in the flux through the metabolic pathways that they control[66].

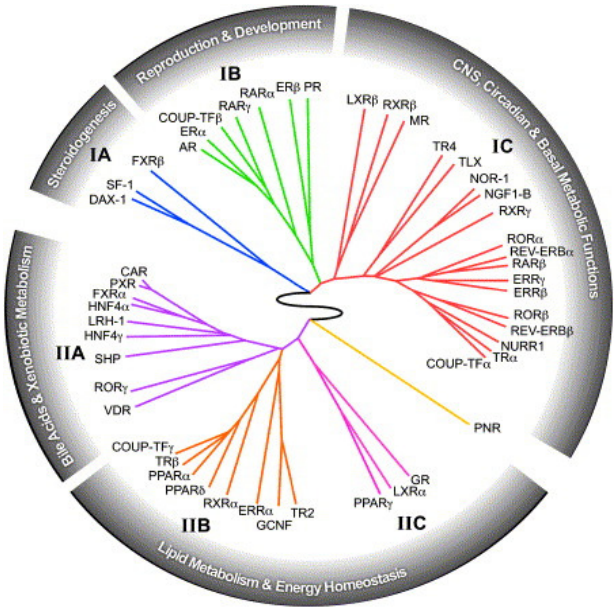

Figure 6. The nuclear receptor ring of physiology. The relationship between receptor expression, function, and physiology is depicted as a circular dendrogram65.

4.2 LXR and LXR agonists

Liver X receptors (LXRs) are sterol-responsive nuclear receptors that regulate expression of genes involved in cholesterol metabolism and homeostasis[67]. LXRs act as cholesterol sensors. When cellular oxysterols accumulate as a result of increasing concentrations of cholesterol, LXR induces the transcription of genes that protect cells from cholesterol overload[68]. LXR agonists have potent anti-atherogenic effects, shown in different hyperlipidemic mouse models. Several studies have demonstrated that activation of LXR with compounds, such as T0901317, significantly up-regulates cholesterol efflux activity and inhibits development of atherosclerosis, providing direct evidence for an atheroprotective effect of LXR agonists[69,70]. T0901317 treatment was associated with reduced cholesterol absorption and promoted biliary cholesterol excretion[71,72,73]. Furthermore, LXR agonist significantly increased the generation of HDL particles in plasma. Table 1 summarizes the studies of LXR agonists performed in mouse models to study atherosclerotic progression or regression.

4.3 PNPLA3

Patatin-like phospholipase domain-containing protein 3 (PNPLA3), also knows as adiponutrin (ADPN) or calcium-independent phospholipase A2-epsilon, is an enzyme that in humans is encoded by the PNPLA*3* gene[74,75]. High human PNPLA3 activity is associated with increased liver fat content and liver injury. Variation in PNPLA3 contributes to ancestry-related and inter-individual differences in hepatic fat content, risk of hepatic steatosis, and susceptibility to NAFLD[76,77].

4.4 CETP

Cholesteryl ester transfer protein (CETP) is a 74-kDa hydrophobic plasma glycoprotein that has an established role in mediation of neutral lipid transport among lipoproteins[78]. In humans, CETP mRNA is expressed predominantly in adipose tissue, liver, and spleen, with lower levels of expression in the small intestine, adrenal gland, kidney, skeletal muscle, and heart[79,80]. In addition, Van Eck *et al*[81] have demonstrated that bone marrow-derived cells, including macrohpages, are an important contributor to total serum CETP activity and mass in mice.

Cholesteryl ester transfer protein (CETP) is a key modulator not only of the intravascular metabolism of HDL and apoA-I but also of triglyceride-rich lipoproteins (TRL). CETP modifies the lipid composition of the plasma by mediating the transfer of cholesteryl esters from HDL to pro-atherogenic apoB-lipoproteins, with heterotransfer of TG mainly from very low-density lipoprotein to HDL, thereby decreasing plasma HDL-C concentrations and increasing the proportion of lipids present in the atherogenic LDL-C and VLDL-C fractions[82,83] (Figure 7). The overall effect of CETP is to promote a net mass transfer of CE from HDL to TRL and LDL and of TG from TRL to LDL and HDL. CETP plays a significant role in reverse cholesterol transport (RCT)[84]. Pharmacological inhibition of CETP in humans therefore presents a preferential target to improve the lipid profile of dyslipidemic patients, not only by increasing HDL-C levels but also by reducing LDL-C levels[85].

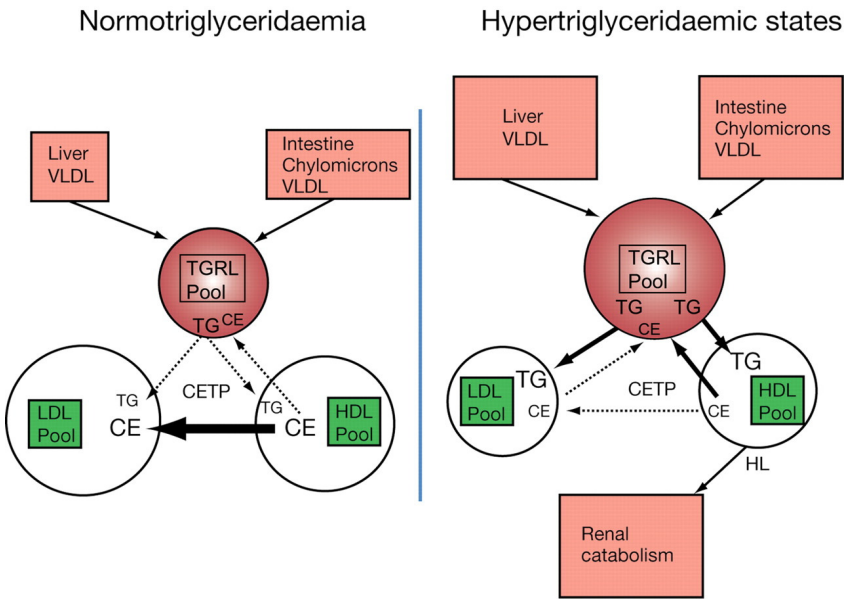

Figure 7. Role of CETP in plasma lipoprotein transport82.

4.5 GPR109A, niacin, and niacin derivatives

The G protein-coupled receptor GPR109A, also known as PUMA-G in mouse and HM74A in humans, has been identified as a high-affinity receptor for nicotinic acid, also known as niacin[86,87]. GPR109A is dominantly expressed in adipose tissue and spleen[88,89]. It is also highly expressed in macrophages and other immune cells, such as lymphocytes[90,91,92,93]. The lipid-lowering effect of niacin on plasma (V)LDL-TG is the consequence of a direct interaction between niacin and its receptor GPR109A in adipose tissue[94].

Niacin is the most effective agent currently available to treat dyslipidaemic disorders [95] . It lowers plasma levels of pro-atherogenic lipids, including chylomicrons, very-low-density lipoproteins (VLDL), low-density lipoproteins (LDL), and triglycerides (TG) in normolipidemic as well as hypercholesterolemic subjects[96]. Several clinical trials have shown that nicotinic acid reduces cardiovascular disease and myocardial infarction incidence, providing a solid rationale for the use of nicotinic acid in the treatment of atherosclerosis[97,98]. The effects of niacin on lipid metabolism in human have been summarized in Figure 8. Recently, we showed that niacin also reduces the hepatic expression and plasma levels of the pro-atherogenic cholesteryl ester transfer protein (CETP) in mouse models [99]. A summary of studies on effects of niacin on lipid metabolism and CETP regulation in mouse models are shown in Table 2.

LIPOPROTEIN	EFFECT
Chylomicrons	↓
VLDL	↓
β-VLDL	↓
IDL	↓
LDL	↓
sdLDL	↓
HDL	↑
HDL_2	↑
LP(a)	↓

Figure 8. Summary of the effects of niacin on plasma lipoprotein classes in human[100].

Despite its established cardiovascular benefits, the clinical use of niacin has been limited due to the cutaneous flushing, a well-recognized adverse skin effect from nicotinic acid therapy[101]. The niacin receptor GPR109A expressed in the skin is a critical mediator of nicotinic acid-induced flushing[102]. Nicotinic acid stimulates GPR109A in epidermal Langerhans cells and keratinocytes, causing the cells to produce vasodilatory prostaglandin D_2 (PGD_2) and prostaglandin E_2 (PGE_2), which leads to cutaneous vasodilation[103,104,105,106]. For the past decade, the pharmacology of GPR109A has been studied and its full or partial agonists, including acipimox, acifran, 3-pyridine-acetic acid, 5-methylnicotinic acid, pyridazine-4-carboxylic acid, and pyrazine-2-carboxylic acid, have been developed in an attempt to achieve the beneficial effects of nicotinic acid while avoiding the unwanted flushing side effect[107,108,109].

5. THESIS OUTLINE

Atherosclerosis is a chronic disease causing many cardiovascular complications, among which atherosclerotic coronary heart disease is the leading cause of morbidity and mortality worldwide. Atherosclerosis is a progressive inflammatory disease which has an onset by vascular obstruction from the deposits of plaque, subsequently developing into athero-thrombosis and abnormal blood flow. The evidence to support a cholesterol-atherosclerosis link has been revealed in the past three decades. There is a growing consensus that therapeutic lowering of plasma cholesterol level will reduce the risk of cardiovascular incidence. In **Chapter 1**, established mechanisms underlying lipid metabolism and atherosclerotic pathology are reviewed, including the important players involved in plasma / hepatic lipoprotein metabolism pathways and atherosclerotic plaque progression / regression process.

The first part of the thesis focuses on the hepatic lipid metabolism and the pharmaceutical interventions in the liver. In **Chapter 2**, we have composed the hepatic cell type-specific expression profile of NRs to provide the most complete quantitative assessment of NRs distribution in liver reported to date. We have identified several liver-enriched orphan NRs as potential novel targets for pharmaceutical interventions in liver. In **Chapter 3**, we have determined the hepatic expression profile of NAFLD-related gene PNPLA3 and its metabolic effects. PNPLA3 is highly responsive to metabolic changes in hepatocytes within the liver and its relative change in expression level suggests an essential function in lipogenesis. In **Chapter 4** the mechanism underlying the hepatic and plasma CETP-lowering effect of niacin in mice is investigated. The clinical use of niacin has been limited due to the cutaneous flushing effect, which is mediated by the nicotinic acid receptor GPR109A. Therefore, in **Chapter 5**, we assessed the properties of two partial agonists for GPR109A compared to niacin. We showed that these two partial agonists are promising drug candidates to achieve the beneficial lipid-lowering effects while successfully avoiding the unwanted flushing side effect.

The second part of the thesis focuses on the concept of atherosclerotic lesion regression, shedding insights in the roles of LXR activation and application of mouse models in regression studies. In both **Chapter 6** and **Chapter 7** it is examined whether rapidly improved plasma lipoprotein profiles combined with LXR activation can lead to atherosclerotic lesion regression. In **Chapter 6** $LDLr^{-/-}$ mice are used and it is shown that intact LDL receptor function is crucial to overcome LXR-induced hyperlipidemia. In **Chapter 7** we used $ApoE^{-/-}$ mice reconstituted with bone marrow from C57BL/6 mice as a novel mouse model with chow diet feeding, providing an alternative model to investigate atherosclerotic plaque regression without robust surgical measures. Both of these two chapters demonstrate that rapidly optimized plasma lipoprotein profiles combined with LXR agonist induce favorable gene expression profiles leading to regression of pre-existing atherosclerotic plaques.

In **Chapter 8**, the results obtained from all the experiments mentioned above are summarized and discussed with respect to the implications of these studies for future investigations.

Table 1. Summary of studies of LXR agonists on atherosclerotic progression and regression in mouse models

Name	Mouse model	Diet during treatment	Treatment duration	Plasma TC	Plasma (V)LDL	Plasma TG	Plasma HDL	Lesion size (aortic root)	Lesion size (en face)	Reference
T0901317	C57BL/6	Chow	7 days	↑	↑	↑	↑			110
T0901317	LDLr–/–	AD	8 weeks	→	↓	→ (transient increase)	↑	Inhibited progression		111
T0901317	C57BL/6	Chow	3 days	↑		→	↑			112
T0901317	C57BL/6	Chow	6 days	↑	↑	↑	↑			113
T0901317	LDLR–/–	WTD	Baseline: 8 weeks WTD Regression study: 6weeks WTD±T0901317	↓	↓	↑	→	Inhibited progression. Macrophage content ↓ Collagen content ↑	Regression	114
T0901317	LDLr–/–	WTD	12 weeks	↑	↑	↑	↓	Inhibited progression Macrophage content ↓ Collagen content ↑	Inhibited progression Macrophage content ↑	115
T0901317	ApoE–/–	AD	Baseline: AD 8 weeks Regression study: 6weeks AD±T0901317	↑	→	↑	↑	Regression Macrophage content ↓	Regression	116,117
T0901317	ApoE*3Leiden		Baseline: WTD 18 weeks Regression study: 8weeks Chow±T0901317	→	↑	↑	→	Regression		49
T0901317	C57BL/6	Chow	4 days	Hepatic TC →		Hepatic TG ↑				118
T0901317	LXR*α*–/–;LDLr–/–	WTD	12 weeks	→		→		Inhibited progression	→	119
T0901317	LXR*β*–/–;LDLr–/–	WTD	12 weeks	→		↑		Inhibited progression	Inhibited progression	119
T0901317	LDLr–/–	WTD	12 weeks	→		↑		Inhibited progression	Inhibited progression	119
T0901317	C57BL/6	Chow	4 weeks	↑	↓	↓	↑			120
T0901317	LDLr–/–	WTD	4 weeks	↑	↑	↑	→			120
T0901317	ApoE–/–	AD	6 weeks	↑		↑	↑	Inhibited progression	Inhibited progression	121
GW3965	LDLr–/–	AD	12 weeks	↓		→	→	Inhibited progression	Inhibited progression	69
GW3965	ApoE–/–	Chow	12 weeks	→	↓	↑	→	Inhibited progression		69

GW3965	C57BL/6	Chow	3 days	→		→	↑			112
GW3965	C57BL/6	Chow	6 days	↑	↑	↑	↑			113
GW3965	C57BL/6	Chow	12 days	↑	↑		↑			122
GW3965	ApoB/CETP Tg	Chow	12 days	↑	↑		↑			122
GW3965	LXR–/–;ApoE–/–	Chow	12 days	↑	→		→			122
GW3965	LXRα–/–;ApoE–/–	WTD	11 weeks	↓	→	→	↑	Inhibited progression	Inhibited progression	123
GW3965	ApoE–/–	WTD	11 weeks	↓		↑	↑	Inhibited progression	Inhibited progression	123
GW3965	LDLr-/-	AD	8 weeks	→		→			Inhibited progression	124
GW3965	C57BL/6	Chow	10 days	↑			↑			125
GW3965	LDLr–/–	Chow	10 days	↑			↑			70
GW3965	APOE*3Leiden	AD	20 weeks	→		↑		inhibited progression Collagen content ↓		126
ATI-111	LDLr–/–	AD	8 weeks	↓	↓	↓	→	inhibited progression	inhibited progression	70
AZ-876	APOE*3Leiden	AD	20 weeks	Low dose: → High dose: ↓		Low dose: → High dose: ↑		Inhibited progression upon low/high dose Lesion composition →		126
ATI-829	LDLr–/–	WTD	12 weeks	→	→	→	→	Inhibited progression Macrophage content ↓ Collagen content ↑	Inhibited progression	127
DMHCA	ApoE–/–	WTD	11 weeks	↓	↓	↓	→	Inhibited progression	Inhibited progression	118
DMHCA	C57BL/6	Chow	15 days	↓		→				118
DMHCA	C57BL/6	WTD	15 days	→		→				118
MHEC	ApoE–/–	AD	6 weeks	→		→	↑	Inhibited progression	Inhibited progression	121

↑: increased; ↓: decreased; →: unchanged.
WTD: Western-type diet; AD: Atherogenic diet; HFD: High-fat Diet; Tg: transgenic

Table 2. Summary of effects of niacin on lipid metabolism and CETP regulation in mouse models

Mouse model	Diet during treatment	Treatment duration (weeks)	Plasma TC	Plasma (V)LDL	Plasma HDL	Plasma TG	Plasma FFA	Effects on liver	Lesion size (aortic root)	Lesion size (en face)	Reference
C57BL/6	AD	4	→		→	↓					128
C57BL/6	WTD	12				↓	↓				129
C57BL/6	Chow	30 min after i.p. injection					↓				93
C57BL/6	Chow	3	↓	↓	↓			cAMP ↓ ABCA1 ↓			130
C57BL/6;Gpr109a–/–	Chow	3	→	→	→			cAMP → ABCA1 →			130
C57BL/6	Chow	2	↓	→	→	↓					131
Human CETP Tg	Chow	2	→	↓	↑	↓					131
Human apo B100 Tg	Chow	2	↓	↓	↓	→					131
Human CETP/apoB100 Tg	Chow	2	↓	↓	↑	↓					131
E3L mice	WTD	3	↓	↓	→	↓					99
E3L.CETP mice	WTD	3	↓	↓	↑	↓		TG, TC, FC, CE ↓ Plasma CETP ↓ Hepatic CETP ↓			99
LDLr–/–;Gpr109a+/+	HFD	10	→	→	→	At 2 weeks: ↓ At 10 weeks: →	→		↓	↓	132
LDLr–/–;Gpr109a–/–	HFD	10	→	→	→	At 2 weeks: ↓ At 10 weeks: →	→		→	→	132
ApoE–/–	AD	14	→		→	→			→		128

↑: increased; ↓: decreased; →: unchanged.
WTD: Western-type diet; AD: Atherogenic diet; HFD: High-fat Diet; Tg: transgenic

REFERENCES

1. Toutouzas K, Drakopoulou M, Skoumas I, Stefanadis C. Advancing therapy for hypercholesterolemia. Expert Opin Pharmacother. 2010;11:1659-1672.
2. Paras C, Hussain MM, Rosenson RS. Emerging drugs for hyperlipidemia. Expert Opin Emerg Drugs. 2010;15:433-451.
3. Lee JM, Choudhury RP. Atherosclerosis regression and high-density lipoproteins. Expert Rev Cardiovasc Ther. 2010;8:1325-1334.
4. Ginsberg HN. Lipoprotein metabolism and its relationship to atherosclerosis. Med Clin North Am. 1994;78:1-20.
5. Champe P, Harvey R. Lippincott's Illustrated Reviews: Biochemistry, Fourth Edition. Philadelphia : Lippincott William & Wilkin. 2008.
6. Ginsberg HN. Lipoprotein physiology. Endocrinol Metab Clin North Am. 1998;27:503-519.
7. Nabel EG. Cardiovascular disease. N Engl J Med. 2003;349:60-72.
8. Taskinen MR, Ginsberg HN. Lipid metabolism: new approaches to old problems. Curr Opin Lipidol. 1998;9:185-187.
9. Link JJ, Rohatgi A, de Lemos JA. HDL cholesterol: physiology, pathophysiology, and management. Curr Probl Cardiol. 2007;32:268-314.
10. Rothblat GH, Phillips MC. High-density lipoprotein heterogeneity and function in reverse cholesterol transport. Curr Opin Lipidol. 2010;21:229-238.
11. Assmann G, Nofer JR. Atheroprotective effects of high-density lipoproteins. Annu Rev Med. 2003;54:321-341.
12. Ragbir S, Farmer JA. Dysfunctional high-density lipoprotein and atherosclerosis. Curr Atheroscler Rep. 2010;12:343-348.
13. Ye D, Lammers B, Zhao Y, Meurs I, Van Berkel T, Van Eck M. ATP-Binding Cassette Transporters A1 and G1, HDL Metabolism, Cholesterol Efflux, and Inflammation: Important Targets for the Treatment of Atherosclerosis. Curr Drug Targets. 2011;12:647-660.
14. Duffy D, Rader DJ. Update on strategies to increase HDL quantity and function. Nat Rev Cardiol. 2009;6:455-463.
15. Van der Velde AE. Reverse cholesterol transport: from classical view to new insights. World J Gastroenterol. 2010;16:5908-5915.
16. Lund-Katz S, Phillips MC. High density lipoprotein structure-function and role in reverse cholesterol transport. Subcell Biochem. 2010;51:183-227.
17. Meurs I, Van Eck M, Van Berkel TJ. High-density lipoprotein: key molecule in cholesterol efflux and the prevention of atherosclerosis. Curr Pharm Des. 2010;16:1445-1467.
18. Davis RA, Hui TY. 2000 George Lyman Duff Memorial Lecture: atherosclerosis is a liver disease of the heart. Arterioscler Thromb Vasc Biol. 2001;21:887-898.
19. Marchesini G, Moscatiello S, Di Domizio S, Forlani G. Obesity-associated liver disease. J Clin Endocrinol Metab. 2008;93:74-80.
20. Marchesini G, Bugianesi E, Forlani G, Cerrelli F, Lenzi M, Manini R, Natale S, Vanni E, Villanova N, Melchionda N, Rizzetto M. Nonalcoholic fatty liver, steatohepatitis, and the metabolic syndrome. Hepatology. 2003;37:917–923.
21. Kotronen A, Yki-Järvinen H. Fatty liver: a novel component of the metabolic syndrome. Arterioscler Thromb Vasc Biol. 2008;28:27-38.
22. Targher G, Marra F, Marchesini G. Increased risk of cardiovascular disease in non-alcoholic fatty liver disease: causal effect or epiphenomenon? Diabetologia. 2008;51:1947-1953.
23. Hamaguchi M, Kojima T, Takeda N, Nagata C, Takeda J, Sarui H, Kawahito Y, Yoshida N, Suetsugu A, Kato T, Okuda J, Ida K, Yoshikawa T. Nonalcoholic fatty liver disease is a novel predictor of cardiovascular disease. World J Gastroenterol. 2007;13:1579-1584.
24. Wisse E. An electron microscopic study of the fenestrated endothelial lining of rat liver sinusoids. J Ultrastruct Res. 1970;31:125-150.
25. Smedsrød B, De Bleser PJ, Braet F, Lovisetti P, Vanderkerken K, Wisse E, Geerts A. Cell biology of liver endothelial and Kupffer cells. Gut. 1994;35:1509-1516.
26. Bouwens L, Baekeland M, De Zanger R, Wisse E. Quantitation, tissue distribution and proliferation kinetics of Kupffer cells in normal rat liver. Hepatology. 1986;6:718-722.
27. Van Berkel TJ, Kruijt JK, Koster JF. Identity and activities of lysosomal enzymes in parenchymal and non-parenchymal cells from rat liver. Eur J Biochem. 1975;58:145-152.
28. Munthe-Kaas AC, Berg T, Seljelid R. Distribution of lysosomal enzymes in different types of rat liver cells. Exp Cell Res. 1976;99:146-154.

29. Mottino AD, Catania VA. Hepatic drug transporters and nuclear receptors: regulation by therapeutic agents. World J Gastroenterol. 2008;14:7068-7074.
30. Karpen SJ, Trauner M. The new therapeutic frontier--nuclear receptors and the liver. J Hepatol. 2010;52:455-462.
31. Kolios G, Valatas V, Kouroumalis E. Role of Kupffer cells in the pathogenesis of liver disease. World J Gastroenterol. 2006;12:7413-7420.
32. Van Berkel TJ, Nagelkerke JF, Harkes L, Kruijt JK. Processing of acetylated human low-density lipoprotein by parenchymal and non-parenchymal liver cells. Involvement of calmodulin? Biochem J. 1982;208:493-503.
33. Nagelkerke JF, Havekes L, Van Hinsbergh VW, Van Berkel TJ. In vivo catabolism of biologically modified LDL. Arteriosclerosis. 1984;4:256-264.
34. Nenseter MS, Gudmundsen O, Roos N, Maelandsmo G, Drevon CA, Berg T. Role of liver endothelial and Kupffer cells in clearing low density lipoprotein from blood in hypercholesterolemic rabbits. J Lipid Res. 1992;33:867-877.
35. Stienstra R, Saudale F, Duval C, Keshtkar S, Groener JE, van Rooijen N, Staels B, Kersten S, Müller M. Kupffer cells promote hepatic steatosis via interleukin-1beta-dependent suppression of peroxisome proliferator-activated receptor alpha activity. Hepatology. 2010;51:511-522.
36. Prudêncio M, Rodriguez A, Mota MM. The silent path to thousands of merozoites: the Plasmodium liver stage. Nat Rev Microbiol. 2006;4:849-856.
37. McGovern PG, Pankow JS, Shahar E, Doliszny KM, Folsom AR, Blackburn H, Luepker RV. Recent trends in acute coronary heart disease--mortality, morbidity, medical care, and risk factors. The Minnesota Heart Survey Investigators. N Engl J Med. 1996;334:884-890.
38. Boehm M, Nabel EG. The cell cycle and cardiovascular diseases. Prog Cell Cycle Res. 2003;5:19-30.
39. Shibata N, Glass CK. Macrophages, oxysterols and atherosclerosis. Circ J. 2010;74:2045-2051.
40. Brown MS, Goldstein JL. Lipoprotein metabolism in the macrophage: implications for cholesterol deposition in atherosclerosis. Annu Rev Biochem. 1983;52:223-261.
41. Hansson GK. Inflammation, atherosclerosis, and coronary artery disease. N Engl J Med. 2005;352:1685-1695.
42. Hansson GK, Robertson AK, Söderberg-Nauclér C. Inflammation and atherosclerosis. Annu Rev Pathol. 2006;1:297-329.
43. Heinecke J. HDL and cardiovascular-disease risk--time for a new approach? N Engl J Med. 2011;364:170-171.
44. Bennett MR. Life and death in the atherosclerotic plaque. Curr Opin Lipidol. 2010;21:422-426.
45. Schrijvers DM, De Meyer GR, Herman AG, Martinet W. Phagocytosis in atherosclerosis: Molecular mechanisms and implications for plaque progression and stability. Cardiovasc Res. 2007;73:470-480.
46. Zhang T, Zhai Y, Chen Y, Zhou Z, Yang J, Liu H. Effects of emotional and physiological stress on plaque instability in apolipoprotein E knockout mice. J Physiol Biochem. 2011 [Epub ahead of print].
47. Trogan E, Feig JE, Dogan S, Rothblat GH, Angeli V, Tacke F, Randolph GJ, Fisher EA. Gene expression changes in foam cells and the role of chemokine receptor CCR7 during atherosclerosis regression in ApoE-deficient mice. Proc Natl Acad Sci U S A. 2006;103:3781-3786.
48. Feig JE, Pineda-Torra I, Sanson M, Bradley MN, Vengrenyuk Y, Bogunovic D, Gautier EL, Rubinstein D, Hong C, Liu J, Wu C, Van Rooijen N, Bhardwaj N, Garabedian M, Tontonoz P, Fisher EA. LXR promotes the maximal egress of monocyte-derived cells from mouse aortic plaques during atherosclerosis regression. J Clin Invest. 2010;120:4415-4424.
49. Verschuren L, De Vries-Van Der Weij J, Zadelaar S, Kleemann R, Kooistra T. LXR agonist suppresses atherosclerotic lesion growth and promotes lesion regression in apoE*3Leiden mice: time course and mechanisms. J Lipid Res. 2009;50:301-311.
50. Raffai RL, Loeb SM, Weisgraber KH. Apolipoprotein E promotes the regression of atherosclerosis independently of lowering plasma cholesterol levels. Arterioscler Thromb Vasc Biol. 2005;25:436-441.
51. Potteaux S, Gautier EL, Hutchison SB, Van Rooijen N, Rader DJ, Thomas MJ, Sorci-Thomas MG, Randolph GJ. Suppressed monocyte recruitment drives macrophage removal from atherosclerotic plaques of Apoe-/- mice during disease regression. J Clin Invest. 2011;121:2025-2036.
52. Kolovou G, Anagnostopoulou K, Mikhailidis DP, Cokkinos DV. Apolipoprotein E knockout models. Curr Pharm Des. 2008;14:338-351.
53. Getz GS. Overview of murine atherosclerosis series. Curr Drug Targets. 2007;8:1144-1149.
54. Schreyer SA, Wilson DL, LeBoeuf RC. C57BL/6 mice fed high fat diets as models for diabetes-accelerated atherosclerosis. Atherosclerosis. 1998;136:17-24.

55. Paigen B, Mitchell D, Reue K, Morrow A, Lusis AJ, LeBoeuf RC. Ath-1, a gene determining atherosclerosis susceptibility and high density lipoprotein levels in mice. Proc Natl Acad Sci U S A. 1987;84:3763-3767.
56. Liao F, Andalibi A, DeBeer FC, Fogelman AM, Lusis AJ. Genetic control of inflammatory gene induction and NF-kappa B-like transcription factor activation in response to an atherogenic diet in mice. J Clin Invest. 1993;91:2572-2579.
57. Paigen B, Ishida BY, Verstuyft J, Winters RB, Albee D. Atherosclerosis susceptibility differences among progenitors of recombinant inbred strains of mice. Arteriosclerosis. 1990;10:316-323.
58. Johnston TP. The P-407-induced murine model of dose-controlled hyperlipidemia and atherosclerosis: a review of findings to date. J Cardiovasc Pharmacol. 2004;43:595-606.
59. Kowala MC, Recce R, Beyer S, Gu C, Valentine M. Characterization of atherosclerosis in LDL receptor knockout mice: macrophage accumulation correlates with rapid and sustained expression of aortic MCP-1/JE. Atherosclerosis. 2000;149:323-330.
60. Knowles JW, Maeda N. Genetic modifiers of atherosclerosis in mice. Arterioscler Thromb Vasc Biol. 2000;20:2336–2345.
61. Zadelaar S, Kleemann R, Verschuren L, De Vries-Van Der Weij J, Van Der Hoorn J, Princen HM, Kooistra T. Mouse models for atherosclerosis and pharmaceutical modifiers. Arterioscler Thromb Vasc Biol. 2007;27:1706-1721.
62. Doggrell SA. Statins in the 21st century: end of the simple story? Expert Opin Investig Drugs. 2001;10:1755-1766.
63. Shah PK. Emerging non-statin LDL-lowering therapies for dyslipidemia and atherosclerosis. Rev Cardiovasc Med. 2003;4:136-141.
64. Wierzbicki AS. New lipid-lowering agents. Expert Opin Emerg Drugs. 2003;8:365-376.
65. Bookout AL, Jeong Y, Downes M, Yu RT, Evans RM, Mangelsdorf DJ. Anatomical profiling of nuclear receptor expression reveals a hierarchical transcriptional network. Cell. 2006;126:789-799.
66. Schulman IG. Nuclear receptors as drug targets for metabolic disease. Adv Drug Deliv Rev. 2010;62:1307-1315.
67. Repa JJ, Mangelsdorf DJ. The liver X receptor gene team: potential new players in atherosclerosis. Nat Med. 2002;8:1243-1248.
68. Zhao C, Dahlman-Wright K. Liver X receptor in cholesterol metabolism. J Endocrinol. 2010;204:233-2340.
69. Joseph SB, McKilligin E, Pei L, Watson MA, Collins AR, Laffitte BA, Chen M, Noh G, Goodman J, Hagger GN, Tran J, Tippin TK, Wang X, Lusis AJ, Hsueh WA, Law RE, Collins JL, Willson TM, Tontonoz P. Synthetic LXR ligand inhibits the development of atherosclerosis in mice. Proc Natl Acad Sci U S A. 2002;99:7604-7609.
70. Peng D, Hiipakka RA, Xie JT, Dai Q, Kokontis JM, Reardon CA, Getz GS, Liao S. A novel potent synthetic steroidal liver X receptor agonist lowers plasma cholesterol and triglycerides and reduces atherosclerosis in LDLR-/- mice. Br J Pharmacol. 2011;162:1792-1804
71. Yu L, Li-Hawkins J, Hammer RE, Berge KE, Horton JD, Cohen JC, Hobbs HH. Overexpression of ABCG5 and ABCG8 promotes biliary cholesterol secretion and reduces fractional absorption of dietary cholesterol. J Clin Invest. 2002;110:671-680.
72. Yu L, York J, von Bergmann K, Lutjohann D, Cohen JC, Hobbs HH. Stimulation of cholesterol excretion by the liver X receptor agonist requires ATP-binding cassette transporters G5 and G8. J Biol Chem. 2003;278:15565-15570.
73. Calpe-Berdiel L, Rotllan N, Fiévet C, Roig R, Blanco-Vaca F, Escolà-Gil JC. Liver X receptor-mediated activation of reverse cholesterol transport from macrophages to feces in vivo requires ABCG5/G8. J Lipid Res. 2008;49:1904-1911.
74. Dunham I, Shimizu N, Roe BA, Chissoe S, Hunt AR, Collins JE, Bruskiewich R, Beare DM, Clamp M, Smink LJ, Ainscough R, Almeida JP, Babbage A, Bagguley C, Bailey J, Barlow K, Bates KN, Beasley O, Bird CP, Blakey S, Bridgeman AM, Buck D, Burgess J, Burrill WD, O'Brien KP, et al. The DNA sequence of human chromosome 22. Nature. 1999;402:489-495.
75. Collins JE, Goward ME, Cole CG, Smink LJ, Huckle EJ, Knowles S, Bye JM, Beare DM, Dunham I. Reevaluating human gene annotation: a second-generation analysis of chromosome 22. Genome Res. 2003;13:27-36.
76. Romeo S, Kozlitina J, Xing C, Pertsemlidis A, Cox D, Pennacchio LA, Boerwinkle E, Cohen JC, Hobbs HH. Genetic variation in PNPLA3 confers susceptibility to nonalcoholic fatty liver disease. Nat Genet. 2008;40:1461-1465.
77. Kotronen A, Johansson LE, Johansson LM, Roos C, Westerbacka J, Hamsten A, Bergholm R, Arkkila P, Arola J, Kiviluoto T, Fisher RM, Ehrenborg E, Orho-Melander M, Ridderstråle M, Groop L,

Yki-Järvinen H. A common variant in PNPLA3, which encodes adiponutrin, is associated with liver fat content in humans. Diabetologia. 2009;52:1056-1060.
78. De Grooth GJ, Klerkx AH, Stroes ES, Stalenhoef AF, Kastelein JJ, Kuivenhoven JA. A review of CETP and its relation to atherosclerosis. J Lipid Res. 2004;45:1967-1974.
79. Jiang XC, Moulin P, Quinet E, Goldberg IJ, Yacoub, Agellon LB, Compton D, Schnitzer-Polokoff R, Tall AR. Mammalian adipose tissue and muscle are major sources of lipid transfer protein mRNA. J. Biol. Chem. 1991;266: 4631-4639.
80. Drayna D., Jarnagin AS, McLean J, Henzel W, Kohr W, Fielding C, Lawn R. Cloning and sequencing of human cholesteryl ester transfer protein cDNA. Nature. 1987;327:632–634.
81. Van Eck M, Ye D, Hildebrand RB, Kar Kruijt J, De Haan W, Hoekstra M, Rensen PC, Ehnholm C, Jauhiainen M, Van Berkel TJ. Important role for bone marrow-derived cholesteryl ester transfer protein in lipoprotein cholesterol redistribution and atherosclerotic lesion development in LDL receptor knockout mice. Circ Res. 2007;100:678-685.
82. Chapman MJ, Le Goff W, Guerin M, Kontush A. Cholesteryl ester transfer protein: at the heart of the action of lipid-modulating therapy with statins, fibrates, niacin, and cholesteryl ester transfer protein inhibitors. Eur Heart J. 2010;31:149-164.
83. Vourvouhaki E, Dedoussis GV. Cholesterol ester transfer protein: a therapeutic target in atherosclerosis? Expert Opin Ther Targets. 2008;12:937-948.
84. Kolovou GD, Anagnostopoulou KK, Kostakou PM, Mikhailidis DP. Cholesterol ester transfer protein (CETP), postprandial lipemia and hypolipidemic drugs. Curr Med Chem. 2009;16:4345-4360.
85. Hunt JA, Lu Z. Cholesteryl ester transfer protein (CETP) inhibitors. Curr Top Med Chem. 2009;9:419-427.
86. Lorenzen A, Stannek C, Lang H, Andrianov V, Kalvinsh I, Schwabe U. Characterization of a G protein-coupled receptor for nicotinic acid. Mol Pharmacol. 2001;59:349-357.
87. Wise A, Foord SM, Fraser NJ, Barnes AA, Elshourbagy N, Eilert M, Ignar DM, Murdock PR, Steplewski K, Green A, Brown AJ, Dowell SJ, Szekeres PG, Hassall DG, Marshall FH, Wilson S, Pike NB. Molecular identification of high and low affinity receptors for nicotinic acid. J Biol Chem. 2003;278: 9869-9874.
88. Soga T, Kamohara M, Takasaki J, Matsumoto S, Saito T, Ohishi T, Hiyama H, Matsuo A, Matsushime H, Furuichi K. Molecular identification of nicotinic acid receptor. Biochem Biophys Res Commun. 2003;303:364-369.
89. Tunaru S, Kero J, Schaub A, Wufka C, Blaukat A, Pfeffer K, Offermanns S. PUMA-G and HM74 are receptors for nicotinic acid and mediate its anti-lipolytic effect. Nat. Med. 2003;9:352-355.
90. Meyers CD, Liu P, Kamanna VS, Kashyap ML. Nicotinic acid induces secretion of prostaglandin D2 in human macrophages: an in vitro model of the niacin flush. Atherosclerosis. 2007;192:253-258.
91. Benyó Z, Gille A, Kero J, Csiky M, Suchánková MC, Nüsing RM, Moers A, Pfeffer K, Offermanns S. GPR109A (PUMA-G/HM74A) mediates nicotinic acid-induced flushing. J Clin Invest. 2005;115:3634-3640.
92. Papaliodis D, Boucher W, Kempuraj D, Michaelian M, Wolfberg A, House M, Theoharides TC. Niacin-induced "flush" involves release of prostaglandin D2 from mast cells and serotonin from platelets: evidence from human cells in vitro and an animal model. J Pharmacol Exp Ther. 2008;327:665-672.
93. Walters RW, Shukla AK, Kovacs JJ, Violin JD, DeWire SM, Lam CM, Chen JR, Muehlbauer MJ, Whalen EJ, Lefkowitz RJ. beta-Arrestin1 mediates nicotinic acid-induced flushing, but not its antilipolytic effect, in mice. J Clin Invest. 2009;119:1312-1321.
94. Carlson LA, Oro L. The effect of nicotinic acid on the plasma free fatty acid; demonstration of a metabolic type of sympathicolysis. Acta Med Scand. 1962;172:641-645.
95. Benhalima K, Muls E. Niacin, an old drug with new perspectives for the management of dyslipidaemia. Acta Clin Belg. 2010;65:23-28.
96. Carlson L.A. Niaspan, the prolonged release preparation of nicotinic acid (niacin), the broad-spectrum lipid drug. Int J Clin Pract. 2004;58:706-713.
97. Lee JM, Robson MD, Yu LM, Shirodaria CC, Cunnington C, Kylintireas I, Digby JE, Bannister T, Handa A, Wiesmann F, Durrington PN, Channon KM, Neubauer S, Choudhury RP. Effects of high-dose modified-release nicotinic acid on atherosclerosis and vascular function: a randomized, placebo-controlled, magnetic resonance imaging study. J Am Coll Cardiol. 2009;54:1787-1794.
98. Taylor AJ, Villines TC, Stanek EJ, Devine PJ, Griffen L, Miller M, Weissman NJ, Turco M. Extended-release niacin or ezetimibe and carotid intima-media thickness. N Engl J Med. 2009;361:2113-2122.

99. Van Der Hoorn JW, De Haan W, Berbée JF, Havekes LM, Jukema JW, Rensen PC, Princen HM. Niacin increases HDL by reducing hepatic expression and plasma levels of cholesteryl ester transfer protein in APOE*3Leiden.CETP mice. Arterioscler Thromb Vasc Biol. 2008;28:2016-2022.
100. Carlson LA. Nicotinic acid: the broad-spectrum lipid drug. A 50th anniversary review. J Intern Med. 2005;258:94-114.
101. Davidson MH. Niacin use and cutaneous flushing: mechanisms and strategies for prevention. Am J Cardiol. 2008;101:14B-19B.
102. Benyó Z, Gille A, Kero J, Csiky M, Suchánková MC, Nüsing RM, Moers A, Pfeffer K, Offermanns S. GPR109A (PUMA-G/HM74A) mediates nicotinic acid-induced flushing. J Clin Invest. 2005;115:3634-3640.
103. Cheng K, Wu TJ, Wu KK, Sturino C, Metters K, Gottesdiener K, Wright SD, Wang Z, O'Neill G, Lai E, Waters MG. Antagonism of the prostaglandin D2 receptor 1 suppresses nicotinic acid-induced vasodilation in mice and humans. Proc Natl Acad Sci U S A. 2006;103:6682-6687.
104. Dunbar RL, Gelfand JM. Seeing red: flushing out instigators of niacin-associated skin toxicity. J Clin Invest. 2010;120:2651-2655.
105. Hanson J, Gille A, Zwykiel S, Lukasova M, Clausen BE, Ahmed K, Tunaru S, Wirth A, Offermanns S. Nicotinic acid- and monomethyl fumarate-induced flushing involves GPR109A expressed by keratinocytes and COX-2-dependent prostanoid formation in mice. J Clin Invest. 2010;120:2910-2919.
106. Morrow JD, Awad JA, Oates JA, Roberts LJ. Identification of skin as a major site of prostaglandin D2 release following oral administration of niacin in humans. J Invest Dermatol. 1992;98:812-815.
107. Wanders D, Judd RL. Future of GPR109A agonists in the treatment of dyslipidemia. Diabetes Obes Metab. 2011;13:685-691.
108. Kamanna VS, Kashyap ML. Nicotinic acid (niacin) receptor agonists: Will they be useful therapeutic agents? Am J Cardiol. 2007;100:53N-1N.
109. Soudijn W, Van Wijngaarden I, IJzerman AP. Nicotinic acid receptor subtypes and their ligands. Med Res Rev. 2007;27:417-433.
110. Schultz JR, Tu H, Luk A, Repa JJ, Medina JC, Li L, Schwendner S, Wang S, Thoolen M, Mangelsdorf DJ, Lustig KD, Shan B. Role of LXRs in control of lipogenesis. Genes Dev. 2000;14:2831-2838.
111. Terasaka N, Hiroshima A, Koieyama T, Ubukata N, Morikawa Y, Nakai D, Inaba T. T-0901317, a synthetic liver X receptor ligand, inhibits development of atherosclerosis in LDL receptor-deficient mice. FEBS Lett. 2003;536:6-11.
112. Miao B, Zondlo S, Gibbs S, Cromley D, Hosagrahara VP, Kirchgessner TG, Billheimer J, Mukherjee R. Raising HDL cholesterol without inducing hepatic steatosis and hypertriglyceridemia by a selective LXR modulator. J Lipid Res. 2004;45:1410-1417.
113. Quinet EM, Savio DA, Halpern AR, Chen L, Miller CP, Nambi P. Gene-selective modulation by a synthetic oxysterol ligand of the liver X receptor. J Lipid Res. 2004;45:1929-1942.
114. Levin N, Bischoff ED, Daige CL, Thomas D, Vu CT, Heyman RA, Tangirala RK, Schulman IG. Macrophage liver X receptor is required for antiatherogenic activity of LXR agonists. Arterioscler Thromb Vasc Biol. 2005;25:135-142.
115. Peng D, Hiipakka RA, Reardon CA, Getz GS, Liao S. Differential anti-atherosclerotic effects in the innominate artery and aortic sinus by the liver X receptor agonist T0901317. Atherosclerosis. 2009;203:59-66.
116. Ou X, Dai X, Long Z, Tang Y, Cao D, Hao X, Hu Y, Li X, Tang C. Liver X receptor agonist T0901317 reduces atherosclerotic lesions in apoE-/- mice by up-regulating NPC1 expression. Sci China C Life Sci. 2008;51:418-429.
117. Dai XY, Ou X, Hao XR, Cao DL, Tang YL, Hu YW, Li XX, Tang CK. The effect of T0901317 on ATP-binding cassette transporter A1 and Niemann-Pick type C1 in apoE-/- mice. J Cardiovasc Pharmacol. 2008;51:467-475.
118. Kratzer A, Buchebner M, Pfeifer T, Becker TM, Uray G, Miyazaki M, Miyazaki-Anzai S, Ebner B, Chandak PG, Kadam RS, Calayir E, Rathke N, Ahammer H, Radovic B, Trauner M, Hoefler G, Kompella UB, Fauler G, Levi M, Levak-Frank S, Kostner GM, Kratky D. Synthetic LXR agonist attenuates plaque formation in apoE-/- mice without inducing liver steatosis and hypertriglyceridemia. J Lipid Res. 2009;50:312-326.
119. Bischoff ED, Daige CL, Petrowski M, Dedman H, Pattison J, Juliano J, Li AC, Schulman IG. Non-redundant roles for LXRalpha and LXRbeta in atherosclerosis susceptibility in low density lipoprotein receptor knockout mice. J Lipid Res. 2010;51:900-906.

120.Peng D, Hiipakka RA, Xie JT, Reardon CA, Getz GS, Liao S. Differential effects of activation of liver X receptor on plasma lipid homeostasis in wild-type and lipoprotein clearance-deficient mice. Atherosclerosis. 2010;208:126-133.
121.Yan W, Zhang T, Cheng J, Zhou X, Qu X, Hu H. Liver X receptor agonist methyl-3β-hydroxy-5α,6α-epoxycholanate attenuates atherosclerosis in apolipoprotein E knockout mice without increasing plasma triglyceride. Pharmacology. 2010;86:306-312.
122.Naik SU, Wang X, Da Silva JS, Jaye M, Macphee CH, Reilly MP, Billheimer JT, Rothblat GH, Rader DJ. Pharmacological activation of liver X receptors promotes reverse cholesterol transport in vivo. Circulation. 2006;113:90-97.
123.Bradley MN, Hong C, Chen M, Joseph SB, Wilpitz DC, Wang X, Lusis AJ, Collins A, Hseuh WA, Collins JL, Tangirala RK, Tontonoz P. Ligand activation of LXR beta reverses atherosclerosis and cellular cholesterol overload in mice lacking LXR alpha and apoE. J Clin Invest. 2007;117:2337-2346.
124.Quinet EM, Basso MD, Halpern AR, Yates DW, Steffan RJ, Clerin V, Resmini C, Keith JC, Berrodin TJ, Feingold I, Zhong W, Hartman HB, Evans MJ, Gardell SJ, DiBlasio-Smith E, Mounts WM, LaVallie ER, Wrobel J, Nambi P, Vlasuk GP. LXR ligand lowers LDL cholesterol in primates, is lipid neutral in hamster, and reduces atherosclerosis in mouse. J Lipid Res. 2009;50:2358-2370.
125.Yasuda T, Grillot D, Billheimer JT, Briand F, Delerive P, Huet S, Rader DJ. Tissue-specific liver X receptor activation promotes macrophage reverse cholesterol transport in vivo. Arterioscler Thromb Vasc Biol. 2010;30:781-786.
126.Van Der Hoorn J, Lindén D, Lindahl U, Bekkers M, Voskuilen M, Nilsson R, Oscarsson J, Lindstedt E, Princen H. Low dose of the liver X receptor agonist, AZ876, reduces atherosclerosis in APOE*3Leiden mice without affecting liver or plasma triglyceride levels. Br J Pharmacol. 2011;162:1553-1563.
127.Peng D, Hiipakka RA, Dai Q, Guo J, Reardon CA, Getz GS, Liao S. Antiatherosclerotic effects of a novel synthetic tissue-selective steroidal liver X receptor agonist in low-density lipoprotein receptor-deficient mice. J Pharmacol Exp Ther. 2008;327:332-342.
128.Declercq V, Yeganeh B, Moshtaghi-Kashanian GR, Khademi H, Bahadori B, Moghadasian MH. Paradoxical effects of fenofibrate and nicotinic acid in apo E-deficient mice. J Cardiovasc Pharmacol. 2005;46:18-24.
129.Hernandez C, Molusky M, Li Y, Li S, Lin JD. Regulation of hepatic ApoC3 expression by PGC-1β mediates hypolipidemic effect of nicotinic acid. Cell Metab. 2010;12:411-419.
130.Li X, Millar JS, Brownell N, Briand F, Rader DJ. Modulation of HDL metabolism by the niacin receptor GPR109A in mouse hepatocytes. Biochem Pharmacol. 2010;80:1450-1457.
131.Hernandez M, Wright SD, Cai TQ. Critical role of cholesterol ester transfer protein in nicotinic acid-mediated HDL elevation in mice. Biochem Biophys Res Commun. 2007;355:1075-1080.
132.Lukasova M, Malaval C, Gille A, Kero J, Offermanns S. Nicotinic acid inhibits progression of atherosclerosis in mice through its receptor GPR109A expressed by immune cells. J Clin Invest. 2011;121:1163-1673.

Chapter 2

Gene Expression Profiling of Nuclear Receptors in Mouse Liver Parenchymal, Endothelial, and Kupffer Cells

Zhaosha Li, J. Kar Kruijt, Theo J.C. Van Berkel, Menno Hoekstra

Division of Biopharmaceutics, Leiden/Amsterdam Center for Drug Research, Leiden University, The Netherlands

Submitted for publication

ABSTRACT

Background & Aims: Liver utilizes nuclear receptors (NRs) for hepatic functions, and NRs have been increasingly appreciated by hepatic researchers. Liver consists of parenchymal and non-parenchymal cells which synchronize crucial roles in liver metabolic homeostasis. To gain insight into the pharmacological potential of the remaining liver-enriched orphan NRs, we have composed the hepatic cell type-specific expression profile of NRs.
Methods and Results: C57BL/6 mice liver parenchymal, endothelial, and Kupffer cells were isolated using collagenase perfusion and counter-flow centrifugal elutriation. The hepatic expression pattern of 48 NRs was generated by real-time quantitative PCR. FXRalpha, COUP-TF3, HNF4alpha, LXRalpha, and CAR were the most abundantly expressed NRs in parenchymal cells. In contrast, NGFIB, COUP-TF2, LXRs, FXRalpha, and COUP-TF3 were the most highly expressed NRs in endothelial and Kupffer cells. Interestingly, members of orphan receptor COUP-TF family showed distinct expression patterns. COUP-TF3 was highly and exclusively expressed in parenchymal cells, with an expression level higher than LXRalpha, while COUP-TF2 was moderately and exclusively expressed in endothelial and Kupffer cells. Another orphan receptor TR4 is ubiquitously expressed in liver at a comparable level as PPARgamma, suggesting that TR4 may function as a lipid sensor as PPARgamma in liver and macrophages.
Conclusions: Our study provides the most complete quantitative assessment of NRs distribution in liver reported to date. It is suggested that orphan NRs such as COUP-TF2, COUP-TF3, and TR4 may be of significant importance as novel targets for pharmaceutical interventions in liver.
Keywords: Nuclear receptor, liver, parenchymal cell, endothelial cell, Kupffer cell

INTRODUCTION

The nuclear receptor (NR) superfamily describes a related but diverse array of ligand-activated transcription factors. NR binds DNA and translates physiological signals into gene regulation involved in biological processes including metabolism. Liver is considered as the major organ with significant therapeutic importance for the maintenance of metabolic homeostasis. Liver utilizes many NRs for hepatic functions, and NRs have been increasingly appreciated by researchers in the hepatic field [1]. Many of the liver-enriched NRs with identified ligands have been demonstrated to be important sensors and regulators. Toxin-activated NRs, such as CAR and PXR, are key sensors to regulate xenobiotic clearance in the liver [2]. Lipid-activated NRs, such as PPAR and LXR, are attractive targets for therapeutic agents to regulate glucose metabolism, lipid metabolism, and inflammation [3]. However, the function of orphan NRs whose endogenous and synthetic ligand(s) is unknown has not been fully exploited. It is thus of interest to quantitatively assess the expression and distribution of NRs in liver to discover the pharmacological potential of the remaining liver-enriched orphan NRs.

The liver consists of different types of cells, including parenchymal cells, namely hepatocytes, and a variety of non-parenchymal cells. Non-parenchymal cells are comprised of mainly liver sinusoidal endothelial cells and Kupffer cells. Liver endothelial cells form a continuous but fenestrated lining of the hepatic sinusoids, while Kupffer cells are found in the sinusoidal lumen on top of or between endothelial cells [4]. Liver endothelial cells free the bloodstream from a variety of macromolecular waste products during inflammation [5]. Kupffer cells are a population of hepatic resident macrophages. They constitute 80-90% of the tissue macrophages present in the body [6]. Although non-parenchymal cells count for only 6.5% of the liver volume, they contain 55% of the lipid droplets in the liver and 43% of the lysosomes, and specific activities of enzymes are generally higher in non-parenchymal cells than in parenchymal cells [7,8]. Parenchymal and non-parenchymal cells synchronize crucial roles in liver metabolic homeostasis as well as inflammation. The majority of studies upon NRs in liver has focused on the array of target genes and metabolic pathways within parenchymal cells [9,10]. However, non-parenchymal cells are also intimately involved in the pathogenesis of various liver metabolic diseases including steatohepatitis, non-alcoholic fatty liver, and liver fibrosis [11]. Previous studies have shown that diet-induced hypercholesterolemia results in marked changes in the hepatic distribution of LDL and significant accumulation of cholesteryl ester/lipid droplets in liver endothelial and Kupffer cells, suggesting a prominent role of liver non-parenchymal cells in removing modified LDL from blood [12-14]. Other studies showed that depletion of liver Kupffer cells and targeted inactivation of scavenger receptor A and CD36 expressed in Kupffer cells reduced hepatic inflammation and tissue destruction associated with diet-induced hepatic steatosis, indicating the role for liver macrophages in hepatic lipid metabolism and insulin sensitivity [15,16]. It has been shown that cross-talk between Kupffer cells and hepatocytes regulates glycogenolysis [17] and hepatic lipid storage [18]. It is thus of interest to further investigate the potential cross-talk between NRs in non-parenchymal and parenchymal cells involved in hepatic metabolism regulation.

NRs may have different distribution patterns in liver parenchymal and non-parenchymal cells. It has been shown that RXRalpha and RXRbeta expression

levels are 5- to 10-fold higher in Kupffer cells than in other non-parenchymal cells while all the subtypes of RAR family have similar expression level in both cell types [19]. Hoekstra *et al* have also demonstrated that for studies of certain NRs and their regulation in liver, their cellular localization should be taken into account, allowing proper interpretation of metabolic changes which are directly related to their intra-cellular expression level [20]. Therefore, a systematic assessment of NR distribution in liver is necessary in order to determine their distinctive contributions in parenchymal, endothelial, and Kupffer cells.

To our knowledge, there has been no study illustrating the full expression pattern of 48 NRs in different liver cell types. In the current study, mouse liver parenchymal and non-parenchymal cells were isolated using counter-flow centrifugal elutriation, and gene expression profiling of NRs in parenchymal, endothelial, and Kupffer cells was performed to compose the hepatic expression pattern. NRs with abundant expression in non-parenchymal cells were identified as novel targets for pharmaceutical interventions in the liver.

MATERIALS AND METHODS

Animals

Female C57BL/6 mice over 8 weeks old were fed on regular chow diet containing 4.3% (w/w) fat without supplemented cholesterol (RM3, Special Diet Services, Witham, UK) for 8 weeks. Animal care and procedures were performed in accordance with the national guidelines for animal experimentation. All protocols were approved by the Ethics Committee for Animal Experiments of Leiden University.

Parenchymal and non-parenchymal cell isolation

Liver cells were isolated from mice at the same time of the day (10-11 AM). Mice were anesthetized, liver tissue was dissociated, and parenchymal cells were isolated after collagenase perfusion, while non-parenchymal cells were collected as described previously [21].

Endothelial and kupffer cell separation

The endothelial cells and Kupffer cells were further separated by counter-flow centrifugal elutriation which consists of a J2-MC centrifuge (Beckman, California, USA) connected with a peristaltic pump (LKB, Bromma, Sweden). The elutriation was performed at 4°C at a speed of 3250 RPM. Endothelial and Kupffer cells were separated at flow rate of 25 mL/min and 70 mL/min respectively.

RNA isolation and gene expression analysis

Total RNA was isolated using acid guanidinium thiocyanate (GTC)-phenol-chloroform extraction. Quantitative real-time PCR was carried out using ABI Prism 7700 Sequence Detection system (Applied Biosystems, CA, USA) according to the manufacturer's instructions. Beta-actin was used as an internal housekeeping gene. The primer sequences for all NRs assessed in the current study were obtained from literature [22] and available on the NURSA website at www.nursa.org. The relative expression of each NR was calculated as $\Delta\Delta Ct=(Ct_{Beta\text{-}actin} - Ct_{NR})$. The numerical fold changes were calculated and the amount of target mRNA relative to

housekeeping genes was expressed as $2^{-(\Delta\Delta Ct)}$. Relative expression mean and standard error of the mean (SEM) were calculated using ΔΔCt formula.

Statistical analysis
Statistical analyses were performed using ANOVA for independent samples after confirmation of gaussion distribution using the test of Golmogorov and Smirnov (Instat GraphPad software, San Diego, USA). Statistical significance was defined as $P<0.05$. Data are expressed as means±SEM.

RESULTS

Expression of NRs in liver
Real-time quantitative PCR was performed to analyze the relative mRNA expression of 48 NRs in mouse liver. The expression profile revealed that 36 (75%) of the 48 NRs were expressed in liver, while the other 12 NRs were undetectable (Ct>34), including DAX, ERbeta, ERRbeta, HNF4gamma, NOR1, NURR1, PNR, PR, RORbeta, SF-1, TLX, and VDR. FXRalpha was identified as the most abundantly expressed NR in liver. The 10 most highly expressed NRs in liver were ranked in the following order: FXRalpha > COUP-TF3 > HNF4alpha > LXRalpha > CAR > LXRbeta > RXRalpha > SHP > PXR > NGFIB (Fig. 1A). There were 15 NRs expressed at a moderate level, including PPARalpha > RORgamma > COUP-TF2 > REV-ERBalpha > LRH-1 > RXRbeta > RXRgamma > AR > ERRalpha > RORalpha > REV-ERBbeta > GR > TR4> ERalpha > PPARgamma (Fig. 1B). Interestingly, the second most highly expressed NR in the liver was the orphan receptor COUP-TF3, with mRNA level slightly higher than HNF4alpha and LXRalpha. Another member from this orphan receptor family, COUP-TF2, was moderately expressed in liver, with expression level similar to LRH-1 but 3.5-fold higher than PPARgamma. Expression of COUP-TF1 in liver was very low, approximately 40-fold lower than that of COUP-TF2.

Expression of NRs in liver parenchymal, endothelial, and Kupffer cells
To generate cell type-specific expression patterns of NRs in liver, parenchymal, endothelial, and Kupffer cells were isolated using centrifugal elutriation. The cell separation was confirmed by real-time quantitative PCR characterization of specific gene markers. Expression of parenchymal cell marker CYP7A1 was detected only in parenchymal cell fraction (Fig. 2A), indicating the success of parenchymal cell separation and no contamination of parenchymal cells in non-parenchymal cell fractions. Similarly, expression of endothelial cell marker PECAM-1 (Fig. 2B) and macrophage marker CD68 (Fig. 2C) were only detected in non-parenchymal cell fractions and significantly higher in endothelial ($p<0.001$) or Kupffer ($p<0.01$) cell fraction respectively, indicating the purity of endothelial and Kupffer cell separation.

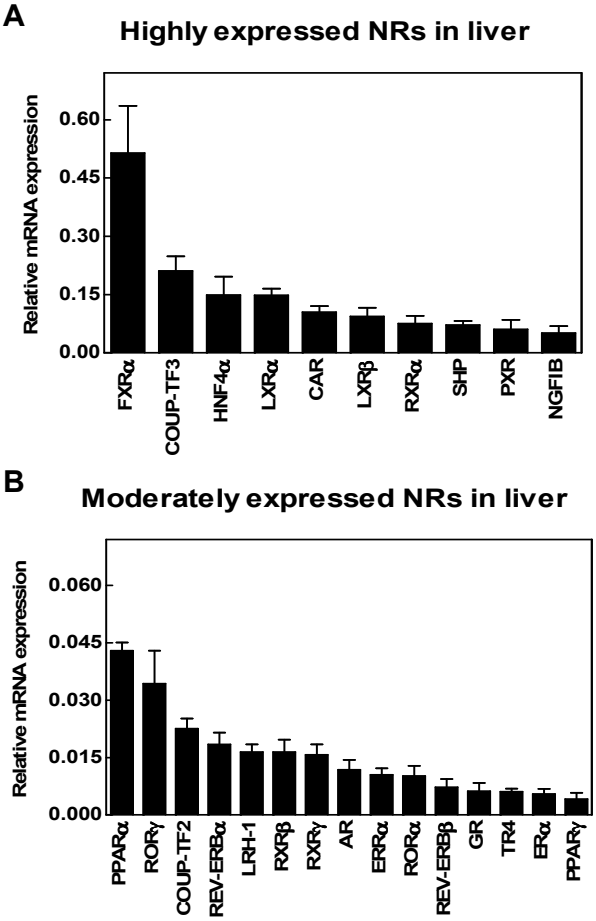

Fig. 1. Expression of NRs in liver. Relative mRNA expression levels of 10 most highly expressed NRs (A) and 15 moderately expressed NRs (B) in total liver, as determined by real time quantitative PCR in C57BL/6 mice and ranked in decreasing order according to gene expression levels. Gene expression data are presented as fold change compared to beta-actin. Values are means ± SEM (N=6).

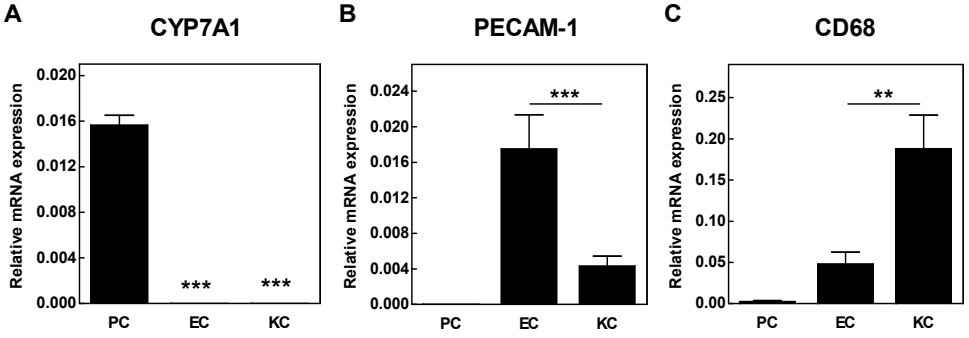

Fig. 2. Expression of cell markers in isolated cell fractions. Relative mRNA expression levels of liver parenchymal cell marker CYP7A1 (A), endothelial cell marker PECAM-1 (B), and Kupffer cell marker CD68 (C) as determined by quantitative PCR in isolated liver parenchymal cell (PC), endothelial cell (EC), and Kupffer cell (KC) fractions. Values are means ± SEM (N=6). **P<0.01, ***P<0.001.

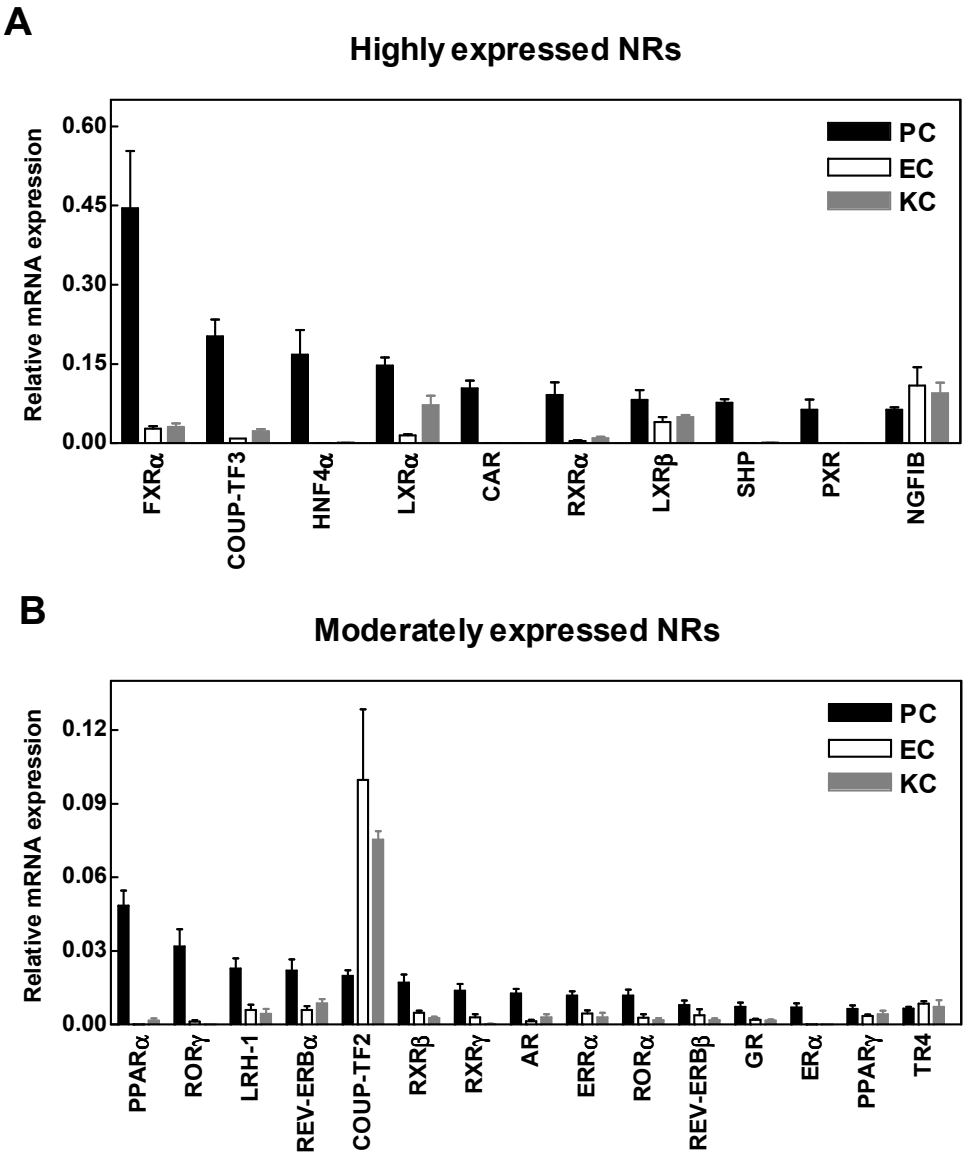

Fig. 3. Expression of NRs in parenchymal and non-parenchymal cells. Expression profile of 10 most highly expressed NRs (A) and 15 moderately expressed NRs (B) in liver parenchymal cells (PC), endothelial cells (EC), and Kupffer cells (KC), as determined by quantitative PCR and ranked in decreasing order according to gene expression levels in PC.

The hepatic expression pattern of 48 NRs in parenchymal, endothelial, and Kupffer cells was generated by real-time quantitative PCR. Among the 36 NRs expressed in liver, 33 (92%) of them were expressed in parenchymal cells. The same 10 NRs were most highly expressed in parenchymal cells as those in whole liver (Fig. 3A). The 15 NRs moderately expressed in parenchymal cells were

shown in Fig. 3B. In non-parenchymal cells, 29 (78%) of the liver-expressed NRs were detected. NGFIB, COUP-TF2, LXRalpha, LXRbeta, FXRalpha, and COUP-TF3 were identified as the most abundantly expressed NRs in both endothelial and Kupffer cells.

Comparison of NR expression in liver parenchymal and non-parenchymal cells

To further characterize the potential relationship between NRs, the liver-expressed NRs were grouped into three clusters according to the substantial differences in their distribution patterns over parenchymal and non-parenchymal cells.

Twenty NRs showed dominant expression in parenchymal cells. HNF4alpha, CAR, SHP, PXR, PPARalpha, RORgamma, ERalpha, and TRbeta were exclusively expressed in parenchymal cells. FXRalpha, COUP-TF3, and RXRalpha showed significantly dominant expression in parenchymal cells, which was 20- to 10-fold higher than in non-parenchymal cells ($p<0.001$). LRH-1, REV-ERBalpha, RXRbeta, RXRgamma, AR, ERRalpha, RORalpha, GR, and TR2 showed an averagely 5-fold higher expression in parenchymal than in endothelial and Kupffer cells ($p<0.01$).

Expression of four NRs, including COUP-TF1, COUP-TF2, RARalpha, and RARbeta, was low in parenchymal cells but significantly higher in non-parenchymal cells, namely in both endothelial and Kupffer cells. In contrast to the exclusive expression of COUP-TF3 in parenchymal cells, COUP-TF1 was exclusively expressed in endothelial and Kupffer cells. COUP-TF2 showed approximately 5-fold higher expression in non-parenchymal cells than in parenchymal cells (Fig. 4A).

In contrast to NRs discussed above which were mainly characterized by significantly high expression in either parenchymal or non-parenchymal cells, five NRs were observed as ubiquitously expressed in all three cell types, including LXRbeta and NGFIB which were highly expressed in the liver, and REV-ERBbeta, PPARgamma, and TR4 which were moderately expressed. For these five NRs, there was no significant difference in expression level in parenchymal, endothelial, and Kupffer cells. Total expression of LXRbeta in liver was 2-fold lower than LXRalpha. However, expression of LXRbeta was comparable to LXRalpha in Kupffer cells and 3-fold higher than LXRalpha in endothelial cells (Fig. 4B).

Interestingly, two orphan receptors which were not highly expressed in whole liver showed considerable expression in non-parenchymal cells. The expression of COUP-TF2 in endothelial and Kupffer cells was similar to that of NGFIB (Fig. 4C), despite a 3-fold lower total expression in liver than NGFIB. In addition, TR4 was 2-fold higher expressed in endothelial and Kupffer cells than PPARgamma (Fig. 4D), although the total expression of TR4 in liver was slightly lower than PPARgamma.

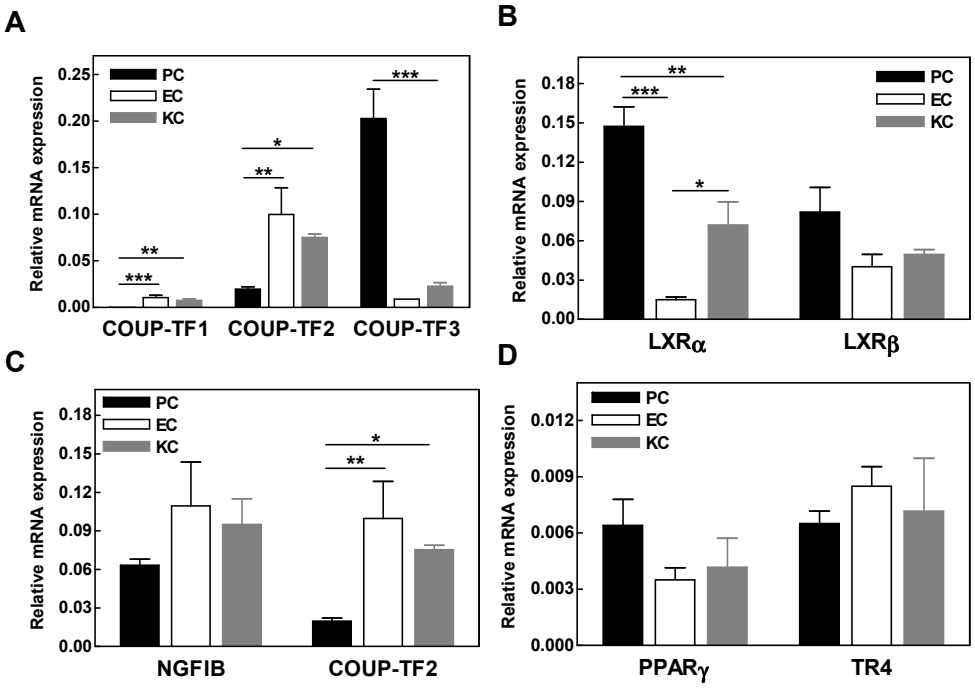

Fig. 4. Relative mRNA expression levels of COUP-TFs (A), LXRs (B), NGFIB versus COUP-TF2 (C), and PPARgamma versus TR4 (D) in liver parenchymal cells (PC), endothelial cells (EC), and Kupffer cells (KC). Values are means ± SEM (N=6). *P<0.05, **P<0.01, ***P<0.001.

DISCUSSION

Real-time quantitative PCR is a standardized method in the NR field to characterize the expression pattern of individual receptors in tissue or cells. It provides a simple but powerful way to obtain comprehensive understanding of the distribution and relational biological functions of NRs [23]. Real-time quantitative PCR has been applied in numerous studies to profile the expression pattern of NRs in tissues representing diverse anatomical systems under various pharmacological conditions and genotypes [24,25]. However, there has been no study establishing NR expression pattern in different liver cell types. Liver is a highly differentiated organ which composes of parenchymal cells and non-parenchymal cells. They play independent but also co-operative roles in health and disease. Thus, separation of liver cells are essential to discover the pharmacological potential of cell type-specific NRs. In the current study, mouse liver parenchymal, endothelial, and Kupffer cells were isolated using counter-flow centrifugal elutriation. This separation method has been confirmed as an ideal gentle process to isolate parenchymal and non-parenchymal cells with high purity and maintained cell function [26]. In the following sections, discussion focuses on NRs expressed at high to moderate levels in the liver, assuming that high mRNA levels are likely to be more relevant for NR function. Majority of the abundantly expressed NRs in liver are expressed dominantly in parenchymal cells, with exception of LXRbeta, NGFIB,

COUP-TF2, and TR4.

LXRalpha has emerged as an important drug target for metabolic regulation of cholesterol efflux based upon its high expression in macrophages. The present study showed that LXRalpha and LXRbeta are both abundant in total liver and liver macrophages, which is in accordance with published data implying similar efficacy of the two LXR subtypes in stimulating macrophage cholesterol efflux [27]. In addition, our observation that LXRbeta is 2-fold lower expressed in parenchymal cells compared to LXRalpha supports the hypothesis that LXRalpha is the primary isotype responsible for the undesirable effects of LXR pan-agonists via activating SREBP-1c in parenchymal cells [28], and LXRbeta-specific agonists may preferentially activate macrophage cholesterol efflux without or to a lesser extent causing adverse hypertriglyceridemia.

NGFIB, also known as Nur77, is highly and ubiquitously expressed in parenchymal and non-parenchymal cells. It has been revealed that NGFIB is highly expressed in vascular endothelial cells and plays a role in angiogenesis and vascular inflammation by negatively regulating endothelial cell activation [29]. Meanwhile, NGFIB regulates lipid metabolism and the inflammatory response in macrophages [30]. The ubiquitously high expression of NGFIB over different liver cell types supports further investigation of NGFIB in both hepatic lipid metabolic process and vascular modulation in multiple tissues.

Interestingly, members of the orphan receptor family COUP-TFs showed distinguished distributions in liver. COUP-TF3 was abundantly and exclusively expressed in liver parenchymal cells, while the other two members, COUP-TF1 and COUP-TF2, were expressed exclusively in non-parenchymal cells. Despite the moderate to high expression level in the liver, the physiological functions of COUP-TFs have not been fully exploited, and the ligand for COUP-TFs has not been identified. Our data suggest the physiologic importance of COUP-TF3 in hepatocytes, and that of COUP-TF2 in endothelial cells and macrophages. Previous studies have shown that the activity of COUP-TFs is associated with the transcriptional regulations of a number of genes expressed mainly in the liver [31]. COUP-TF2 and COUP-TF3 have been generally considered to be repressors or regulators for transcription of NRs such as RARs, TRs, PPARs, and HNF4alpha [32]. Distribution pattern from the present study further suggests that COUP-TF3, given its high expression in liver parenchymal cells, may have a potential role in hepatic lipid and xenobiotic metabolism regulation via cross-talking with other liver-enriched NRs. Our study identifies COUP-TF2 as highly expressed in endothelial cells, which is in accordance with published data upon the role of COUP-TF2 in angiogenesis and generation of haematopoietic cell clusters [33]. In addition, COUP-TF2 was shown to have a potential role in regulation of cholesterol homeostasis [34]. The observation from current study that expression of COUP-TF2 is as high as NGFIB in Kupffer cells raises interest to further investigate whether COUP-TF2 is involved, similarly as NGFIB, in lipid metabolism in macrophages.

TR4 is also an orphan receptor. Similarly as COUP-TFs, TR4 employs repression and gene-silencing events to control basal activities or hormonal responsiveness of numerous target genes [35]. TR4 is ubiquitously expressed in the liver at a comparable level as PPARgamma, with a 2-fold higher expression in Kupffer cells compared to PPARgamma. This suggests that TR4 may function as a lipid sensor as PPARgamma. Recently published data have revealed an important

signaling pathway where TR4 modulates CD36 expression in macrophages and controls CD36-mediated foam cell formation [36]. CD36 is a target gene of PPARgamma. Given the comparable expression patterns of TR4 and PPARgamma, it is of interest to investigate the potential regulatory cross-talk between these two NRs in liver and macrophages.

In conclusion, we composed the cell type-specific expression pattern of 48 NRs in mouse liver parenchymal, endothelial, and Kupffer cells. Our study provides the most complete quantitative assessment of NR distribution in the liver reported to date. The results may give a predictive indication for further investigation. It is suggested that certain orphan NRs such as COUP-TF2, COUP-TF3, and TR4 which are highly expressed in a specific liver cell type may be of significant importance in hepatic function and metabolism. Further investigation into the biology of these receptors will be necessary to understand the functional implication of their hepatic expression patterns. Ultimately, cell-specific targeting systems have been developed for liver [37,38], and the identification of hepatic cell-specific NRs may lead to the development of cell-specific therapeutic molecules to reduce off-target side-effects.

ACKNOWLEDGEMENTS

This work was supported by TIPharma Grant T2-110 (Z.L., T.J.C.V.B., M.H.) and Netherlands Heart Foundation Grant 2008T070 (M.H.).

REFERENCES

1. Karpen SJ (2002) Nuclear receptor regulation of hepatic function. J Hepatol 36:832-850.
2. Di Masi A, Marinis ED, Ascenzi P, Marino M (2009) Nuclear receptors CAR and PXR: Molecular, functional, and biomedical aspects. Mol Aspects Med 30:297-343.
3. Hong C, Tontonoz P (2008) Coordination of inflammation and metabolism by PPAR and LXR nuclear receptors. Curr Opin Genet Dev 18:461-467.
4. Wisse E (1970). An electron microscopic study of the fenestrated endothelial lining of rat liver sinusoids. J Ultrastruct Res 31:125-150.
5. Smedsrød B, De Bleser PJ, Braet F, Lovisetti P, Vanderkerken K, et al. (1994) Cell biology of liver endothelial and Kupffer cells. Gut 35:1509-1516.
6. Bouwens L, Baekeland M, De Zanger R, Wisse E (1986) Quantitation, tissue distribution and proliferation kinetics of Kupffer cells in normal rat liver. Hepatology 6:718-722.
7. Van Berkel TJ, Kruijt JK, Koster JF (1975) Identity and activities of lysosomal enzymes in parenchymal and non-parenchymal cells from rat liver. Eur J Biochem 58:145-152.
8. Munthe-Kaas AC, Berg T, Seljelid R (1976) Distribution of lysosomal enzymes in different types of rat liver cells. Exp Cell Res 99:146-154.
9. Mottino AD, Catania VA (2008) Hepatic drug transporters and nuclear receptors: regulation by therapeutic agents. World J Gastroenterol 14:7068-7074.
10. Karpen SJ, Trauner M (2010) The new therapeutic frontier--nuclear receptors and the liver. J Hepatol 52:455-462.
11. Kolios G, Valatas V, Kouroumalis E (2006) Role of Kupffer cells in the pathogenesis of liver disease. World J Gastroenterol 12:7413-7420.
12. Van Berkel TJ, Nagelkerke JF, Harkes L, Kruijt JK (1982) Processing of acetylated human low-density lipoprotein by parenchymal and non-parenchymal liver cells. Involvement of calmodulin? Biochem J 208:493-503.
13. Nagelkerke JF, Havekes L, van Hinsbergh VW, van Berkel TJ (1984) In vivo catabolism of biologically modified LDL. Arteriosclerosis 4:256-264.
14. Nenseter MS, Gudmundsen O, Roos N, Maelandsmo G, Drevon CA, et al. (1992) Role of liver endothelial and Kupffer cells in clearing low density lipoprotein from blood in hypercholesterolemic rabbits. J Lipid Res 33:867-877.
15. Huang W, Metlakunta A, Dedousis N, Zhang P, Sipula I, et al. (2010) Depletion of liver Kupffer cells prevents the development of diet-induced hepatic steatosis and insulin resistance. Diabetes 59:347-357.
16. Bieghs V, Wouters K, Van Gorp PJ, Gijbels MJ, De Winther MP, et al. (2010) Role of scavenger receptor A and CD36 in diet-induced nonalcoholic steatohepatitis in hyperlipidemic mice. Gastroenterology 138:2477-2486.
17. Kuiper J, De Rijke YB, Zijlstra FJ, Van Waas MP, Van Berkel TJ (1988) The induction of glycogenolysis in the perfused liver by platelet activating factor is mediated by prostaglandin D2 from Kupffer cells. Biochem Biophys Res Commun 157:1288-1295.
18. Stienstra R, Saudale F, Duval C, Keshtkar S, Groener JE, et al. (2010) Kupffer cells promote hepatic steatosis via interleukin-1beta-dependent suppression of peroxisome proliferator-activated receptor alpha activity. Hepatology 51:511-522.
19. Ohata M, Yamauchi M, Takeda K, Toda G, Kamimura S, et al. (2000) RAR and RXR expression by Kupffer cells. Exp Mol Pathol 68:13-20.
20. Hoekstra M, Kruijt JK, Van Eck M, Van Berkel TJ (2003) Specific gene expression of ATP-binding cassette transporters and nuclear hormone receptors in rat liver parenchymal, endothelial, and Kupffer cells. J Biol Chem 278:25448-25453.
21. Hoekstra M, Li Z, Kruijt JK, Van Eck M, Van Berkel TJ, et al. (2010) The expression level of non-alcoholic fatty liver disease-related gene PNPLA3 in hepatocytes is highly influenced by hepatic lipid status. J Hepatol 52:244-251.
22. Fu M, Sun T, Bookout AL, Downes M, Yu RT, et al. (2005) A Nuclear Receptor Atlas: 3T3-L1 adipogenesis. Mol Endocrinol 19:2437-2450.
23. Bookout AL, Mangelsdorf DJ (2003) Quantitative real-time PCR protocol for analysis of nuclear receptor signaling pathways. Nucl Recept Signal 1:e012.
24. Bookout AL, Jeong Y, Downes M, Yu RT, Evans RM, et al. (2006) Anatomical profiling of nuclear receptor expression reveals a hierarchical transcriptional network. Cell 126:789-799.
25. Yang X, Downes M, Yu RT, Bookout AL, He W, et al. (2006) Nuclear receptor expression links the circadian clock to metabolism. Cell 126:801-810.

26. Nagelkerke JF, Barto KP, van Berkel TJ (1983) In vivo and in vitro uptake and degradation of acetylated low density lipoprotein by rat liver endothelial, Kupffer, and parenchymal cells. J Biol Chem 258:12221-12227.
27. Quinet EM, Savio DA, Halpern AR, Chen L, Schuster GU, et al. (2006) Liver X receptor (LXR)-beta regulation in LXRalpha-deficient mice: implications for therapeutic targeting. Mol Pharmacol 70:1340-1349.
28. Scott J (2007) The liver X receptor and atherosclerosis. N Engl J Med 357:2195-2197.
29. You B, Jiang YY, Chen S, Yan G, Sun J (2009) The orphan nuclear receptor Nur77 suppresses endothelial cell activation through induction of IkappaBalpha expression. Circ Res 104:742-749.
30. Bonta PI, van Tiel CM, Vos M, Pols TW, van Thienen JV, et al. (2006) Nuclear receptors Nur77, Nurr1, and NOR-1 expressed in atherosclerotic lesion macrophages reduce lipid loading and inflammatory responses. Arterioscler Thromb Vasc Biol 26:2288-2294.
31. Lazennec G, Kern L, Valotaire Y, Salbert G (1997) The nuclear orphan receptors COUP-TF and ARP-1 positively regulate the trout estrogen receptor gene through enhancing autoregulation. Mol Cell Biol 17:5053-5066.
32. Park JI, Tsai SY, Tsai MJ (2003) Molecular mechanism of chicken ovalbumin upstream promoter-transcription factor (COUP-TF) actions. Keio J Med 52:174-181.
33. You LR, Lin FJ, Lee CT, DeMayo FJ, Tsai MJ, et al. (2005) Suppression of Notch signaling. by the COUP-TFII transcription factor regulates vein identity. Nature 435:98-104.
34. Stephen A. Myers, S.-C. Mary Wang, George E.O.Muscat (2006) The chicken ovalbumin upstream promoter-transcription factors modulate genes and pathways involved in skeletal muscle cell metabolism. J Biol Chem 281:24149-24160.
35. Zhang Y, Dufau ML (2004) Gene silencing by nuclear orphan receptors. Vitam Horm 68:1-48.
36. Xie S, Lee YF, Kim E, Chen LM, Ni J, et al. (2009) TR4 nuclear receptor functions as a fatty acid sensor to modulate CD36 expression and foam cell formation. Proc Natl Acad Sci USA 106:13353-13358.
37. Biessen EA, Vietsch H, Rump ET, Fluiter K, Kuiper J, et al. (1999) Targeted delivery of oligodeoxynucleotides to parenchymal liver cells in vivo. Biochem J 340:783-792.
38. Rensen PC, Gras JC, Lindfors EK, van Dijk KW, Jukema JW, et al. (2006) Selective targeting of liposomes to macrophages using a ligand with high affinity for the macrophage scavenger receptor class A. Curr Drug Discov Technol 3:135-144.

Chapter 3

The expression level of non-alcoholic fatty liver disease-related gene PNPLA3 in hepatocytes is highly influenced by hepatic lipid status

Menno Hoekstra, Zhaosha Li, J. Kar Kruijt, Miranda Van Eck, Theo J.C. Van Berkel, Johan Kuiper

Division of Biopharmaceutics, Leiden/Amsterdam Center for Drug Research, Leiden University, The Netherlands

J Hepatol. 2010;52:244-251

ABSTRACT

Background & Aims: Recent studies have suggested that variations in PNPLA3 are associated with non-alcoholic fatty liver disease (NAFLD). To gain insight in the potential function of PNPLA3 in liver, we have determined the effect of metabolic shifts on the hepatic expression profile of PNPLA3 in mice.
Methods and Results: PNPLA3 expression in wild-type C57BL/6 and NAFLD-susceptible LDL receptor knockout (LDLR-/-) mice was determined using microarray and real-time PCR analysis. PNPLA3 expression in livers is 50- to 100-fold lower as compared to (cardiac) muscle and adipose tissue in regular chow diet-fed mice. Feeding a Western-type diet stimulated the hepatic relative PNPLA3 expression level 23-fold ($P<0.001$) both in C57BL/6 mice and LDLR-/- mice, suggesting that PNPLA3 does become an important player in hepatic lipid metabolism under conditions of lipid excess. Subjecting mice to fasting fully reversed the effect of the Western-type diet on hepatic PNPLA3 expression. Under these conditions, also the expression level of PNPLA3 in adipose tissue is 90% decreased ($P<0.001$). Cellular distribution analysis revealed that PNPLA3 is expressed in hepatocytes, but not liver endothelial and Kupffer cells. Microarray-based gene profiling showed that the expression level of PNPLA3 in hepatocytes is correlated to that of genes associated with the lipogenic pathway such as ME1, SPOT14, and SCD1.
Conclusions: It appears that the NAFLD-related gene PNPLA3 is highly responsive to metabolic changes in hepatocytes within the liver and its relative change in expression level suggests an essential function in lipogenesis.
Keywords: Liver, PNPLA3, mice, hepatocytes, gene expression, lipogenesis, NAFLD

INTRODUCTION

Atherosclerosis is the primary cause of cardiovascular diseases such as ischemic (coronary) heart disease, diabetes, and myocardial infarction, which form the major cause of mortality and morbidity in the Western world. Although atherosclerosis is a progressive disease of the arteries, recent studies have indicated that the occurrence of non-alcoholic fatty liver disease (NAFLD) is also a strong risk factor for atherosclerotic lesion development in humans [1,2].

NAFLD is characterized by the accumulation of lipid in liver cells (hepatic steatosis) and is the most common cause of liver disease with a prevalence of 15-25% in the general population [3-5]. The intra-hepatic lipid balance is maintained by different processes including receptor-mediated uptake of lipids from the blood, hepatic degradation of lipids, de novo synthesis of lipids, secretion of lipids into the bile and the blood compartment, and hepatic storage of lipids. Perturbations in the activity of essential mediators functioning in these processes can induce disturbances in the intra-hepatic lipid homeostasis. More specifically, when the input of lipid exceeds the output of lipid from the liver this will induce excessive storage of lipid and thus lead to the development of hepatic steatosis. NAFLD may slowly progress into non-alcoholic steatohepatitis (NASH), which is characterized by excessive liver inflammation. NASH is an established risk factor for the development of end-stage liver disease (i.e. cirrhosis), a condition that can generally only be treated by performing a liver transplantation.

Interestingly, recent genome-wide association studies have suggested that variations in the patatin-like phospholipase domain containing 3 (PNPLA3) gene contribute to differences in hepatic lipid content and the susceptibility to NAFLD [6-8]. PNPLA3, formerly also known as adiponutrin and iPLAε, is predominantly expressed in adipose tissue and is highly responsive to changes in energy balance [9]. It belongs to the patatin-like phospholipase family of proteins that also contains the key protein involved in the hydrolysis of triglycerides to diglycerides in adipocytes, adipose triglyceride lipase (ATGL; PNPLA2). Although PNPLA3 possesses lipase and acylglycerol transacylase activities in adipocytes in vitro [10], the function of PNPLA3 in the liver in vivo remains to be determined. To gain more insight in the potential function of PNPLA3 in liver, in the current study we have determined the effect of metabolic shifts on the hepatic expression profile of PNPLA3 in mice.

MATERIALS AND METHODS

Animals

Wild-type C57BL/6 mice and homozygous LDL receptor knockout (LDLR-/-) mice were obtained from The Jackson Laboratory as mating pairs and bred at the Gorlaeus Laboratories, Leiden, The Netherlands. Mice were maintained on a regular chow diet containing 5.7% (wt/wt) fat and no cholesterol or were fed a semi-synthetic Western-type diet containing 15% (wt/wt) cacao butter and 0.25% (wt/wt) cholesterol (Diet W, Hope Farms, Woerden, The Netherlands). Mice were fed ad libitum or fasted overnight (~16 hours) before whole body perfusion with PBS and subsequent sacrifice. Organs were isolated and immediately frozen in

liquid N_2 and stored at -80°C until RNA extraction. Animal experiments were performed at the Gorlaeus Laboratories of the Leiden/Amsterdam Center for Drug Research in accordance with national laws. All experimental protocols were approved by the Ethics Committee for Animal Experiments of Leiden University.

Hepatic cell separation
Mice were anaesthetized and the vena cava inferior was cannulated. Subsequently, the vena porta was ligated and the liver was perfused for 10 min (14 ml/min) with oxygenated Hanks' buffer pH 7.4, containing HEPES (1.6 g/l). The perfusion was continued for 10 min with Hanks'/HEPES buffer containing 0.05% (w/v) collagenase (type IV, Sigma) and 1 mM $CaCl_2$. Hepatocytes were isolated after mincing the liver in Hanks' buffer containing 0.3% BSA, filtering through nylon gauze and centrifugation for three times 10 min at 50 × g. The pellets consisted of pure (>99%) hepatocytes (PC) as judged by light microscopy. The supernatants were centrifuged for 10 min at 500 × g in order to harvest the non-parenchymal cells. By the modified method as described previously [11], liver endothelial cells (EC) and Kupffer cells (KC) were isolated at 4°C by density-gradient centrifugation and centrifugal elutriation (3250 rev/min at 26 ml/min for endothelial cells and 65 ml/min for Kupffer cells). The purity of the cell preparations was checked by peroxidase staining, which showed that Kupffer and endothelial cells were >80% and >95% pure, respectively.

Serum lipid analyses
Serum concentrations of total cholesterol and triglycerides were determined using enzymatic colorimetric assays (Roche Diagnostics). The cholesterol and triglyceride distribution over the different lipoproteins in serum was analysed by fractionation of 30 µl serum of each mouse using a Superose 6 column (3.2×30 mm, Smart-system, Pharmacia). Total cholesterol and triglyceride content of the effluent was determined using enzymatic colorimetric assays (Roche Diagnostics).

Analysis of gene expression by real-time quantitative PCR
Quantitative gene expression analysis on perfused organs was performed as described [12]. In short, total RNA was isolated according to Chomczynski and Sacchi [13] and reverse transcribed using RevertAid™ reverse transcriptase. Gene expression analysis was performed using real-time SYBR Green technology (Eurogentec). Beta-actin was used as the standard housekeeping gene. Relative gene expression numbers of were calculated by subtracting the threshold cycle number (Ct) of the gene of interest from the Ct of beta-actin and raising 2 to the power of this difference.

Microarray analysis
The Mouse Genome Survey Arrays used in the study contained 33.012 different probes representing 26.514 genes, which included transcripts from the public domain as well as from the Celera library. Total RNA from hepatocytes from LDLR-/- mice fed a regular chow diet or Western-type diet for 2, 4, or 6 weeks ad libitum was isolated according to Chomczynski and Sacchi [13]. Double stranded cDNA was prepared from 2 µg of total RNA. An in vitro transcription (IVT) reaction was used to synthesize 50-100 µg of UTP-digoxigenin-labeled cRNA. Equal amounts of cRNA (10 µg) from 2 pooled RNA samples of 2 mice (total of 4 mice) per time point

was hybridized to Mouse Genome Survey Arrays for 16 hours at 55°C. Subsequently, an alkalic phosphatase-linked digoxigenin antibody was incubated with the array and the phosphatase activity was initiated to start the chemiluminescent signal. The chemiluminescent (cRNA) and fluorescent (spot backgound) signals of the cRNA and standard controls spots were scanned for 5 and 25 seconds using an AB1700 Chemiluminescence Analyzer (Applied Biosystems). Using the software supplied with the AB1700 apparatus, the spot chemiluminescent signal was normalized over the fluorescent signal of the same spot (using the standard control signals) to obtain the normalized signal value that was used for further analysis. In the analysis, the median value of the normalized signal of two independent arrays for each time point was calculated as an indication for the relative gene expression number at that time point. Profile similarity search was performed using a Euclidean distance-based comparison.

Statistical analysis

The significance of differences in relative gene expression numbers between fasted or ad libitum fed mice and between mice on a chow or a Western-type diet was calculated using a two-tailed unpaired Student's t-test on the differences in Ct (Ct β-actin – Ct PNPLA3). The difference in Ct values was tested for normality using Graphpad Instat 3 software (Graphpad Instat Software, San Diego, CA). The significance of differences in serum lipid levels between the different groups of mice was tested using analysis of variance and the Student-Newman-Keuls multicomparison test (Graphpad Instat Software, San Diego, CA). Probability values less than 0.05 were considered significant.

RESULTS

The relative expression level of PNPLA3 in livers from wild-type C57BL/6 mice and low-density lipoprotein receptor knockout (LDLR-/-) mice, an established diet-induced atherosclerosis and NASH mouse model [14,15], under ad libitum feeding conditions was determined to gain insight in the basal role for hepatic PNPLA3. The mRNA expression of PNPLA3 in livers of regular chow-fed C57BL/6 mice and LDLR-/- mice as measured with quantitative real-time PCR was extremely low, since the threshold cycle for the fluorescent signal in the real-time quantitative PCR was rather high (Ct=30-32). In parallel, Baulande et al. showed that PNPLA3 mRNA was virtually undetectable in livers from SWISS mice under ad libitum feeding conditions [16]. As a result, the hepatic expression level of PNPLA3 was 50- to 1000-fold lower as compared to the level of expression detected in (cardiac) muscle, brown and white adipose tissue isolated from LDLR-/- mice (Fig.1), suggesting that PNPLA3 does not play a major role in liver metabolism under basal feeding conditions.

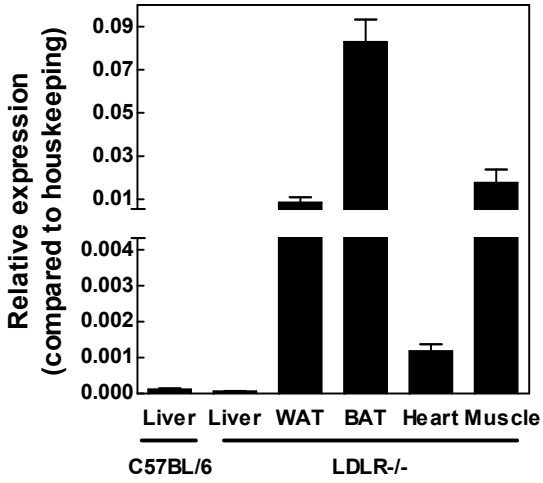

Fig. 1. Relative mRNA levels of PNPLA3 in livers and other metabolic tissues from C57BL/6 wild-type mice and LDL receptor knockout (LDLR-/-) mice fed a regular chow diet. Values represent means+SEM (n=5).

The human association studies suggested that PNPLA3 expression in liver is positively related to obesity and liver fat content [7]. Previously, it has been shown that feeding a Western-type diet containing fat and cholesterol not only stimulates atherosclerotic lesion development, but also induces obesity and fatty liver development in LDLR-/- mice [17]. We therefore determined the effect of Western-type diet feeding on the expression of PNPLA3 in livers of wild-type and LDLR-/- mice. Two weeks of feeding a Western-type diet containing 0.25% 9w/w) cholesterol and 15% (w/w) high fat, which for humans compares to an unhealthy high fat diet [18], induced an increase in plasma total cholesterol and triglyceride levels in C57BL/6 and LDLR-/- mice (Fig.2A). In LDLR-/- mice, the increase in plasma cholesterol could be primarily attributed to a rise in the level of the pro-atherogenic lipoproteins very-low-density lipoprotein (VLDL) and LDL, while in C57BL/6 mice Western-type diet feeding led to an increase in the plasma level of both pro- (VLDL/LDL) and anti-atherogenic high-density lipoproteins (HDL)(Fig.2B). Importantly, an increase in dietary lipid levels was associated with a significant 23-fold stimulation ($P<0.001$) of the relative expression level of PNPLA3 in livers of both C57BL/6 and LDLR-/- mice (Fig.3). The marked induction of its expression upon Western-type diet feeding suggests that PNPLA3 probably does play an important role in hepatic lipid metabolism under conditions of lipid excess. Furthermore, it thus seems that hepatic PNPLA3 levels in mice are positively related to plasma/liver fat content, similarly as observed in the human situation [7].

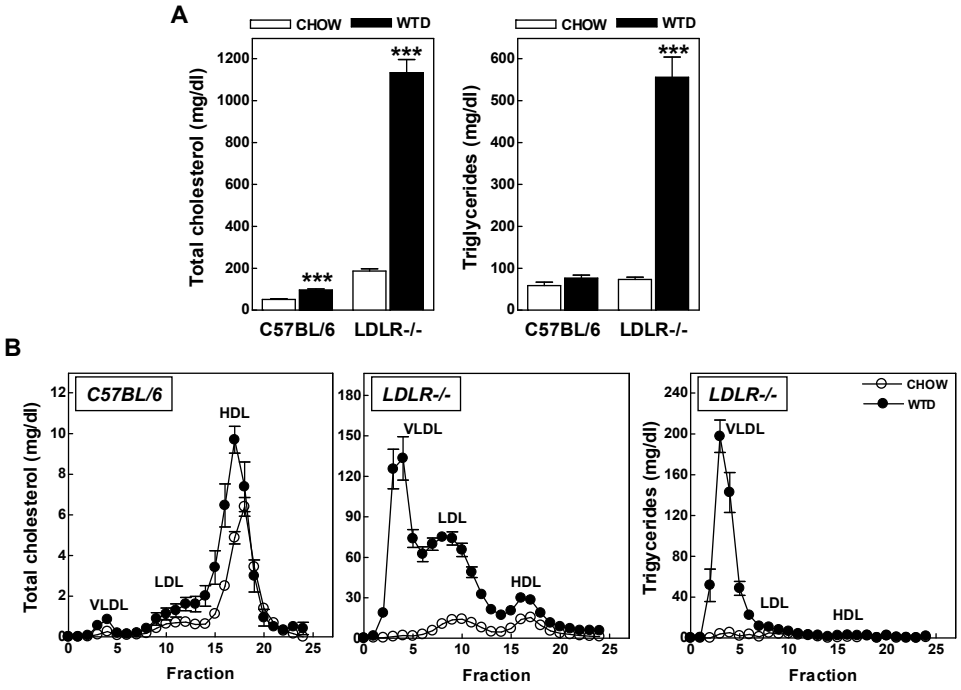

Fig. 2. A) Plasma total cholesterol and triglyceride levels, and B) plasma lipoprotein cholesterol and triglyceride distribution in C57BL/6 wild-type mice and LDL receptor knockout (LDLR-/-) mice fed a chow diet (white bars / open circles) or an atherogenic Western-type diet (WTD; black bars / closed circles) for two weeks. Fractions 2-6 represent VLDL, fractions 7-13 represent LDL, and fractions 14-20 represent HDL, respectively. Values represent means±SEM (n=5). *** P<0.001 compared to chow diet values.

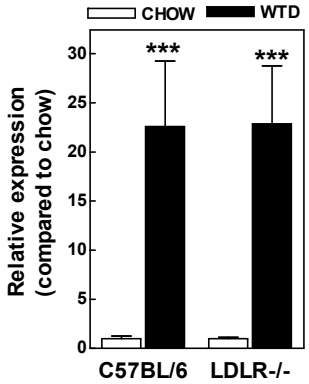

Fig. 3. Relative mRNA levels of PNPLA3 in livers from C57BL/6 wild-type mice and LDL receptor knockout (LDLR-/-) mice fed a chow diet (white bars) or an atherogenic Western-type diet (WTD; black bars) for two weeks. Values are expressed as fold compared to the chow diet and represent means+SEM of 5 mice. *** P<0.001 compared to chow diet values.

In accordance with a possibly important role for PNPLA3 in the protection against tissue lipid excess, several studies have shown that adipose tissue

PNPLA3 levels become virtually undetectable upon food restriction (i.e. external lipid depletion) [16,19,20]. To investigate whether external lipid depletion does also induce changes in hepatic PNPLA3 levels, we determined the effect fasting on PNPLA3 mRNA levels in livers and white adipose tissue of chow-fed (basal conditions) and Western-type diet-fed (lipid excess). Hepatic PNPLA3 expression was decreased by fasting in chow-fed C57BL/6 mice, while it actually increased in chow-fed LDLR-/- mice (Fig.4A). Strikingly, the 23-fold increase in the PNPLA3 expression in liver upon feeding the Western-type diet was completely abolished after a subsequent 16 hour fasting period, resulting in a relative hepatic expression level of PNPLA3 in fasted Western-type diet-fed mice identical to that of chow-fed animals (Fig.4A). As anticipated, fasting induced a ~90% decrease in white adipose tissue PNPLA3 mRNA expression of mice that were fed either the regular chow or the atherogenic Western-type diet (Fig.4B). Combined, these data show that fasting induces a similar response in PNPLA3 expression in fatty liver and white adipose tissue, suggesting that PNPLA3 may have a comparable function in adipose tissue and livers that exhibit an adipocyte-like (i.e. fatty) phenotype.

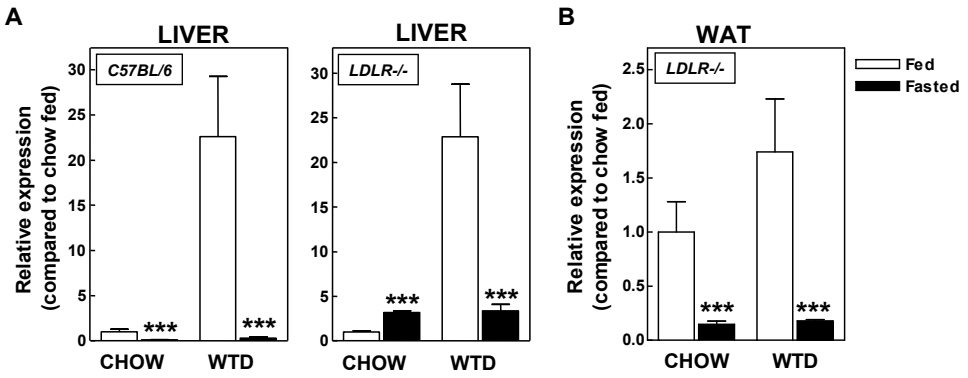

Fig. 4. A) Relative mRNA levels of PNPLA3 in livers from C57BL/6 wild-type mice and/or LDL receptor knockout mice (LDLR-/-) that were fed a chow diet (CHOW) or an atherogenic Western-type diet (WTD) for two weeks ad libitum (Fed) or that were subsequently subjected to 16h of fasting (Fasted). B) Relative mRNA levels of PNPLA3 in white adipose tissues (WAT) from LDLR-/- mice. Values represent means+SEM of 5 mice. *** P<0.001 compared to ad libitum fed values.

The liver consists of several different cell types which each play a distinct role in hepatic metabolism. In earlier experiments we have observed that for studies on the function of genes it is important to take their intra-hepatic cellular localization into account [12,21]. Feeding mice a Western-type diet enriched in cholesterol induces hepatic inflammation [15], ultimately leading to an increased number of macrophages within the liver. To exclude that the rise in hepatic PNPLA3 expression upon Western-type diet feeding could be attributed to an influx of monocytes in response the hepatic inflammation, we examined the relative PNPLA3 expression level in isolated hepatocytes, liver endothelial, and Kupffer cells (tissue macrophages). Importantly, expression of PNPLA3 was detected (although at low levels; Ct=31) in hepatocytes from C57BL/6 mice, while it was absent (Ct>35) in both liver endothelial and Kupffer cells (Fig.5). This suggests that effects measured in total liver PNPLA3 expression actually represent changes in the relative expression of PNPLA3 specifically in hepatocytes.

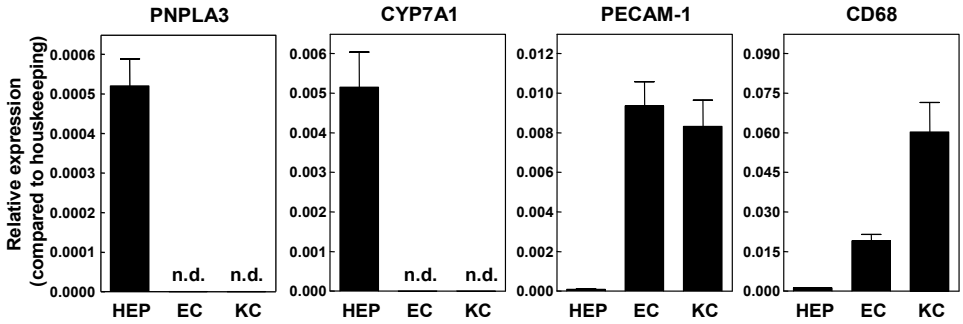

Fig. 5. Relative mRNA levels of PNPLA3 in hepatocytes (HEP), liver endothelial (EC), and Kupffer cells (KC). For comparison, the relative expression levels of the hepatocytes-specific gene cholesterol 7alpha-hydroxylase (CYP7A1), and the respective non-parenchymal and macrophage markers platelet endothelial cell adhesion molecule-1 (PECAM-1) and CD68 are also indicated. Values represent means+SEM of 4-6 different cell isolations. n.d., not detectable.

Previously, we have performed microarray-based gene expression profiling of hepatocytes isolated from livers of LDLR-/- mice to identify genes involved hepatic lipid metabolism specifically under conditions of high lipid pressure [22]. In our original analysis we used a quite stringent signal-to-noise ratio threshold to identify genes as being expressed. Because PNPLA3 did not reach the required signal-to-noise threshold value in normal fed LDLR-/- mice, our primary analysis suggested that PNPLA3 is not expressed in isolated hepatocytes. Re-analysis of our original data-set without the signal-to-noise limitation showed that out of a total of 27.857 transcripts detected PNPLA3 was the most highly upregulated one upon feeding mice the atherogenic Western-type diet. Verification by real-time quantitative PCR showed a very similar expression profile as observed in the microarray with a marked ~50-fold higher PNPLA3 expression in hepatocytes after two weeks of Western-type diet feeding, which remained elevated until the end of the feeding period (6 weeks)(Fig.6A).

To gain insight in the possible role for PNPLA3 in hepatocytes, we performed profile similarity analysis on the microarray data in which we compared the time-dependent expression profile of PNPLA3 to that of all transcripts detected (Fig.6B). In Table 1 the 10 genes whose time-dependent expression profile closely resembled that of PNPLA3 in hepatocytes are shown, including fatty acid binding protein 5 (FABP5), several unassigned FABP5-like proteins, malic enzyme 1 (ME1), stearoyl-CoA desaturase 1 (SCD1), and SPOT14. Interestingly, the expression of glucose-6-phosphate dehydrogenase 2 (G6PD2) and PNPLA3 followed the most similar pattern. As observed for PNPLA3, the expression of G6PD2 was extremely low under basal feeding conditions, while it was markedly induced by the Western-type diet. As a result, the relative expression level of PNPLA3 and G6PD2 in hepatocytes of LDL receptor knockout mice after different times of Western-type diet feeding was significantly correlated (R=0.96; P=0.038; Fig.6C). No expression of G6PD2 was observed in livers of C57BL/6 wild-type mice on a chow or Western-type diet (Ct>35), suggesting that in contrast to in the LDL receptor knockout mice the expression of G6PD2 in C57BL/6 does not reach a detectable level even under conditions of lipid excess. However, real-time PCR profiling of other genes that

were subject to coordinate regulation with PNPLA3 in hepatocytes of LDL receptor knockout mice showed that feeding the Western-type diet led to a significant stimulation of the relative expression level of FABP5 (3.1-fold; P=0.032), ME1 (2.6-fold; P=0.046), SCD1 (5.4-fold; P=0.002), and SPOT14 (3.1-fold; P=0.046) in livers of C57BL/6 wild-type mice (Fig.7). It thus seems that the expression of PNPLA3 in liver of both LDL receptor knockout mice and C57BL/6 wild-type mice is coordinately regulated with that of key lipogenic genes.

Table 1. Ten genes whose time-dependent expression profile was most comparable to that of PNPLA3 in hepatocytes of LDL receptor knockout mice.

Celera ID	Gene Name	Fold change on Western-type diet compared with chow diet		
		2 Weeks	4 Weeks	6 Weeks
mCG121722	Patatin-like phospholipase domain containing 3 (PNPLA3)	47.7	38.0	72.1
mCG50373	Glucose-6-phosphate dehydrogenase 2 (G6PD2)	15.6	10.6	16.8
mCG5289	Fatty acid binding protein (unassigned)	16.6	10.4	11.9
mCG22653	Fatty acid binding protein (unassigned)	16.5	10.6	11.1
mCG16174	PDZK1 interacting protein 1 (PDZK1IP1)	10.2	8.4	11.4
mCG22278	Fatty acid binding protein (unassigned)	19.3	7.4	7.7
mCG9729	Fatty acid binding protein (unassigned)	14.3	9.2	7.2
mCG7050	Thyroid hormone responsive SPOT14 homolog (THRSP)	16.5	8.1	6.9
mCG11880	Malic enzyme 1 (ME1)	8.1	8.4	10.6
mCG131749	Stearoyl-Coenzyme A desaturase 1 (SCD1)	7.3	8.1	10.6
mCG1638	Fatty acid binding protein 5, epidermal (FABP5)	22.3	5.9	5.5

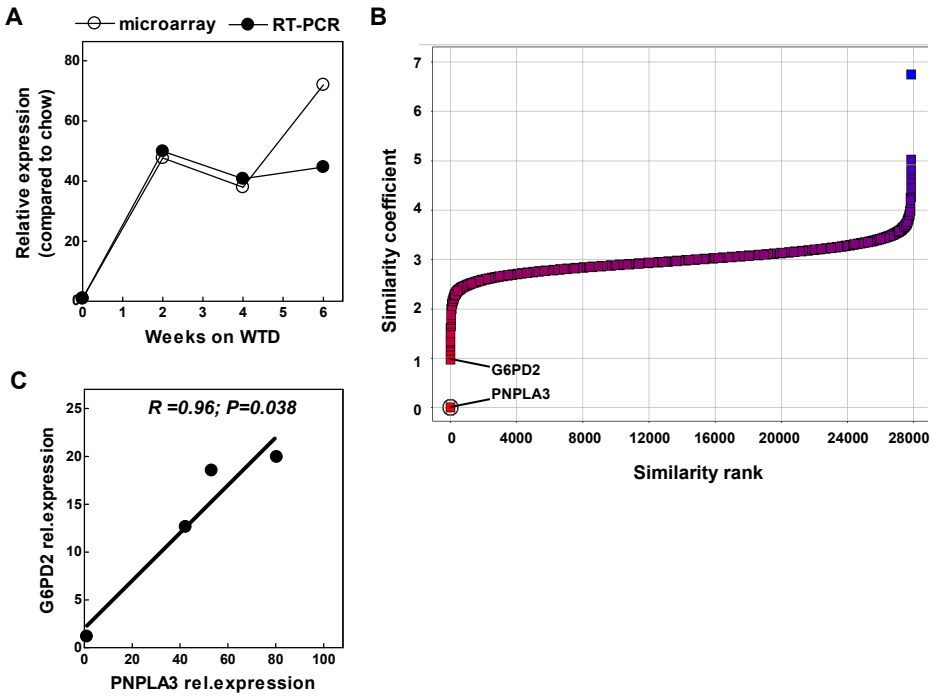

Fig. 6. A) Real-time quantitative PCR validation (closed circles) of the Western-type diet (WTD)-induced changes in the expression of PNPLA3 in hepatocytes from LDL receptor knockout mice, as observed with microarray analysis (open circles). B) Graphical representation of the results from the profile similarity analysis on the 27.857 transcripts present on the microarray. A higher similarity coefficient indicates a lower degree of profile comparison with the input gene PNPLA3. Marked dots represent PNPLA3 and glucose-6-phoshate dehydrogenase 2 (G6PD2), respectively. C) Correlation of the relative mRNA levels of PNPLA3 and G6PD2 in hepatocytes from LDL receptor knockout mice. Values are significantly correlated (P=0.038; R=0.96) and are relative to the expression on chow diet.

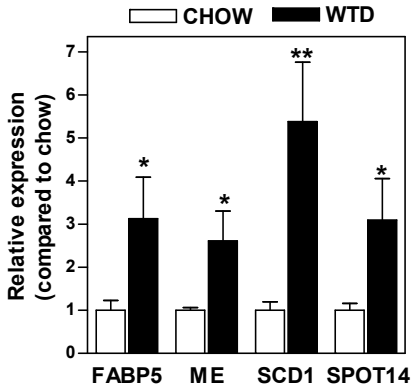

Fig. 7. Relative mRNA levels in livers of C57BL/6 wild-type mice that were fed a chow diet (CHOW) or an atherogenic Western-type diet (WTD) for two weeks ad libitum of genes showing a coordinate regulation with PNPLA3 in hepatocytes of LDL receptor knockout mice. Values represent means+SEM of 5 mice and are relative to the expression on chow diet. * P<0.05 and ** P<0.01 compared to chow diet values.

DISCUSSION

Non-alcoholic fatty liver disease (NAFLD), the presence of hepatic steatosis due to non-alcoholic causes, is a commonly observed phenomenon in Western societies. Although factors such as obesity, diabetes, and insulin resistance promote the accumulation of triglycerides in the liver, it has become clear that genetic variation is also a prominent risk factor for the development of NAFLD. Recent association studies have identified PNPLA3 as a possible important player in liver lipid metabolism as variations in the PNPLA3 gene are linked to an increased susceptibility for NAFLD [6-8]. However, no data are present on the exact role of PNPLA3 within the liver. In the current study, we have shown that PNPLA3 is expressed in the primary metabolic cell type in the liver, namely the hepatocytes, but not in liver endothelial cells or tissue macrophages (Kupffer cells). The relatively low hepatic expression of PNPLA3 upon chow diet feeding argues against a major role for this protein under basal conditions. As PNPLA3 among 27.857 transcripts is the most highly induced gene in hepatocytes upon exposure to exogenous lipid (i.e. upon Western-type diet feeding) we anticipate, however, that it does play a major role in liver under conditions of high lipid exposure.

A microarray profile similarity search indicated that the Western-type diet-induced change in the expression profiles of PNPLA3 and glucose-6-phosphate dehydrogenase (G6PD) type 2 was highly similar in hepatocytes of LDL receptor knockout mice. G6PD is a cytosolic enzyme that takes part in the pentose phosphate pathway. It transforms glucose-6-phosphate into 6-phosphoglucono-δ-lactone and NADP to NADPH that is subsequently used for the biosynthesis of fatty acids, making it a key enzyme involved in the synthesis of triglycerides from glucose (lipogenesis) [23,24]. As the PNPLA3 expression pattern follows that of G6PD2 it is suggested that PNPLA3 may also play an important role in hepatocyte lipogenesis. Importantly, other genes that had a comparable time-dependent expression profile as observed for PNPLA3 in hepatocytes in LDL receptor knockout mice and that are also significantly upregulated in livers of wild-type mice upon feeding a Western-type diet, i.e. SPOT14 and malic enzyme, are also established mediators of lipogenesis [24]. In agreement with a related function for PNPLA3 and G6PD2 in lipid metabolism, they respond similarly to changes in metabolic conditions. Moldes et al. have shown that PNPLA3 expression is significantly stimulated in adipose tissue upon infusion of insulin [25]. In parallel, Kastrouni et al. detected an enhanced activity of G6PD in adipose tissue upon administration of insulin, which is related to an increased transcription rate of the G6PD gene [26]. G6PD expression in liver and brain is significantly decreased upon fasting [27]. In accordance with the functional overlap between G6PD and PNPLA3, in the current study we observed that fasting also significantly diminished the expression level of PNPLA3 in adipose tissue and livers from Western-type diet-fed mice. Combined, these findings suggest that the mRNA expression level of PNPLA3 and G6PD is tightly controlled by the same upstream regulator. The lipogenic transcription factor sterol regulatory element binding protein 1 (SREBP-1) has been identified as a possible regulator of G6PD expression in liver [24,28]. It will therefore be interesting to study whether SREBP can also act as a transcriptional regulator of hepatic PNPLA3 expression.

In conclusion, we have shown that, in mice, the NAFLD-related gene PNPLA3 is expressed in hepatocytes within the liver and that its relative expression level is

highly influenced by the intra-hepatic lipid status. Furthermore, our studies suggest that the function of PNPLA3 in liver is related to lipogenesis.

ACKNOWLEDGEMENTS

This research was supported by Top Institute Pharma (TIPharma project T2-110; M.H. and T.V.B.), by Grant 2008T070 (M.H.) from the Netherlands Heart Foundation, and by VIDI Grant 917.66.301 from the Netherlands Organization for Scientific Research (M.V.E.). M.V.E. is an Established Investigator of the Netherlands Heart Foundation (Grant 2007T056).

REFERENCES

[1] A. Brea, D. Mosquera, E. Martín, A. Arizti, J.L. Cordero and E. Ros, Nonalcoholic fatty liver disease is associated with carotid atherosclerosis: a case-control study, Arterioscler Thromb Vasc Biol 25 (2005), pp. 1045–1050.

[2] G. Targher, L. Bertolini, R. Padovani, F. Poli, L. Scala and L. Zenari et al., Non-alcoholic fatty liver disease is associated with carotid artery wall thickness in diet-controlled type 2 diabetic patients, J Endocrinol Invest 29 (2006), pp. 55–60.

[3] A.J. McCullough, The clinical features, diagnosis and natural history of nonalcoholic fatty liver disease, Clin Liver Dis 8 (2004), pp. 521–533.

[4] G. Marchesini, R. Marzocchi, F. Agostini and E. Bugianesi, Nonalcoholic fatty liver disease and the metabolic syndrome, Curr Opin Lipidol 16 (2005), pp. 421–427.

[5] L.A. Adams and P. Angulo, Recent concepts in non-alcoholic fatty liver disease, Diabet Med 22 (2005), pp. 1129–1133.

[6] S. Romeo, J. Kozlitina, C. Xing, A. Pertsemlidis, D. Cox and L.A. Pennacchio et al., Genetic variation in PNPLA3 confers susceptibility to nonalcoholic fatty liver disease, Nat Genet 40 (2008), pp. 1461–1465.

[7] A. Kotronen, L.E. Johansson, L.M. Johansson, C. Roos, J. Westerbacka and A. Hamsten et al., A common variant in PNPLA3, which encodes adiponutrin, is associated with liver fat content in humans, Diabetologia 52 (2009), pp. 1056–1060.

[8] S. Sookoian, G.O. Castaño, A.L. Burgueño, T. Fernández Gianotti, M.S. Rosselli and C.J. Pirola, A nonsynonymous gene variant in adiponutrin gene is associated with nonalcoholic fatty liver disease severity, J Lipid Res 50 (2009), pp. 2111–2116.

[9] Y.M. Liu, M. Moldes, J.P. Bastard, E. Bruckert, N. Viguerie and B. Hainque et al., Adiponutrin: A new gene regulated by energy balance in human adipose tissue, J Clin Endocrinol Metab 89 (2004), pp. 2684–2689.

[10] C.M. Jenkins, D.J. Mancuso, W. Yan, H.F. Sims, B. Gibson and R.W. Gross, Identification, cloning, expression, and purification of three novel human calcium-independent phospholipase A2 family members possessing triacylglycerol lipase and acylglycerol transacylase activities, J Biol Chem 279 (2004), pp. 48968–48975.

[11] A.G. Van Velzen, R.P. Da Silva, S. Gordon and T.J. Van Berkel, Characterization of a receptor for oxidized low-density lipoproteins on rat Kupffer cells: similarity to macrosialin, Biochem J 322 (1997), pp. 411–415.

[12] M. Hoekstra, J.K. Kruijt, M. Van Eck and T.J. Van Berkel, Specific gene expression of ATP-binding cassette transporters and nuclear hormone receptors in rat liver parenchymal, endothelial, and Kupffer cells, J Biol Chem 278 (2003), pp. 25448–25453.

[13] P. Chomczynski and N. Sacchi, Single-step method of RNA isolation by acid guanidinium thiocyanate–phenol–chloroform extraction, Anal Biochem 162 (1987), pp. 156–159.

[14] S. Ishibashi, J.L. Goldstein, M.S. Brown, J. Herz and D.K. Burns, Massive xanthomatosis and atherosclerosis in cholesterol-fed low density lipoprotein receptor-negative mice, J Clin Invest 93 (1994), pp. 1885–1893.

[15] K. Wouters, P.J. van Gorp, V. Bieghs, M.J. Gijbels, H. Duimel and D. Lütjohann et al., Dietary cholesterol, rather than liver steatosis, leads to hepatic inflammation in hyperlipidemic mouse models of nonalcoholic steatohepatitis, Hepatology 48 (2008), pp. 474–486.

[16] S. Baulande, F. Lasnier, M. Lucas and J. Pairault, Adiponutrin, a transmembrane protein corresponding to a novel dietary- and obesity-linked mRNA specifically expressed in the adipose lineage, J Biol Chem 276 (2001), pp. 33336–33344.

[17] K.R. Coenen and A.H. Hasty, Obesity potentiates development of fatty liver and insulin resistance, but not atherosclerosis, in high-fat diet-fed agouti LDLR-deficient mice, Am J Physiol Endocrinol Metab 293 (2007), pp. E492–E499.

[18] F.M. Sacks, G.A. Bray, V.J. Carey, S.R. Smith, D.H. Ryan and S.D. Anton et al., Comparison of weight-loss diets with different compositions of fat, protein, and carbohydrates, N Engl J Med 360 (2009), pp. 859–873.

[19] G. Wiesner, B.A. Morash, E. Ur and M. Wilkinson, Food restriction regulates adipose-specific cytokines in pituitary gland but not in hypothalamus, J Endocrinol 180 (2004), pp. R1–R6.

[20] F. Bertile and T. Raclot, Differences in mRNA expression of adipocyte-derived factors in response to fasting, refeeding and leptin, Biochim Biophys Acta 1683 (2004), pp. 101–109.

[21] D. Ye, M. Hoekstra, R. Out, I. Meurs, J.K. Kruijt and R.B. Hildebrand et al., Hepatic cell-specific ATP-binding cassette (ABC) transporter profiling identifies putative novel candidates for lipid homeostasis in mice, Atherosclerosis 196 (2008), pp. 650–658.

[22] M. Hoekstra, M. Stitzinger, E.J. van Wanrooij, I.N. Michon, J.K. Kruijt and J. Kamphorst et al., Microarray analysis indicates an important role for FABP5 and putative novel FABPs on a Western-type diet, J Lipid Res 47 (2006), pp. 2198–2207.
[23] J. Park, H.K. Rho, K.H. Kim, S.S. Choe, Y.S. Lee and J.B. Kim, Overexpression of glucose-6-phosphate dehydrogenase is associated with lipid dysregulation and insulin resistance in obesity, Mol Cell Biol 25 (2005), pp. 5146–5157.
[24] H. Shimano, N. Yahagi, M. Amemiya-Kudo, A.H. Hasty, J. Osuga and Y. Tamura et al., Sterol regulatory element-binding protein-1 as a key transcription factor for nutritional induction of lipogenic enzyme genes, J Biol Chem 274 (1999), pp. 35832–35839.
[25] M. Moldes, G. Beauregard, M. Faraj, N. Peretti, P.H. Ducluzeau and M. Laville et al., Adiponutrin gene is regulated by insulin and glucose in human adipose tissue, Eur J Endocrinol 155 (2006), pp. 461–468.
[26] E. Kastrouni, T. Pegiou, P. Gardiki and A. Trakatellis, Activity changes of glucose-6-phosphate dehydrogenase in response to diet and insulin, Int J Biochem 16 (1984), pp. 1353–1358.
[27] V.P. Titanji, J. Ngogang and P. Gouater, The effects of alloxan diabetes, insulin and epinephrine on glucose-6-phosphate dehydrogenase from rat liver and brain, Ups J Med Sci 86 (1981), pp. 33–38.
[28] G.P. Laliotis, I. Bizelis, A. Argyrokastritis and E. Rogdakis, Cloning, characterization and computational analysis of the 5′ regulatory region of ovine glucose 6-phosphate dehydrogenase gene, Comp Biochem Physiol B Biochem Mol Biol 147 (2007), pp. 627–634.

Chapter 4

Niacin reduces plasma CETP levels by diminishing liver macrophage content in CETP transgenic mice

Zhaosha Li[1], Yanan Wang[2], Reeni B. Hildebrand[1], José W.A. van der Hoorn[3], Hans M.G. Princen[3], Miranda Van Eck[1], Theo J.C. Van Berkel[1], Patrick C.N. Rensen[2], Menno Hoekstra[1]

[1]Division of Biopharmaceutics, Leiden/Amsterdam Center for Drug Research, Leiden University, The Netherlands.
[2]Department of General Internal Medicine, Endocrinology, and Metabolic Diseases, Leiden University Medical Center, The Netherlands.
[3]Netherlands Organization for Applied Scientific Research-Metabolic Health Research, Gaubius Laboratory, Leiden, The Netherlands.

Submitted for publication

ABSTRACT

Background & Aims: The anti-dyslipidemic drug niacin has been recently shown to reduce the hepatic expression and plasma levels of CETP. Since liver macrophages contribute to hepatic CETP expression, the aim of the current study was to investigate the role of macrophages in the CETP-lowering effect of niacin in mice.
Methods and Results: *In vitro* studies showed that niacin does not directly attenuate CETP expression in macrophages. Treatment of human CETP transgenic mice, fed with a Western-type diet, with 2% (w/w) niacin for 4 weeks significantly reduced hepatic cholesterol concentration (-20%), hepatic CETP gene expression (-20%), and plasma CETP mass (-30%). Concomitantly, niacin decreased hepatic expression of CD68 (-44%) and ABCG1 (-32%), both of which are specific markers for the hepatic macrophage content. The decrease in hepatic CETP expression was significantly correlated with the reduction of hepatic macrophage content. Furthermore, niacin treatment attenuated atherogenic diet-induced inflammation in liver, as shown in decreased expression of MCP-1 (-32%) and TNFalpha (-43%). Post hoc analysis showed that niacin also decreased the macrophage content in APOE*3-Leiden.CETP transgenic mice on a Western-type diet.
Conclusions: Niacin decreases hepatic CETP expression and plasma CETP mass by attenuating liver inflammation and macrophage content in response to its primary lipid-lowering effect, rather than by attenuating CETP expression in the macrophage.
Keywords: CETP, niacin, macrophages, lipoprotein, liver, inflammation

INTRODUCTION

The anti-dyslipidemic drug niacin, also known as nicotinic acid, lowers plasma levels of pro-atherogenic lipids/lipoproteins, including very-low-density lipoproteins (VLDL) and low-density lipoproteins (LDL) as well as triglycerides (TG). The lipid-lowering effect of niacin has been widely recognized as an action on adipose tissue[1]. Niacin rapidly inhibits intracellular TG lipolysis, reduces the mobilization of free fatty acids (FFA) from adipose tissue to liver, and lowers plasma FFA levels acutely. In addition, niacin reduces hepatic synthesis and secretion of VLDL into the circulation[2]. Concomitantly, niacin increases the level of anti-atherogenic high-density lipoprotein (HDL) in normolipidemic as well as hypercholesterolemic subjects[3]. Several clinical trials have shown that niacin reduces cardiovascular disease and myocardial infarction incidence, providing an emerging rationale for the use of niacin in the treatment of atherosclerosis[4,5].

Recently, we showed that niacin increases HDL by reducing the hepatic expression and plasma levels of the pro-atherogenic cholesteryl ester transfer protein (CETP)[6]. CETP, as a lipid transfer protein, has an established role in cholesterol metabolism[7]. It modifies the arterial intima cholesterol content via altering the concentration and function of plasma lipoproteins. Human population investigations favor low CETP as atheroprotective; this is supported by animal models where overexpression of CETP increased concentration of apoB-lipoprotein-cholesterol[8] and atherosclerosis[9]. We have demonstrated, by using APOE*3-Leiden.CETP versus APOE*3-Leiden mice, that niacin markedly reduces hepatic CETP expression and plasma CETP mass. Since CETP expression is driven by liver X receptor (LXR) activation, the reduction in hepatic CETP expression may be secondary to reduced liver lipid levels. However, the exact mechanism behind the hepatic CETP-lowering effect of niacin is still unresolved.

The liver consists of several different types of cells, including hepatocytes and non-parenchymal cells such as resident macrophages, also known as Kupffer cells. Kupffer cells reside in the sinusoidal space of the liver and represent approximately 80-90% of the body's resident macrophages[10,11]. Kupffer cells are derived from monocytes that arise from bone marrow progenitors and migrate from the circulation[12]. Interestingly, Van Eck *et al*[13] have shown a 47-fold higher expression of CETP mRNA in liver Kupffer cells than in hepatocytes. CETP expression in Kupffer cells contributes approximately 50% to the total hepatic CETP expression, indicating that bone marrow-derived CETP is an important contributor to hepatic CETP expression and plasma CETP mass. As the niacin receptor GPR109A is expressed in macrophages[14,15], it is important to determine whether there is a direct action of niacin on liver macrophages. Therefore, the aim of the current study was to investigate the mechanism underlying the hepatic CETP-lowering effect of niacin in CETP transgenic mice.

MATERIALS AND METHODS

Animals

Female CETP transgenic mice expressing the human CETP transgene under the control of its natural flanking regions (CETP Tg; C57BL/6 background) were used

in the present study. The animals were fed with semi-synthetic Western-type diet (WTD) containing 15% (w/w) fat and 0.25% (w/w) cholesterol (Diet W, Special Diet Services, Witham, UK) for 3 weeks (run-in), after which the diet for the treatment group was supplemented with 2% niacin (Sigma-Aldrich) for 4 weeks, while the control group was continuously fed with WTD. After euthanization, mice were bled via orbital exsanguination, and perfused *in situ* through the left cardiac ventricle with ice-cold PBS (pH 7.4) for 20 minutes. Tissues were dissected and snap-frozen in liquid nitrogen. One lobe of the liver was dissected free of fat and stored in 3.7% neutral-buffered formalin (Formal-fixx, Shandon Scientific Ltd., UK) for histological analysis. Animal care and procedures were performed in accordance with the national guidelines for animal experimentation. All protocols were approved by the Ethics Committee for Animal Experiments of Leiden University.

Culture of bone marrow-derived macrophages

Bone marrow-derived macrophages were obtained from CETP transgenic mice. Single-cell suspensions were harvested as described above. Cell concentration was adjusted to 8 x 10^6 cells/mL, and cells were placed on a non-tissue culture treated Petri dish in RPMI1640 (PAA Laboratories) containing 20% (v/v) fetal calf serum (FCS), 2 mM/L L-glutamine, 100 U/mL penicillin, 100 µg/mL streptomycin, 1% (v/v) non-essential amino acids, 1% (v/v) pyruvate, and 30% (v/v) L929-conditioned media. Cells were cultured in a humidified incubator with 5% CO_2 at 37°C for 7 days. After bone marrow cell differentiation, adherent macrophages were harvested and cultured on 12-well plate in DMEM (PAA Laboratories) containing 10% (v/v) FCS, 2 mM/L L-glutamine, 100 U/mL penicillin, and 100 µg/mL streptomycin at a density of 0.5 x 10^6 cells/mL. After 24 hours, non-adherent cells were removed, and macrophages were incubated in the absence or presence of niacin (Sigma-Aldrich) at a concentration of 0.1 µM, 1 µM, and 10 µM for 24 hours. Total RNA was extracted and gene expression analysis was performed as described above.

Hepatic lipid analysis

Lipid analysis was performed when the animals received 4 weeks of WTD with or without 2% niacin. Mice were fasted overnight prior to euthanization. Lipids were extracted from liver using the Folch method. Briefly, 100 mg of tissue was homogenized with chloroform/methanol (1:2). The homogenate was centrifuged to recover the upper phase, which was further washed with chloroform-0.9% NaCl (1:1, pH 1.0). After centrifugation, the lower chloroform phase containing lipids was evaporated and the retained lipids were resolubilized in 2% Triton X-100 by sonification. Protein contents were analyzed by BCA assay (Pierce Biotechnology, Thermo Fisher Scientific BV, IL, USA). Total cholesterol content of lipid extracts was measured using the enzymatic colorimetric assay with 0.025 U/mL cholesterol oxidase, 0.065 U/mL peroxidase, and 15 µg/mL cholesteryl esterase (Roche Diagnostics, Mannheim, Germany). Data were expressed as milligrams of lipid per milligram of protein.

RNA isolation and gene expression analysis

Total RNA from liver was isolated using acid guanidinium thiocyanate (GTC)-phenol-chloroform extraction. Briefly, 500 µL of GTC solution (4 M guanidine isothiocyanate, 25 mM sodium citrate, 0.5% N-lauroylsarcosine) was added to

each sample, followed by acid phenol:chloroform extraction. The RNA in aqueous phase was precipitated with isopropanol. The quantity and purity of the isolated RNA were examined using ND-1000 Spectrophotometer (Nanodrop, Wilmington, DE, USA). One microgram of the isolated RNA from each sample was converted into cDNA by reverse transcription with RevertAid™ M-MuLV Reverse Transcriptase (Promega, Madison, WI, USA). Negative controls without addition of reverse transcriptase were prepared for each sample. Quantitative real-time PCR was carried out using ABI Prism 7700 Sequence Detection system (Applied Biosystems, Foster City, CA, USA) according to the manufacturer's instructions. 36B4, Beta-actin, and GAPDH were used as internal housekeeping genes. Amplification curves were analyzed using 7500 Fast System SDS software V1.4 (Applied Biosystems, Foster City, CA, USA). The relative expression of each gene was expressed as comparative numerical fold changes $2^{-(\Delta\Delta CT)}$. Standard error of the mean (SEM) and statistical significance were calculated using ΔΔCt formula.

CETP mass determination in plasma
Plasma CETP mass was determined by ELISA, using a commercially available immunoturbidimetry kit (Daiichi Pure Chemicals, Tokyo, Japan) according to the manufacturer's instructions.

Immunohistochemistry
Macrophage content in livers of APOE*3-Leiden.CETP mice treated with or without 1% of niacin6 was analyzed by immunohistochemistry staining. The liver was embedded in O.C.T™ Compound (Tissue-Tek, Sakura finetek, Tokyo, Japan), and subsequently sectioned using a Leica CM 3050S cryostat at 8 µm intervals. After incubation with blocking solution (5% goat serum), macrophages were detected using F4/80 antibody (rat antibody directed against murine macrophages, AbD Serotec, Oxford, UK). A rabbit anti rat IgG/HRP was used as second antibody (Dako, Heverlee, Belgium). Sections were developed using NovaRED Peroxidase Substrate Kit (Vector Laboratories, Peterborough, UK) according to the manufacturer's instructions. Slides were counterstained with hematoxylin (Sigma-Aldrich).

Statistical analysis
Statistical analyses were performed by the unpaired Student's t-test for independent samples (Instat GraphPad software, San Diego, USA). Statistical significance was defined as $p<0.05$. Data are expressed as means ± SEM.

RESULTS

Niacin reduces hepatic lipid content, plasma CETP mass, and hepatic CETP expression
CETP Tg mice were utilized to analyze the effects of niacin on hepatic CETP expression and plasma levels of CETP. Four weeks of niacin treatment significantly reduced hepatic cholesterol concentration by 20% ($p=0.005$, Figure 1). In addition, in line with our previous data[6], niacin treatment resulted in a significant 30% reduction ($p=0.0002$) in plasma CETP mass (Figure 1). In parallel, gene expression of CETP in liver was also significantly reduced by 20% ($p=0.034$, Figure 1).

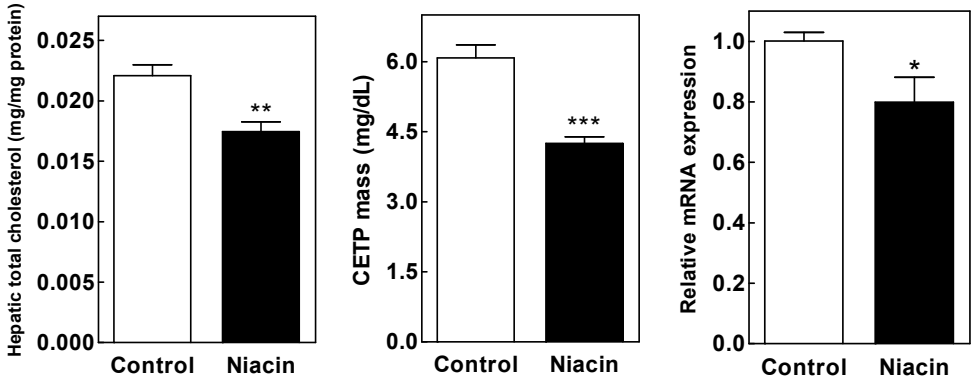

Figure 1. Effect of niacin on hepatic cholesterol concentration, plasma CETP mass, and hepatic CETP expression in CETP Tg mice. After 4 weeks of Western-type diet (WTD) feeding with or without 2% niacin supplement, mice were euthanized and lipids were extracted from liver. Total cholesterol concentration was measured. Plasma CETP mass was determined by ELISA. Total RNA was isolated from liver. Relative mRNA expression of CETP was determined by quantitative PCR and presented as fold-change relative to control group. Values are means ± SEM (6 mice per group). *P<0.05; **P<0.01; ***P<0.001.

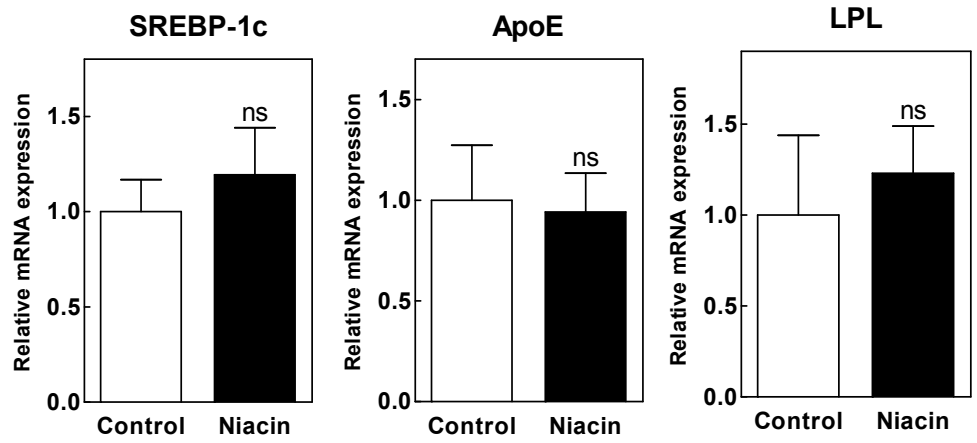

Figure 2. Effect of niacin on LXR-target genes in CETP Tg mice. Total RNA was isolated from liver. Relative mRNA expression of the LXR-target genes SREBP-1c, ApoE, and LPL were determined by quantitative PCR and presented as fold-change relative to control group. Values are means ± SEM (6 mice per group). ns, not significant.

Niacin does not directly regulate LXR activity in the liver

To evaluate whether niacin decreased hepatic CETP expression by attenuating LXR activation, we measured the effect of niacin on the LXR target genes SREPB-1c, ApoE, and LPL. The hepatic expression of these three genes remained unchanged after niacin treatment (Figure 2), indicating that the reduction of hepatic CETP expression was not due to a direct regulation of niacin on LXR.

Niacin does not directly regulate CETP expression in bone marrow-derived macrophages

To assess whether niacin directly attenuates CETP expression in macrophages, bone marrow-derived macrophages isolated from CETP Tg mice were exposed to various concentrations of niacin (0.1 μM, 1 μM, and 10 μM) for 24 hours. Niacin treatment did not alter CETP expression (Figure 3). In addition, niacin did not affect expression of the LXR-regulated targets SREBP-1c or apoE, or the cholesterol metabolism-related genes ABCA1, ABCG1, SR-B1, CD36 (data not shown).

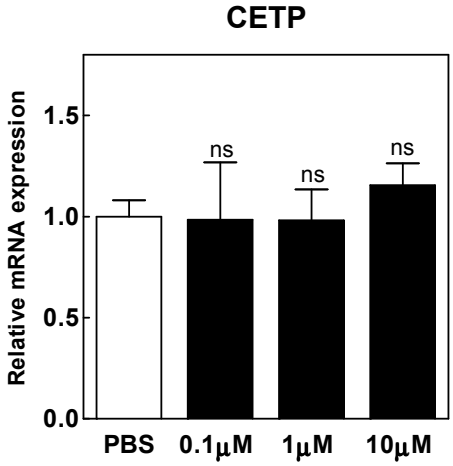

Figure 3. Effect of niacin on CETP expression in bone marrow-derived macrophages from CETP Tg mice. Bone marrow-derived macrophages isolated from CETP Tg mice were incubated in medium in the absence or presence of niacin at a concentration of 0.1 μM, 1 μM, and 10 μM for 24 hours. Total RNA was extracted and CETP mRNA expression was assessed by quantitative PCR and presented as fold-change compared to PBS-control group. Values are presented as means ± SEM (5 independent cell isolations). ns, not significant.

Niacin reduces macrophage content and inflammation in the liver

Since these data indicated that niacin may reduce hepatic CETP expression by reducing the liver macrophage content, we evaluated the effect of niacin on CD68 and ABCG1, both of which have been defined as reliable markers to assess the hepatic macrophage content[16, 17, 18]. Interestingly, niacin treatment significantly decreased hepatic expression of CD68 by 44% (p=0.027) and ABCG1 by 32% (p=0.001) (Figure 4A). In addition, niacin did not affect the CETP/ABCG1 and ABCG1/CD68 expression ratios (Figure 4A). This suggests that niacin does not directly reduce the expression of CETP or ABCG1 by on macrophages, in line with our previous results from *in vitro* study, but in fact reduces the liver macrophage content, thereby

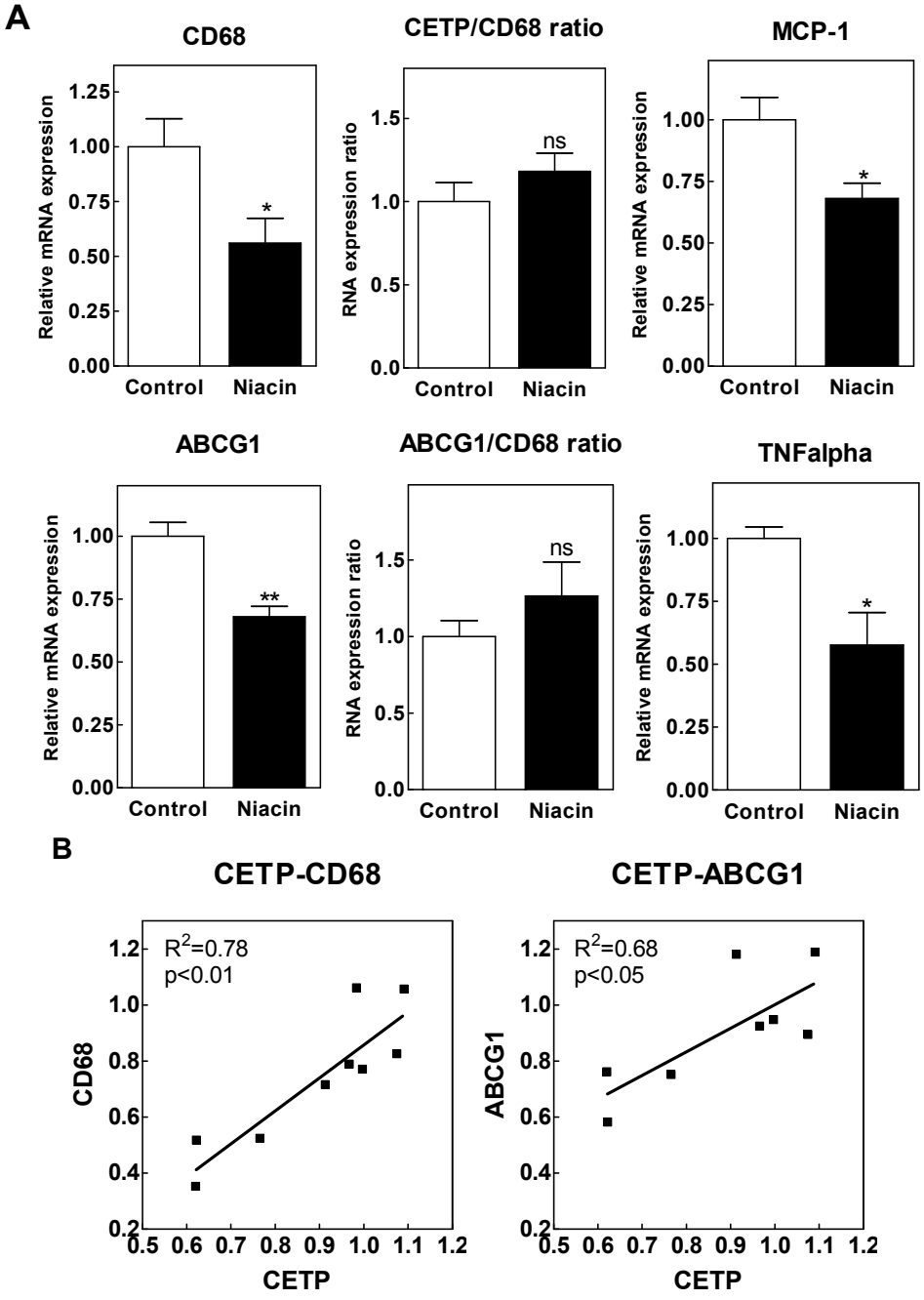

Figure 4. Effect of niacin on hepatic macrophage gene expression in CETP Tg mice. Total RNA was extracted from liver and relative mRNA expression of CD68, ABCG1, MCP-1, and TNFalpha were assessed by quantitative PCR and presented as fold-change relative to control group (A). Ratio between the expression level of CETP and CD68, ABCG1 and CD68 were calculated (A). Correlation between hepatic CETP and CD68 / ABCG1 expression upon niacin treatment was linearly plotted (B). Values are means ± SEM (6 mice per group). ns, not significant. *P<0.05; **P<0.01.

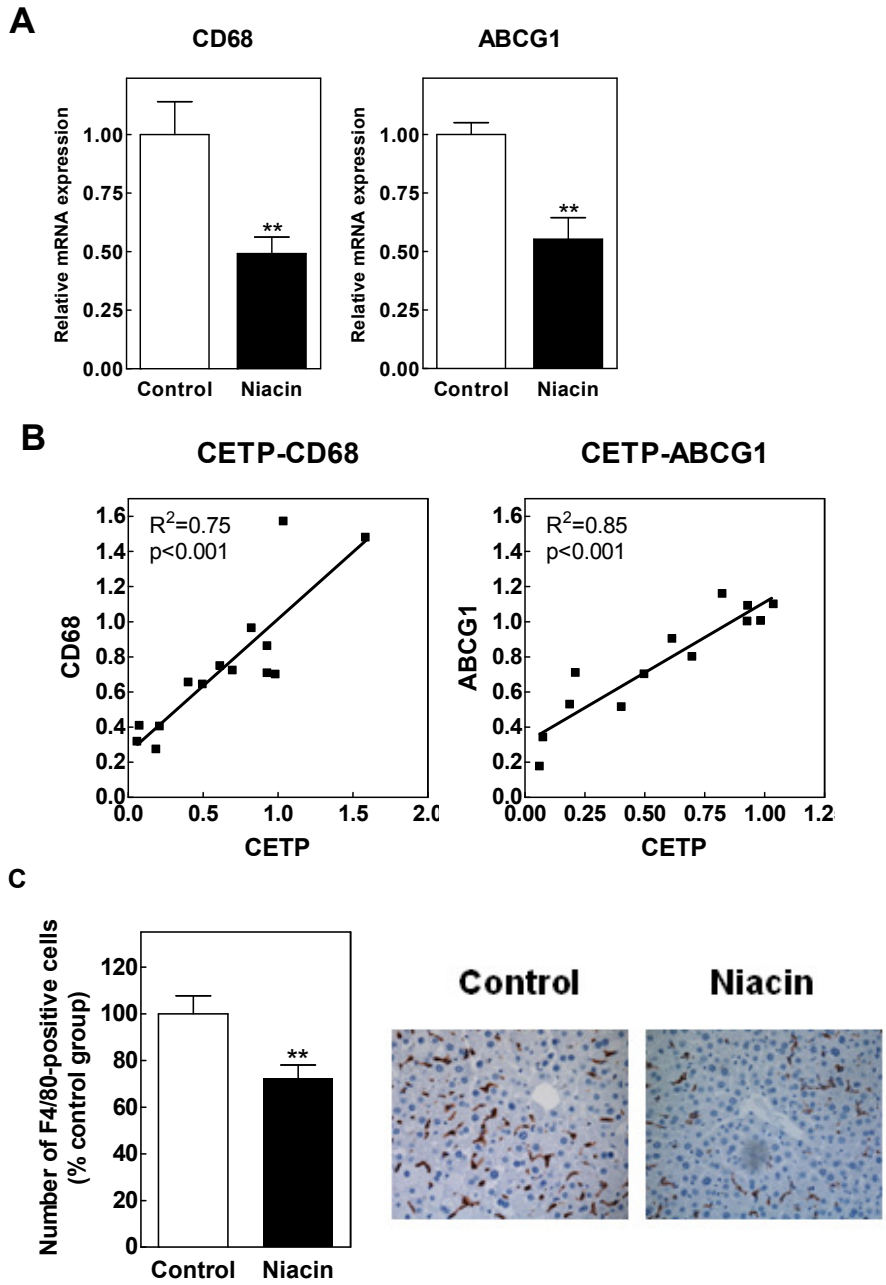

Figure 5. Effect of niacin on hepatic macrophage gene expression and number of macrophages in APOE*3-Leiden.CETP mice. Total RNA was extracted from liver and relative mRNA expression of CD68 and ABCG1 were assessed by quantitative PCR and presented as fold-change relative to control group (A). Correlation between hepatic CETP and CD68 / ABCG1 expression upon niacin treatment was linearly plotted (B). Macrophage content in the liver was visualized via immunohistochemistry staining with F4/80 antibody, and the number of positive cells were counted and expressed as percentage of control group. Representative pictures are shown (C). Values are means ± SEM (8 mice per group). ns, not significant. *P<0.05; **P<0.01.

reducing CETP expression. In accordance with the decreased liver macrophage content, gene expression of the inflammatory markers MCP-1 and TNFalpha in the liver both decreased substantially by 32% (p=0.016) and 43% (p=0.011), respectively, after niacin treatment (Figure 4A), suggesting attenuated high-fat diet-induced inflammation in liver.

The comparable reductions of hepatic CETP, liver macrophage markers, and liver inflammation markers suggest that the decrease of hepatic CETP expression is caused by a reduced amount of inflammatory macrophages in liver. Indeed, linear regression showed a very significant and strong positive correlation between hepatic CETP and CD68 expression ($p<0.01$; $R^2=0.78$), as well as between hepatic CETP and ABCG1 expression ($p<0.05$, $R^2=0.68$).

Consistent with our current results, post-hoc analysis on livers of APOE*3-Leiden.CETP mice treated with 1% niacin, from our previous study, in which the CETP-lowering effect of niacin was first observed[6], revealed similar significant reductions in hepatic gene expression of CD68 (-51%, p=0.007) and ABCG1 (-45%, p=0.001) (Figure 5A). In addition, there were also significant correlations between hepatic CETP and CD68 ($p<0.001$; $R^2=0.75$) or ABCG1 ($p<0.001$; $R^2=0.85$) expression (Figure 5B). The reduction of hepatic macrophage content was further visualized by staining of F4/80-positive cells, where niacin significantly reduced the number of macrophages in the liver by 28% (p=0.006) (Figure 5C).

DISCUSSION

To explain the CETP-lowering effect of niacin, we set out to investigate the effect of niacin on macrophages. Our observations *in vitro* showed that niacin at various concentrations did not reduce CETP expression in cultured macrophages derived from CETP Tg mice. Neither did niacin alter cholesterol metabolism-related genes, such as ABCA1, ABCG1, and SR-B1. We thus conclude that niacin does not directly regulate expression of CETP or other lipid-related genes in macrophages, albeit that secondary effects of niacin in an *in vivo* setting, e.g. related to a reduction in the fatty acid flux from adipose tissue to (liver) macrophages, can not be ruled out.

Luo *et al*[19] have previously demonstrated that CETP is trans-activated by nuclear receptor LXR, suggesting its role in regulating CETP expression *in vivo*. We also proposed in our previous study that niacin may decrease the hepatic CETP mRNA expression via LXR responsive element in the CETP promoter following decreased cholesterol content. However, our current *in vitro* data showed that niacin did not directly regulate expression of LXR-regulated target genes, such as ABCA1. Our *in vivo* data further confirmed that niacin did not regulate the expression of classical LXR targets such as SREBP-1c, apoE, or LPL in liver. In addition, although niacin treatment reduced the gene expression of ABCG1 in liver, it did not affect the ABCG1/CD68 expression ratio, indicating that niacin does not directly reduce the expression of ABCG1 on macrophages. The reduction in ABCG1 *in vivo* is thus probably not simply the consequence of reduced LXR activation. Therefore, it is suggested that either direct or indirect regulation of LXRs in the liver is not the main mechanism by which niacin reduces CETP expression.

The liver is a unique immunological site responding to inflammation. Antigen-rich blood from the gastrointestinal tract and the peripheral circulation enters the

hepatic parenchyma, passes through a network of liver sinusoids and is scanned by immune cells including macrophages and lymphocytes [20]. Thus, liver macrophages have profound implications in many aspects of the hepatic inflammatory response[21]. Plasma pro-atherogenic lipoproteins, mainly (V)LDLs, are important determinants of liver inflammation. Recent evidence has indicated an increased hepatic inflammation and macrophage content upon high-fat diet-induced hyperlipidemia. In C57Bl/6J mice fed a high-fat diet, up-regulation of hepatic expression of CD68 was found associated with increased hepatic lipid content[22]. Another study showed that in the LDLr$^{-/-}$ mice fed a high-fat diet, an increase of CD68 expression in the liver was correlated with increased plasma VLDL cholesterol levels. Omitting cholesterol from the diet rapidly reduced plasma TG and VLDL-cholesterol accumulation, associated with significantly lowered CD68 expression in liver together with other inflammatory genes[23]. In humans, a similar correlation between increased presence of CD68-positive Kupffer cells and the histological severity of human hepatic lipid content in fatty liver has been reported[24]. Such correlations between altered macrophage content and circulatory inflammatory factors define macrophage infiltration as a common response against hepatic and circulatory inflammation.

In the current study, niacin treatment reduced cholesterol content in the liver. In line with this attenuated liver fat accumulation, we further observed a significant reduction of pro-inflammatory markers MCP-1 and TNFalpha in liver. MCP-1 is one of the best characterized pro-inflammatory chemokines in liver. It has been reported that dietary fat and cholesterol, inappropriately high in the Western-type diet, are potent metabolic stress inducers of hepatic expression of the MCP-1 gene[25]. An increase in MCP-1 expression contributes to macrophage infiltration and hepatic steatosis in mice[26]. The pro-inflammatory cytokine TNFalpha is also critically involved in the pathophysiology of liver steatosis, and this cytokine is primarily secreted by Kupffer cells and liver-infiltrating macrophages[27]. Taken together, the results suggested an attenuated liver inflammation after niacin treatment.

In line with the attenuated diet-induced inflammation in the liver, the hepatic gene expression of CD68 and ABCG1 were also reduced upon niacin treatment. CD68 has been defined as a reliable macrophage marker and widely used for quantification of macrophage content in numerous studies[28,29,30]. ABCG1 has also been shown to be a good marker to assess Kupffer cell content in the liver, since ABCG1 is not expressed in hepatocytes[31,32]. In the current study, a reduction in the hepatic MCP-1 expression was associated with decreased CD68 and ABCG1 gene expression in liver, and also a reduced number of macrophages in liver, indicating an attenuated macrophage infiltration and/or an increased macrophage efflux from the liver into the liver and thus a decreased liver macrophage content. More importantly, the significant positive correlation between hepatic CETP and both CD68 and ABCG1 expression observed in both the current study and in the present post-hoc analysis of our previous study suggests that the liver macrophage is a primary contributor to hepatic and total plasma CETP mass, and that the hepatic CETP reduction induced by niacin treatment is a direct consequence of a reduced macrophage content of the liver.

Figure 6 illustrates the proposed mechanism underlying the action of niacin on hepatic CETP expression. We propose that the primarily reduced hepatic cholesterol accumulation via the lipid-lowering effect of niacin leads to attenuated

hepatic inflammation, and thus less macrophage infiltration into and/or increased macrophage emigration out of the liver. The decreased amount of hepatic macrophages leads to an overall reduction in hepatic CETP expression and a lower plasma CETP level.

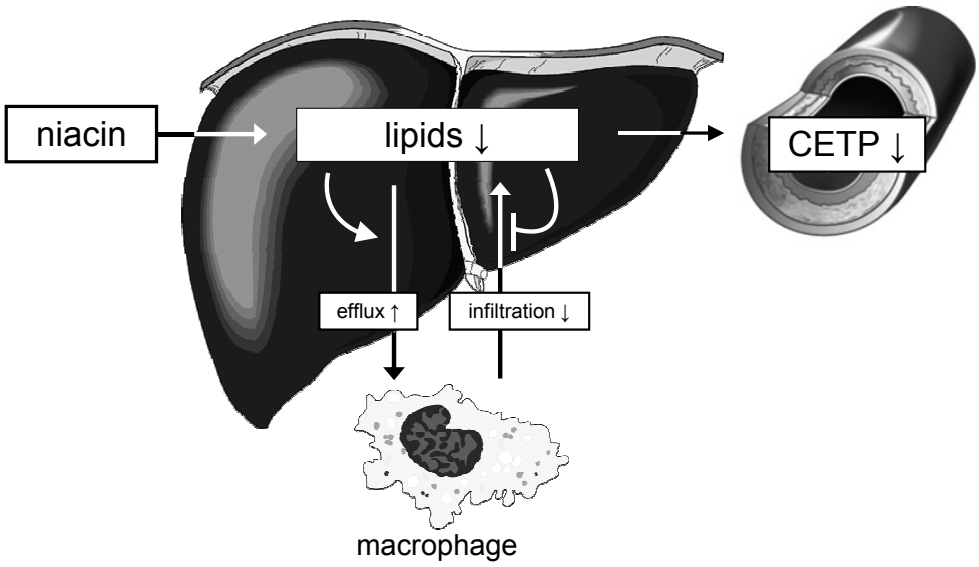

Figure 6. Proposed mechanism underlying the action of niacin on hepatic CETP expression and plasma CETP mass. We propose that the primarily reduced hepatic cholesterol accumulation via the lipid-lowering effect of niacin leads to attenuated hepatic inflammation, and thus less macrophage infiltration into and/or increased macrophage emigration out of the liver. The decreased amount of hepatic macrophages, which are significant contributors of CETP, leads to an overall reduction in hepatic CETP expression and a lower plasma CETP level.

In conclusion, our study sheds new light on the mechanism underlying the CETP-lowering effect of niacin in CETP transgenic mice. We have shown that niacin does not directly alter macrophage CETP expression, but attenuates liver inflammation and the macrophage content in response to its primary lipid-lowering effect, which leads to a decrease in hepatic CETP expression and plasma CETP mass.

ACKNOWLEDGEMENTS

This work was supported by TIPharma (Grant T2-110 to Z.L., T.J.C.V.B., M.H.) and the Netherlands Heart Foundation (Grant 2008T070 to M.H. and grant 2007B81 to P.C.N.R.). M.V.E. and P.C.N.R. are Established Investigators of the Netherlands Heart Foundation (2007T056 and 2009T038, respectively).

REFERENCES

1. Carlson LA, Oro L. The effect of nicotinic acid on the plasma free fatty acid; demonstration of a metabolic type of sympathicolysis. Acta Med Scand. 1962;172:641-645.
2. Grundy SM, Mok HY, Zech L, Berman M. Influence of nicotinic acid on metabolism of cholesterol and triglycerides in man. J Lipid Res. 1981;22:24-36.
3. Carlson LA. Niaspan, the prolonged release preparation of nicotinic acid (niacin), the broad-spectrum lipid drug. Int J Clin Pract. 2004;58:706-713.
4. Lee JM, Robson MD, Yu LM, Shirodaria CC, Cunnington C, Kylintireas I, Digby JE, Bannister T, Handa A, Wiesmann F, Durrington PN, Channon KM, Neubauer S, Choudhury RP. Effects of high-dose modified-release nicotinic acid on atherosclerosis and vascular function: a randomized, placebo-controlled, magnetic resonance imaging study. J Am Coll Cardiol. 2009;54:1787-1794.
5. Taylor AJ, Villines TC, Stanek EJ, Devine PJ, Griffen L, Miller M, Weissman NJ, Turco M. Extended-release niacin or ezetimibe and carotid intima-media thickness. N Engl J Med. 2009;361:2113-2122.
6. van der Hoorn JW, de Haan W, Berbée JF, Havekes LM, Jukema JW, Rensen PC, Princen HM. Niacin increases HDL by reducing hepatic expression and plasma levels of cholesteryl ester transfer protein in APOE*3Leiden.CETP mice. Arterioscler Thromb Vasc Biol. 2008;28:2016-2022.
7. Barter PJ, Brewer HB Jr, Chapman MJ, Hennekens CH, Rader DJ, Tall AR. Cholesteryl ester transfer protein: a novel target for raising HDL and inhibiting atherosclerosis. Arterioscler Thromb Vasc Biol. 2003;23:160-167.
8. Quintão EC, Cazita PM. Lipid transfer proteins: past, present and perspectives. Atherosclerosis. 2010;209:1-9.
9. Westerterp M, van der Hoogt CC, de Haan W, Offerman EH, Dallinga-Thie GM, Jukema JW, Havekes LM, Rensen PC. Cholesteryl ester transfer protein decreases high-density lipoprotein and severely aggravates atherosclerosis in APOE*3-Leiden mice. Arterioscler Thromb Vasc Biol. 2006;26:2552-2559.
10. Wisse E. An electron microscopic study of the fenestrated endothelial lining of rat liver sinusoids. J Ultrastruct Res. 1970;31:125-150.
11. Nemeth E, Baird AW, O'Farrelly C. Microanatomy of the liver immune system. Semin Immunopathol. 2009;31:333-343.
12. Bouwens L, Knook D, Wisse E. Local proliferation and extrahepatic recruitment of liver macrophages (Kupffer cells) in partial-body irradiated rats. Jf Leukoc Biol. 1986;39:687-697.
13. Van Eck M, Ye D, Hildebrand RB, Kar Kruijt J, de Haan W, Hoekstra M, Rensen PC, Ehnholm C, Jauhiainen M, Van Berkel TJ. Important role for bone marrow-derived cholesteryl ester transfer protein in lipoprotein cholesterol redistribution and atherosclerotic lesion development in LDL receptor knockout mice. Circ Res. 2007;100:678-685.
14. Schaub A, Futterer A, Pfeffer K. PUMA-G, an IFN-γ-inducible gene in macrophages is a novel member of the seven transmembrane spanning receptor superfamily. Eur J Immunol. 2001;31:3714-3725.
15. Tunaru S, Kero J, Schaub A, Wufka C, Blaukat A, Pfeffer K, Offermanns S. PUMA-G and HM74 are receptors for nicotinic acid and mediate its anti-lipolytic effect. Nat Med. 2003;9:352-355.
16. Ferenbach D, Hughes J. Macrophages and dendritic cells: what is the difference? Kidney Int. 2008;74:5-7.
17. Ye D, Lammers B, Zhao Y, Meurs I, Van Berkel T, Van Eck M. ATP-Binding Cassette Transporters A1 and G1, HDL Metabolism, Cholesterol Efflux, and Inflammation: Important Targets for the Treatment of Atherosclerosis. Curr Drug Targets. 2010. [Epub ahead of print]
18. Out R, Hoekstra M, Hildebrand RB, Kruit JK, Meurs I, Li Z, Kuipers F, Van Berkel TJ, Van Eck M. Macrophage ABCG1 deletion disrupts lipid homeostasis in alveolar macrophages and moderately influences atherosclerotic lesion development in LDL receptor-deficient mice. Arterioscler Thromb Vasc Biol. 2006;26:2295-2300.
19. Luo Y, Tall AR. Sterol upregulation of human CETP expression in vitro and in transgenic mice by an LXR element. J Clin Invest. 2000;105:513-520.
20. Racanelli V, Rehermann B. The liver as an immunological organ. Hepatology. 2006;43:S54-S62.
21. MacPhee PJ, Schmidt EE, Groom AC. Evidence for Kupffer cell migration along liver sinusoids, from high-resolution in vivo microscopy. Am J Physiol. 1992;263:G17-G23.
22. Lanthier N, Molendi-Coste O, Horsmans Y, van Rooijen N, Cani PD, Leclercq IA. Kupffer cell activation is a causal factor for hepatic insulin resistance. Am J Physiol Gastrointest Liver Physiol. 2010;298:G107-G116.

23. Wouters K, van Gorp PJ, Bieghs V, Gijbels MJ, Duimel H, Lütjohann D, Kerksiek A, van Kruchten R, Maeda N, Staels B, van Bilsen M, Shiri-Sverdlov R, Hofker MH. Dietary cholesterol, rather than liver steatosis, leads to hepatic inflammation in hyperlipidemic mouse models of nonalcoholic steatohepatitis. Hepatology. 2008;48:474-486.
24. Park JW, Jeong G, Kim SJ, Kim MK, Park SM. Predictors reflecting the pathological severity of non-alcoholic fatty liver disease: comprehensive study of clinical and immunohistochemical findings in younger Asian patients. J Gastroenterol Hepatol. 2007;22:491-497.
25. Rull A, Rodríguez F, Aragonès G, Marsillach J, Beltrán R, Alonso-Villaverde C, Camps J, Joven J. Hepatic monocyte chemoattractant protein-1 is upregulated by dietary cholesterol and contributes to liver steatosis. Cytokine. 2009;48:273-279.
26. Kanda H, Tateya S, Tamori Y, Kotani K, Hiasa K, Kitazawa R, Kitazawa S, Miyachi H, Maeda S, Egashira K, Kasuga M. MCP-1 contributes to macrophage infiltration into adipose tissue, insulin resistance, and hepatic steatosis in obesity. J Clin Invest. 2006;116:1494-1505.
27. Tacke F, Luedde T, Trautwein C. Inflammatory pathways in liver homeostasis and liver injury. Clin Rev Allergy Immunol. 2009;36:4-12.
28. Kunisch E, Fuhrmann R, Roth A, Winter R, Lungershausen W, Kinne RW. Macrophage specificity of three anti-CD68 monoclonal antibodies (KP1, EBM11, and PGM1) widely used for immunohistochemistry and flow cytometry. Ann Rheum Dis. 2004;63:774-784.
29. Micklem K, Rigney E, Cordell J, Simmons D, Stross P, Turley H, Seed B, Mason D. A human macrophage-associated antigen (CD68) detected by six different monoclonal antibodies. Br J Haematol. 1989;73:6-11.
30. Huang W, Metlakunta A, Dedousis N, Zhang P, Sipula I, Dube JJ, Scott DK, O'Doherty RM. Depletion of liver Kupffer cells prevents the development of diet-induced hepatic steatosis and insulin resistance. Diabetes. 2010;59:347-357.
31. Hoekstra M, Kruijt JK, Van Eck M, Van Berkel TJ. Specific gene expression of ATP-binding cassette transporters and nuclear hormone receptors in rat liver parenchymal, endothelial, and Kupffer cells. J Biol Chem. 2003;278:25448-25453.
32. Ye D, Hoekstra M, Out R, Meurs I, Kruijt JK, Hildebrand RB, Van Berkel TJ, Van Eck M. Hepatic cell-specific ATP-binding cassette (ABC) transporter profiling identifies putative novel candidates for lipid homeostasis in mice. Atherosclerosis. 2008;196:650-658.

Chapter 5

Effects of pyrazole partial agonists on HCA_2-mediated flushing and hepatic VLDL production in mice

Zhaosha Li[1*], Clara C. Blad[2*], Ronald J. van der Sluis[1], Henk de Vries[2], Theo J.C. Van Berkel[1], Ad P. IJzerman[2], Menno Hoekstra[1]

[1]Division of Biopharmaceutics, Leiden/Amsterdam Center for Drug Research, Leiden University, The Netherlands.
[2]Division of Medicinal Chemistry, Leiden/Amsterdam Center for Drug Research, Leiden University, The Netherlands.
[*]These authors contributed equally to this work.

Submitted for publication

ABSTRACT

Background & Aims: Nicotinic acid, also known as niacin, is the most effective agent currently available to treat dyslipidaemic disorders. However, its clinical use has been limited due to the cutaneous flushing, which is mediated by the nicotinic acid receptor HCA_2. In the current study, we assessed the *in vitro* and *in vivo* properties of two partial agonists for HCA_2, LUF6281 and LUF6283, to evaluate their anti-dyslipidemic potentials and cutaneous flushing side effect compared to nicotinic acid.
Methods and Results: Radioligand competitive binding assay showed the K_i values for LUF6281 and LUF6283 were 3 μM and 0.55 μM, respectively. [^{35}S]-GTPγS binding determined the rank order of their potency: nicotinic acid > LUF6283 > LUF6281. Both LUF6281 and LUF6283 avoided the unwanted flushing side effect as tested in C57BL/6 mice. Furthermore, both agonists significantly reduced plasma VLDL-cholesterol concentration in mice. In the liver, both agonists resulted in a more than 40% reduction in the expression levels of ApoB and MTP as compared to the control group, indicating inhibited hepatic VLDL production.
Conclusions: The current study demonstrates that two HCA_2 partial agonists of the pyrazole class are promising drug candidates to achieve the beneficial lipid-lowering effects while successfully avoiding the unwanted flushing side effect.
Keywords: HCA_2 partial agonists, niacin, lipoprotein, VLDL, liver, flushing

INTRODUCTION

Nicotinic acid, also known as niacin, is the most effective agent currently available to treat dyslipidaemic disorders[1]. It lowers plasma levels of pro-atherogenic lipids, including chylomicrons, very-low-density lipoproteins (VLDL), low-density lipoproteins (LDL), and triglycerides (TG) in normolipidemic as well as hypercholesterolemic subjects[2]. Several clinical trials have shown that nicotinic acid reduces cardiovascular disease and myocardial infarction incidence, providing a solid rationale for the use of nicotinic acid in the treatment of atherosclerosis[3,4]. The G protein-coupled receptor GPR109A, also known as PUMA-G in mouse and HM74A in humans, has been identified as a high-affinity receptor for nicotinic acid[5,6]. We now know that the endogenous ligand for GPR109A is 3-hydroxybutyrate, and this receptor has recently been renamed as hydroxy-carboxylic acid receptor 2 (HCA_2)[7].

Despite its established cardiovascular benefits, the clinical use of nicotinic acid has been limited due to the cutaneous flushing, a well-recognized adverse skin effect from nicotinic acid therapy. Flushing has been cited as the major reason for the discontinuation of this therapy, estimated at rates as high as 25%-40%[8]. The nicotinic acid receptor HCA_2 expressed in the skin is a critical mediator of nicotinic acid-induced flushing[9]. Nicotinic acid stimulates HCA_2 in epidermal Langerhans cells and keratinocytes, causing the cells to produce vasodilatory prostaglandin D_2 (PGD_2) and prostaglandin E_2 (PGE_2), which leads to cutaneous vasodilation[10,11,12,13].

For the past decade, the pharmacology of HCA_2 has been studied and full or partial agonists for HCA_2 have been developed in an attempt to achieve the beneficial effects of nicotinic acid while avoiding the unwanted flushing side effect[14]. Based on the structure-activity relationship of nicotinic acid-related molecules, several potent agonists for HCA_2 have been identified, including acipimox, acifran, 3-pyridine-acetic acid, 5-methylnicotinic acid, pyridazine-4-carboxylic acid, and pyrazine-2-carboxylic acid[15,16]. However, the challenge remains that HCA_2 partial agonists failed to demonstrate the beneficial effects on LDL-cholesterol, triglycerides or HDL-cholesterol despite the absence of flushing events in clinical studies[17]. Further understanding of the medicinal chemistry of HCA_2 is needed to pharmacologically dissociate the antilipolytic and vasodilatory effects of nicotinic acid by acting on HCA_2[16].

In the current study, we assessed the properties of two HCA_2 partial agonists, LUF6281 and LUF6283, of the pyrazole class, which were developed in our laboratory[18]. We first characterized these two compounds *in vitro*, using a radioligand binding assay, [^{35}S]-GTPγS assay and ERK phosphorylation assay. The ERK phosphorylation assay was included because it has been suggested that ERK1/2 phosphorylation downstream from HCA_2 correllates positively with skin flushing[19]. Then, we assessed the cutaneous flushing effect and the therapeutic lipid-lowering potential of these two partial agonists in C57BL/6 mice.

MATERIALS AND METHODS

In vitro experiments

Materials

[^{3}H]-nicotinic acid (60 Ci/mmol) was obtained from BioTrend (Koehln, Germany). [^{35}S]-GTPγS (1250 Ci/mmol) was obtained from Perkin Elmer (Waltham, MA).

Cell culture and membrane preparation

Human embryonic kidney (HEK) 293T cells stably expressing human HCA_2 were cultured in DMEM supplemented with 10% newborn bovine serum, 0.4 mg/mL G418, 50 IU/mL penicillin and 50 µg/mL streptomycin. The cells were harvested by scraping in cold PBS, centrifuged at 1000 xg for 10 minutes and resuspended in cold 50 mM Tris-HCl buffer, pH 7.4. Then a DIAX 900 electrical homogenizer (Heidolph, Schwabach, Germany) was used for 15 seconds to obtain cell lysis. The suspension was centrifuged at 225000 xg for 20 minutes at 4 °C and the supernatant was discarded. The pellet was resuspended in Tris-HCl, and the homogenization and centrifugation steps were repeated. The membranes were resuspended in cold assay buffer (50 mM Tris HCl, 1 mM $MgCl_2$, pH 7.4) and the protein content was determined using BCA assay (Thermo Scientific, Waltham, USA). During membrane preparation the suspension was kept on ice at all times. Membrane aliquots were stored at -80 °C until the day of use.

[^{3}H]-nicotinic acid displacement assay

Membranes of our stable HEK293T-HCA_2 cell line (50 µg protein per tube) were incubated for 1 hour at 25 °C with 20 nM [^{3}H]-nicotinic acid and with increasing concentrations of the test compounds in assay buffer (50 mM Tris HCl, 1 mM $MgCl_2$, pH 7.4). The total assay volume was 100 µL. To assess the total binding, a control without test compound was included. The non-specific binding was determined in the presence of 10 µM unlabeled nicotinic acid. Final DMSO concentration in all samples was ≤ 0.25%. The incubation was terminated by filtering over GF/B filters using a 24-sample harvester (Brandel, Gaithersburg, USA). The filters were washed 3 times with 2 mL cold buffer (50 mM Tris HCl, pH 7.4). Filters were transferred to counting vials and counted in a Perkin Elmer LSA Tri-Carb 2900TR counter after 2 hours of extraction in 3.5 mL Emulsifier Safe liquid scintillation cocktail (Perkin Elmer, Waltham, USA).

[^{35}S]-GTPγS binding assay

This assay was performed in 96-well format in 50 mM Tris-HCl, 1 mM EDTA, 5 mM $MgCl_2$, 150 mM NaCl, pH 7.4 at 25 °C with 1 mM DTT, 0.5% BSA and 50 µg/mL saponin freshly added. HEK-HCA_2 membranes (5 µg protein per well in 25 µL) were pre-incubated with 25 µL of 40 µM GDP and 25 µL increasing concentrations of the test compounds, for 30 minutes at room temperature. Then, 25 µL [^{35}S]-GTPγS was added (final concentration 0.3 nM) and the mixture was incubated for 90 minutes at 25 °C with constant shaking. The incubation was terminated by filtration over GF/B filterplates on a FilterMate harvester (PerkinElmer). The filters were dried and 25 µL Microscint 20 (PerkinElmer) was added to each filter. After ≥3 hours of extraction the bound radioactivity was determined in a Wallac Microbeta Trilux 1450 counter (PerkinElmer, MA, USA).

ERK1/2 phosphorylation assay
The assay was performed using AlphaScreen SureFire Phospho-ERK1/2 kit (PerkinElmer, MA, USA), following the kit protocol. Briefly, a 96-well cell culture plate was coated with poly-D-lysine and HEK cells stably expressing human HCA_2 were seeded at 50000 cells/well in 200 µL DMEM supplemented with 10% newborn bovine serum, 0.4 mg/mL G418, 50 IU/mL penicillin and 50 µg/mL streptomycin. After overnight incubation the cells were serum starved for 4 h in the same medium lacking the serum, and then the medium was replaced by 90 µL prewarmed PBS and incubated for an additional 30 minutes. Increasing concentrations of the test compounds were diluted in prewarmed PBS and 10 µL was added per well for stimulation. After 5 minutes the stimulation solution was removed from the plates, the wells were washed once in ice-cold PBS and 100 µL lysis buffer was added per well. After 15 minutes of incubation and shaking at room temperature, the lysates were mixed by pipetting and 4 µL was transferred to a 384-well OptiPlate (PerkinElmer, MA, USA). The reaction mix was prepared according to the kit protocol (60 µL reaction buffer and 10 µL activation buffer with 1 µL of the donor and acceptor beads each) and 7 µL mix was added to each proxyplate well. After 2 h the plate was read on an EnVision multilabel plate reader (PerkinElmer, MA, USA).

Data analysis
Analysis of the results was performed using Prism 5.0 software (GraphPad Software Inc., La Jolla, USA). Nonlinear regression was used to determine IC_{50} values from competition binding curves. The Cheng-Prusoff equation was then applied to calculate K_i values[20]. [^{35}S]-GTPγS and pERK curves were analysed by nonlinear regression to obtain EC_{50} values.

***In vivo* experiments**

Animals
Female C57BL/6 mice of 12 weeks old were used. Animals were fed a regular cholesterol-free chow diet containing 4.3% (w/w) fat (RM3, Special Diet Services, Witham, UK). Mice received either vehicle (50% DMSO in PBS) or HCA_2 partial agonists LUF6281 and LUF6283 (400 mg/kg/day) once a day for 4 weeks via oral gavage. After euthanization, mice were bled via orbital exsanguination and perfused *in situ* through the left cardiac ventricle with ice-cold PBS (pH 7.4) for 20 minutes. Liver was dissected free of fat and snap-frozen in liquid nitrogen. Animal care and procedures were performed in accordance with the national guidelines for animal experimentation. All protocols were approved by the Ethics Committee for Animal Experiments of Leiden University.

Measurement of skin flushing in mouse
Cutaneous flushing in C57BL/6 mice was assessed by monitoring the change of the skin temperature at the mouse paw location. Temperature measurements were recorded using a non contact infrared thermometer (Pro Exotics PE-1 Infrared Temp Gun, Littleton, USA). The probe was held at a distance of 1 to 2 mm from the metacarpal pad of mouse paw, and temperature readings were taken from a circular area approximately 3 mm in diameter. Animals were habituated to handling and to the infrared probe before use. Skin temperature was initially recorded from

the abdominal area, tail, ear, and paw, after which it was determined that mouse paw skin temperature gave the most reliable and consistent results. During the experiment, the animals were dosed with either vehicle (50% DMSO in PBS) or partial agonists LUF6281 and LUF6283 (400 mg/kg/day) via oral gavage (10:00-11:00 AM), and the paw temperature was measured every 10 minutes for a period of 60 minutes in total. Three readings from the center area of mouse paw were recorded routinely for each time point. Baseline paw temperature was recorded right before animals were dosed. All the administration was performed in conscious mice to avoid the interference of the anesthetics on skin temperature.

Plasma lipid analysis

The distribution of cholesterol over different lipoproteins in plasma was determined by fast protein liquid chromatography (FPLC) through a Superose 6 column (3.2 x 30 mm; Smart-System, Pharmacia, Uppsala, Sweden). Cholesterol content of the lipoprotein fractions was measured using the enzymatic colorimetric assay (Roche Diagnostics, Mannheim, Germany).

RNA isolation and gene expression analysis.

Total RNA from the liver was isolated using acid guanidinium thiocyanate (GTC)-phenol-chloroform extraction. Briefly, 500 µL of GTC solution (4 M guanidine isothiocyanate, 25 mM sodium citrate, 0.5% N-lauroylsarcosine) was added to each sample, followed by acid phenol:chloroform extraction. The RNA in aqueous phase was precipitated with isopropanol. The quantity and purity of the isolated RNA were examined using ND-1000 Spectrophotometer (Nanodrop, Wilmington, DE, USA). One microgram of the isolated RNA from each sample was converted into cDNA by reverse transcription with RevertAid™ M-MuLV Reverse Transcriptase (Promega, Madison, WI, USA). Negative controls without addition of reverse transcriptase were prepared for each sample. Quantitative real-time PCR was carried out using ABI Prism 7700 Sequence Detection system (Applied Biosystems, Foster City, CA, USA) according to the manufacturer's instructions. 36B4, Beta-actin, and GAPDH were used as internal housekeeping genes. The gene-specific primer sequences used are listed in Table 1. Amplification curves were analyzed using 7500 Fast System SDS software V1.4 (Applied Biosystems, Foster City, CA, USA). The relative expression of each gene was expressed as fold changes $2^{-(\Delta\Delta CT)}$ compared to baseline group. Standard error of the mean (SEM) and statistical significance were calculated using ΔΔCt formula.

Statistical analysis

Mean values between 2 groups were analyzed with 2-tailed unpaired Student's t-test. Data sets containing multiple groups were analyzed by ANOVA (Instat GraphPad software, San Diego, USA). Statistical significance was defined as $p<0.05$. Data are expressed as means ± SEM.

Table 1. Murine primers for quantitative real-time PCR analysis

Gene	Forward primer	Reverse Primer
36B4	GGACCCGAGAAGACCTCCTT	GCACATCACTCAGAATTTCAATGG
Beta-actin	AACCGTGAAAAGATGACCCAGAT	CACAGCCTGGATGGCTACGTA
GAPDH	TCCATGACAACTTTGGCATTG	TCACGCCACAGCTTTCCA
ApoB	ATGTCATAATTGCCATAGATAGTGCCA	TCGCGTATGTCTCAAGTTGAGAG
MTP	AGCTTTGTCACCGCTGTGC	TCCTGCTATGGTTTGTTGGAAGT

RESULTS

In this study, we assessed the *in vitro* and *in vivo* properties of two HCA_2 ligands, LUF6281 and LUF6283, to evaluate their anti-dyslipidemic potentials and cutaneous flushing side effect compared to nicotinic acid. The chemical structures of these compounds are shown in Figure 1. For *in vitro* experiments we used HEK293T cell line stably expressing the human HCA_2 receptor.

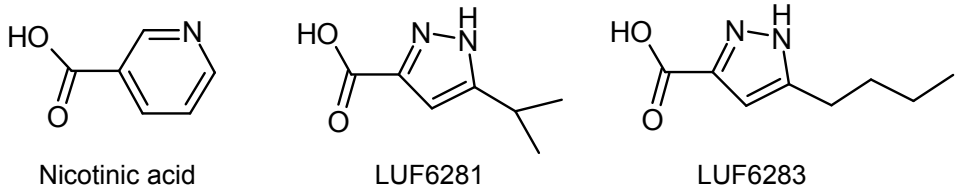

Nicotinic acid LUF6281 LUF6283

Figure 1. Chemical structures of nicotinic acid, LUF6281, and LUF6283.

First, the affinity of the compounds to HCA_2 was determined by a competitive binding assay using radiolabeled nicotinic acid (Figure 2). The K_i values determined for LUF6281 and LUF6283 were 3 μM and 0.55 μM, respectively (Table 2).

Next, we compared the potencies and intrinsic efficacies of nicotinic acid, LUF6281 and LUF6283 by measuring their ability to stimulate [^{35}S]-GTPγS binding. The results clearly showed that LUF6281 and LUF6283 were partial agonists, with intrinsic efficacies of 55 (±4.1) and 76 (±3.4) %, respectively (N=7). The rank order of their potency was nicotinic acid > LUF6283 > LUF6281, with EC_{50} values of 0.41, 3.1 and 8.6 μM, respectively (Figure 3; Table 2).

Table 2. In vitro biochemical characterization of GPR109A agonists nicotinic acid, LUF6281, and LUF6283. Values are mean (±SEM) (N≥3)

	Ki (μM)	**EC_{50}-[^{35}S]-GTPγS (μM)**	**EC_{50}-pERK1/2 (μM)**
Nicotinic acid	0.04 (±0.02)	0.41 (±0.11)	0.02 (±0.004)
LUF6281	3.1 (±0.5)	8.60 (±1.00)	1.37 (±0.31)
LUF6283	0.55 (±0.01)	3.10 (±0.13)	0.32 (±0.06)

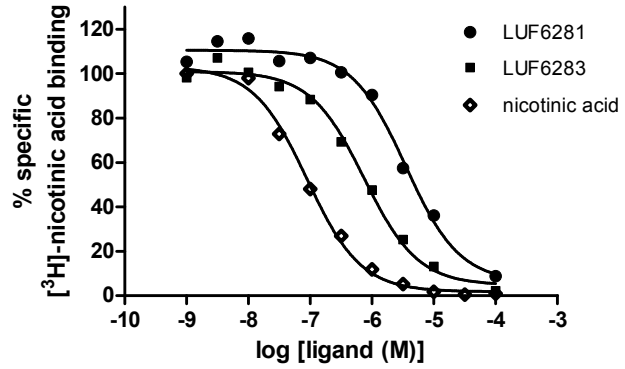

Figure 2. Competitive radioligand binding assay using 20 nM [^{3}H]-nicotinic acid revealing the relative affinities of nicotinic acid, LUF6481 and LUF6483. The assay was performed on HEK293T-HCA_2 membranes (50 µg/tube). The results from one representative experiment are shown (of N=3).

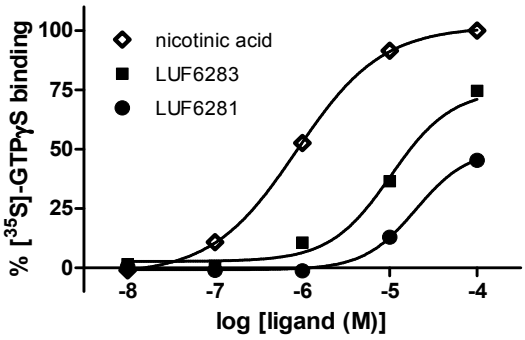

Figure 3. Dose-response curves of nicotinic acid, LUF6481 and LUF6483 in a [^{35}S]-GTPγS binding assay, showing the relative potencies and intrinsic efficacies. Nicotinic acid is a full agonist, whereas LUF6481 and LUF6483 are partial agonists in this assay. The assay was performed on HEK293T-HCA_2 membranes (5 µg/tube). Data from one representative experiment are shown (of N=3).

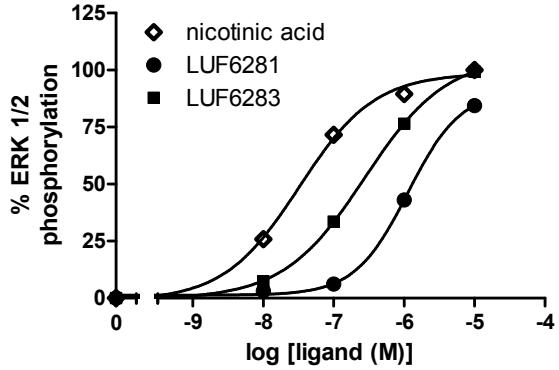

Figure 4. Dose-response curves of nicotinic acid, LUF6481 and LUF6483 in an ERK 1/2 phosphorylation assay, showing the relative potencies and intrinsic efficacies. All ligands are full agonists in this assay. The assay was performed on attached HEK293T-HCA_2 cells. Data from one representative experiment are shown (of N=3-5).

The second functional assay monitored ERK1/2 phosphorylation of the compounds upon HCA_2 activation. Results from this assay showed that the intrinsic efficacy was the same for all compounds (Figure 4; Table 2). The EC_{50} values obtained here were 20 nM for nicotinic acid, 1.6 µM for LUF6281 and 0.26 µM for LUF6283. Thus, all compounds seemed to be more potent in the pERK1/2 assay than in the [^{35}S]-GTPγS assay, but this difference was much more pronounced for nicotinic acid (20-fold) than for LUF6283 (12-fold) and LUF6281 (4-fold) (Table 2).

To examine the vasodilatory effects of these compounds *in vivo*, we used C57BL/6 mice to assess the cutaneous flushing as determined by an increase in mouse paw skin temperature. In mice, the normal paw skin temperature was approximately 26.4°C (*n* = 30). Mice were divided into 3 groups: the control group received vehicle (50% DMSO in PBS), while the treatment groups received LUF6281 and LUF6283 (400 mg/kg/day) respectively via oral gavage. Surprisingly, DMSO induced a time-dependent temperature increase in the control group, with a maximum 3.6 °C (*n* = 10) that occurred at 20 minutes after oral gavage (Figure 5). Similar effects of DMSO have been reported in the literature, and might be due to a release of histamine[21,22,23,24,25]. However, neither of the treatment groups displayed significant temperature raise. At 20 minutes, LUF6281 and LUF6283 induced a maximal temperature increase of only 0.5 or 1.0 °C (*n* = 10 per group), which was significantly lower than the temperature raise observed in the control group ($p < 0.001$; Figure 5) and comparable to the temperature raise induced by PBS at the same time point (data not shown). The results suggested that both of the HCA_2 partial agonists LUF6281 and LUF6283 avoided the unwanted flushing side effect in mice.

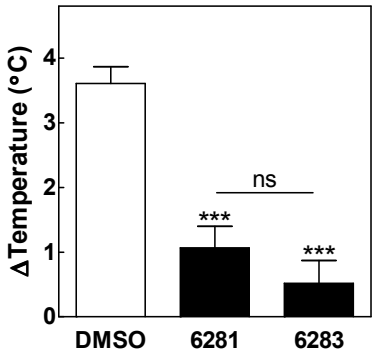

Figure 5. Mouse flushing after administration of nicotinic acid, LUF6281, and LUF6283. The cutaneous vasodilation was determined by change in paw skin temperature in C57BL/6 mice. Mice received vehicle (DMSO), LUF6281, or LUF6283 (400 mg/kg/day) via oral gavage. Data are expressed as the increase of skin temperature at 20 min after dosing compared to before treatment (n=10 per group). ns, not significant. ***P<0.001.

To evaluate the beneficial antilipolytic potentials of the LUF compounds, we tested their effects on plasma lipid homeostasis in C57BL/6 mice. Although treatment with LUF compounds for 4 weeks did not alter plasma total cholesterol or triglycerides concentration, separation of plasma lipoproteins by FPLC in combination with analysis of the lipid content across the FPLC fractions showed that LUF6281 sharply reduced plasma VLDL-cholesterol concentration by 77.4% ($p<0.01$) and LUF6283 also significantly reduced plasma VLDL-cholesterol level by 38.1% ($p<0.05$, Figure 6).

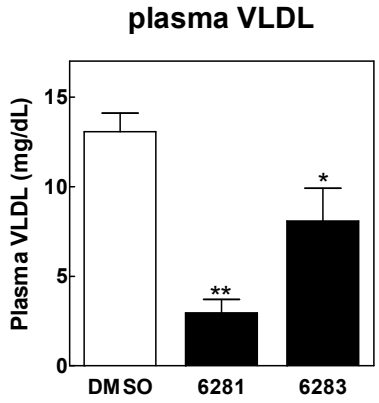

Figure 6. Effects of LUF6281 and LUF6283 on plasma VLDL concentration in C57BL/6 mice. Mice were fed with regular chow diet and received either vehicle (DMSO) or GPR109A partial agonists LUF6281 and LUF6283 (400 mg/kg/day) once a day for 4 weeks. Plasma lipoproteins were separated by FPLC and cholesterol level was measured in each fraction. VLDL represents the sum of cholesterol concentrations from fraction 2 to 7 (VLDL fractions. Values are means ± SEM (n=10 per group). *P<0.05; **P<0.01.

To further understand the mechanism whereby LUF compounds largely reduced the plasma VLDL concentration, hepatic gene expression levels in response to compound treatment were assessed by real-time quantitative PCR. Both LUF6281 and LUF6283 modulated the relative RNA expression level of hepatic VLDL production-associated genes in mouse. Concomitant with the plasma VLDL-lowering effect, treatment of both LUF compounds resulted in a more than 40% reduction in the expression levels of apolipoprotein B (apoB) ($p<0.05$) and microsomal triglyceride transfer protein (MTP) ($p<0.05$) as compared to the control group (Figure 7), indicating inhibited hepatic VLDL production.

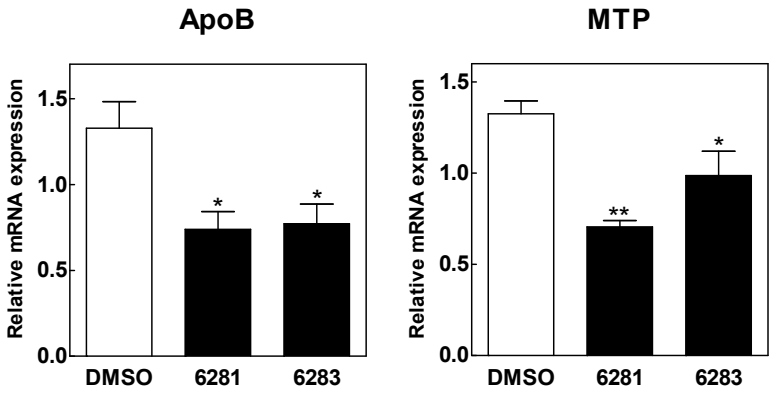

Figure 7. Effects of LUF6281 and LUF6283 on hepatic gene expression in C57BL/6 mice. Total RNA was extracted from liver, and relative mRNA expression levels of ApoB and MTP were determined by quantitative PCR and presented as fold-change relative to control group. Values are means ± SEM (n=10 per group). *P<0.05; **P<0.01.

DISCUSSION

Previous studies have shown that HCA_2 mediates nicotinic acid-induced cutaneous flushing[26]. It seems that the early phase of flushing depends on HCA_2 expressed on Langerhans cells, whereas the late phase is mediated by HCA_2 expressed on keratinocytes[12]. Derivatives of nicotinic acid have been developed to pharmacologically dissociate the antilipolytic and vasodilatory effects by acting as partial and, in the case of MK-0354, biased agonists on HCA_2[18,19,27]. The pyrazole MK-0354 stimulates the G protein pathway that leads to antilipolysis in adipocytes, but does not cause ERK1/2 phosphorylation[27]. This compound showed promising results in mice, since no vasodilation was observed and antilipolytic activity was retained, but in clinical trials this compound failed since it had no effect on plasma lipid levels[17]. In the current study, we characterized the affinity and efficacy of two HCA_2 partial agonists LUF6281 and LUF6283 previously reported by us[18] and we evaluated the cutaneous flushing effect and the therapeutic lipid-lowering potential of these agonists in C57BL/6 mice.

We show that nicotinic acid, LUF6281 and LUF6283 may all have a certain bias, since these compounds all seem to have a higher potency for ERK1/2 phosphorylation than for G protein activation. Furthermore, LUF6281 and LUF6283 were both partial agonists in the [^{35}S]-GTPγS assay but seemed full agonists in the pERK1/2 assay. The fold difference in potency depended on the compound; nicotinic acid was 20-fold more potent for ERK phosphorylation, LUF6283 was 12-fold more potent and LUF6281 was only 5-fold more potent. The high potency of nicotinic acid for activation of the MAP kinase pathway may explain why this compound causes flushing so effectively. Unlike MK-0354, our pyrazole compounds are still active in the ERK1/2 assay, but we hypothetized that their relatively low potency on this pathway might attenuate the flushing response. Indeed, our *in vivo* findings confirm that the pyrazoles do not provoke the flushing response as nicotinic acid does, although it remains unclear what causes this improvement.

In addition, our data suggested that LUF6281 and LUF6283 exerts lipid-lowering effect via inhibiting hepatic VLDL production. LUF6281 and LUF6283 both markedly reduced the hepatic gene expression of apoB and MTP. ApoB is the structural lipoprotein of VLDL, LDL and chylomicrons. ApoB and the MTP are essential for the assembly and secretion of apoB-containing lipoproteins[28]. The assembly and secretion pathway of VLDL in the liver involves the transfer of lipid by MTP to apoB during translation and then the fusion of apoB-containing precursor particles with triglyceride droplets to form mature VLDL[29,30]. The link between hepatic ApoB / MTP gene expression level, hepatic VLDL secretion and plasma VLDL concentration has been illustrated in the literature[31,32].

In conclusion, the current study demonstrated two HCA_2 partial agonists of the pyrazole class as promising drug candidates to achieve the beneficial lipid-lowering effects while successfully avoid the unwanted flushing side effect.

ACKNOWLEDGEMENTS

This work was supported by TIPharma (Grant D1-105 to C.C.B., A.P.IJ.; Grant T2-

110 to Z.L., T.J.C.V.B., M.H.) and the Netherlands Heart Foundation (Grant 2008T070 to M.H.).

REFERENCES

1. Benhalima, K. and E. Muls, Niacin, an old drug with new perspectives for the management of dyslipidaemia. Acta Clin Belg, 2010. 65(1): p. 23-8.
2. Carlson, L.A., Niaspan, the prolonged release preparation of nicotinic acid (niacin), the broad-spectrum lipid drug. Int J Clin Pract, 2004. 58(7): p. 706-13.
3. Lee, J.M., et al., Effects of high-dose modified-release nicotinic acid on atherosclerosis and vascular function: a randomized, placebo-controlled, magnetic resonance imaging study. J Am Coll Cardiol, 2009. 54(19): p. 1787-94.
4. Taylor, A.J., et al., Extended-release niacin or ezetimibe and carotid intima-media thickness. N Engl J Med, 2009. 361(22): p. 2113-22.
5. Lorenzen, A., et al., Characterization of a G protein-coupled receptor for nicotinic acid. Mol Pharmacol, 2001. 59(2): p. 349-57.
6. Wise, A., et al., Molecular identification of high and low affinity receptors for nicotinic acid. J Biol Chem, 2003. 278(11): p. 9869-74.
7. Offermanns, S., et al., International Union of Basic and Clinical Pharmacology. LXXXII: Nomenclature and Classification of Hydroxy-carboxylic Acid Receptors (GPR81, GPR109A, and GPR109B). Pharmacol Rev, 2011. 63(2): p. 269-90.
8. Davidson, M.H., Niacin use and cutaneous flushing: mechanisms and strategies for prevention. Am J Cardiol, 2008. 101(8A): p. 14B-19B.
9. Benyó, Z., et al., GPR109A (PUMA-G/HM74A) mediates nicotinic acid-induced flushing. J Clin Invest, 2005. 115(12): p. 3634-3640.
10. Cheng, K., et al., Antagonism of the prostaglandin D2 receptor 1 suppresses nicotinic acid-induced vasodilation in mice and humans. Proc Natl Acad Sci U S A, 2006. 103(17): p. 6682-7.
11. Dunbar, R.L. and J.M. Gelfand, Seeing red: flushing out instigators of niacin-associated skin toxicity. J Clin Invest, 2010. 120(8): p. 2651-5.
12. Hanson, J., et al., Nicotinic acid- and monomethyl fumarate-induced flushing involves GPR109A expressed by keratinocytes and COX-2-dependent prostanoid formation in mice. J Clin Invest, 2010. 120(8): p. 2910-9.
13. Morrow, J.D., et al., Identification of skin as a major site of prostaglandin D2 release following oral administration of niacin in humans. J Invest Dermatol, 1992. 98(5): p. 812-5.
14. Wanders, D. and R.L. Judd, Future of GPR109A agonists in the treatment of dyslipidemia. Diabetes Obes Metab, 2011.
15. Kamanna, V.S. and M.L. Kashyap, Nicotinic acid (niacin) receptor agonists: Will they be useful therapeutic agents? Am J Cardiol, 2007. 100(11): p. 53N-61N.
16. Soudijn, W., I. van Wijngaarden, and A.P. IJzerman, Nicotinic acid receptor subtypes and their ligands. Med Res Rev, 2007. 27(3): p. 417-433.
17. Lai, E., et al., Effects of a niacin receptor partial agonist, MK-0354, on plasma free fatty acids, lipids, and cutaneous flushing in humans. J Clin Lipidol, 2008. 2(5): p. 375-83.
18. van Herk, T., et al., Pyrazole derivatives as partial agonists for the nicotinic acid receptor. J Med Chem, 2003. 46(18): p. 3945-51.
19. Richman, J.G., et al., Nicotinic acid receptor agonists differentially activate downstream effectors. J Biol Chem, 2007. 282(25): p. 18028-18036.
20. Cheng, Y. and W.H. Prusoff, Relationship between the inhibition constant (K1) and the concentration of inhibitor which causes 50 per cent inhibition (I50) of an enzymatic reaction. Biochem Pharmacol, 1973. 22(23): p. 3099-108.
21. Adamson, J.E., H.H. Crawford, and C.E. Horton, The action of dimethyl sulfoxide on the experimental pedicle flap. Surg Forum, 1966. 17: p. 491-2.
22. Colucci, M., et al., New insights of dimethyl sulphoxide effects (DMSO) on experimental in vivo models of nociception and inflammation. Pharmacol Res, 2008. 57(6): p. 419-25.
23. Jacob, S.W. and R. Herschler, Pharmacology of DMSO. Cryobiology, 1986. 23(1): p. 14-27.
24. Kligman, A.M., Topical Pharmacology and Toxicology of Dimethyl Sulfoxide. 1. JAMA, 1965. 193: p. 796-804.
25. Santos, N.C., et al., Multidisciplinary utilization of dimethyl sulfoxide: pharmacological, cellular, and molecular aspects. Biochem Pharmacol, 2003. 65(7): p. 1035-41.
26. Zhang, Y.Y., et al., Niacin mediates lipolysis in adipose tissue through its G protein-coupled receptor HM74A. Biochem Biophys Res Commun, 2005. 334(2): p. 729-732.
27. Semple, G., et al., 3-(1H-tetrazol-5-yl)-1,4,5,6-tetrahydro-cyclopentapyrazole (MK-0354): A partial agonist of the nicotinic acid receptor, G protein-coupled receptor 109A, with antilipolytic but no vasodilatory activity in mice. J Med Chem, 2008. 51(16): p. 5101-5108.

28. Davidson, N.O. and G.S. Shelness, APOLIPOPROTEIN B: mRNA editing, lipoprotein assembly, and presecretory degradation. Annu Rev Nutr, 2000. 20: p. 169-93.
29. Davis, R.A., Cell and molecular biology of the assembly and secretion of apolipoprotein B-containing lipoproteins by the liver. Biochim Biophys Acta, 1999. 1440(1): p. 1-31.
30. Shelness, G.S. and J.A. Sellers, Very-low-density lipoprotein assembly and secretion. Curr Opin Lipidol, 2001. 12(2): p. 151-7.
31. Bartolomé, N., et al., Kupffer cell products and interleukin 1beta directly promote VLDL secretion and apoB mRNA up-regulation in rodent hepatocytes. Innate Immun, 2008. 14(4): p. 255-66.
32. Basciano, H., et al., LXRalpha activation perturbs hepatic insulin signaling and stimulates production of apolipoprotein B-containing lipoproteins. Am J Physiol Gastrointest Liver Physiol, 2009. 297(2): p. G323-32.

Chapter 6

LXR activation is essential to induce atherosclerotic plaque regression in C57BL/6 mice

Zhaosha Li[1*], Marco van der Stoep[1*], Ronald J. van der Sluis[1], Heather J. McKinnon[2], Martin J. Smit[3], Miranda Van Eck[1], Theo J.C. Van Berkel[1], Menno Hoekstra[1]

[1]Division of Biopharmaceutics, Leiden/Amsterdam Center for Drug Research, Leiden University, The Netherlands.
[2]Schering-Plough (Part of the MSD Organisation), Newhouse, UK.
[3]Merck Research Laboratories, MSD Oss, The Netherlands.
[*]These authors contributed equally to this work.

Submitted for publication

ABSTRACT

Background & Aims: LXR activation leads to a number of favorable changes in lipid metabolism. LXR agonists have been shown to attenuate the progression of atherosclerosis. It is thus interesting to examine whether rapidly improved plasma lipoprotein profiles combined with LXR activation can lead to atherosclerotic lesion regression.
Methods and Results: $LDLr^{-/-}$ and C57BL/6 mice were fed with atherogenic diet to induce atherosclerotic development, after which the diet was switched to chow diet with or without supplementation of LXR agonist T0901317. In $LDLr^{-/-}$ mice, LXR activation did not induce atherosclerotic plaque regression. In C57BL/6 mice, LXR agonist dramatically improved plasma lipoprotein profile, including large reductions in (V)LDL and brisk enhancements in HDL. T0901317 induced favourable hepatic gene expression profiles. T0901317 significantly increased hepatic expression of ABCA1, ABCG1, and SR-BI, suggesting enhanced reverse cholesterol transport. Subsequently, T0901317 supplemented in chow diet significantly reduced the pre-existing atherosclerotic plaque size (-43%).
Conclusions: The current study shows that 1) intact LDL receptor function is crucial to overcome LXR-induced hyperlipidemia; and 2) rapidly optimized plasma lipoprotein profiles combined with LXR agonist induced favorable gene expression profiles can induce regression of pre-existing atherosclerotic plaques.
Keywords: LXR, T0901317, lipoprotein, atherosclerosis, regression

INTRODUCTION

Hypercholesterolemia holds a critical role in the development of atherosclerosis[1]. Lowering of very-low-density lipoprotein- (VLDL-) and low-density lipoprotein- (LDL-) cholesterol levels leads to reduction in cardiovascular morbidity and mortality in individuals at risk for cardiovascular events[2,3]. High-density lipoprotein (HDL) is an anti-atherosclerotic lipoprotein based on its ability to mediate reverse cholesterol transport (RCT), which is a major protective system against atherosclerosis[4]. HDL can remove cholesterol from the periphery, allowing it to be cleared by the liver and then excreted into the bile[5]. Cholesterol efflux from macrophages to HDL is a crucial step in RCT[6]. Modulation of the major molecular mediators in RCT, such as ATP binding cassette transporter A1 (ABCA1), ATP binding cassette transporter G1 (ABCG1), and scavenger receptor class B1 (SR-B1) has consistent beneficial effects on RCT and atherosclerosis[7,8]. Agents that raise HDL and promote RCT, including statins, fibrates, nicotinic acids, and liver X receptor (LXR) agonists thus represent promising treatments for atherosclerotic disease[9].

LXRs play an important role in the maintenance of cellular and systemic cholesterol homeostasis[10]. Pharmacological activation of LXRs *in vivo* leads to a number of favorable changes in lipid metabolism[11,12]. Synthetic LXR agonists promote biliary sterol secretion, reduce cholesterol absorption, and increase fecal sterol excretion[13,14]. In addition, LXR activation significantly enhances the ABCA1- and ABCG1-mediated cholesterol efflux to nascent HDL particles and inhibits the atherosclerosis development in animal models[15,16].

While numerous studies have been dedicated to inhibit the progression of atherosclerosis, recent attention has been focused on reversing atherosclerosis, which is the regression of existing atherosclerotic plaque. The first evidence of dramatic atherosclerotic regression in mice was achieved by Trogan *et al* via robust surgical measures, such as aortic transplantation, to rapidly improve the plaque environment[17]. This study suggested that the essential prerequisite promoting regression of atherosclerosis lesion is the robust improvement in plasma lipoprotein profiles and plaque milieu, including large reductions in plasma atherogenic apoB-lipoproteins and brisk enhancements in efflux of cholesterol from plaques. Recently, the same group has demonstrated that LXR expression in the plaque is required for maximal effects on plaque macrophage egression during atherosclerosis regression in mice[18].

LXR activation has been shown to significantly up-regulate cholesterol efflux activity and inhibit development of atherosclerosis, providing direct evidence for an anti-atherogenic effect of LXR agonists[19,20]. However, in these studies, LXR agonists are only shown to attenuate the progression of atherosclerosis in mouse models, while their potential to abrogate pre-existing cardiovascular disease and to stabilize the established atherosclerotic lesions has not been widely addressed. It is thus interesting to examine whether rapidly improved plasma lipoprotein profiles combined with therapeutic LXR agonist-induced activation of RCT and cholesterol efflux could lead to atherosclerotic lesion regression. In the current study, we specifically evaluated the potential of LXR agonist T0901317 to regress diet-induced pre-existing atherosclerotic plaque in $LDLr^{-/-}$ and C57BL/6 mice.

MATERIALS AND METHODS

Animals
For the study on LDLr$^{-/-}$ mice, male homozygous LDL receptor-deficient mice (LDLr$^{-/-}$; C57BL/6 background) of 12 weeks old were used. The animals were fed with semi-synthetic Western-type diet (WTD) containing 15% (w/w) fat and 0.25% (w/w) cholesterol (Diet W, Special Diet Services, Witham, UK) for 6 weeks to induce the development of atherosclerotic lesions. For the study on C57BL/6 mice, female C57BL/6 mice of 12 weeks old were used. The animals were fed with semi-synthetic cholate-containing cholesterol-enriched atherogenic diet containing 15% (w/w) cocoa butter, 1% (w/w) cholesterol, and 0.5% cholate (AB Diets, Woerden, The Netherlands) for 16 weeks to induce the development of atherosclerotic lesions. After the formation of initial atherosclerotic plaques in both studies, diet was switched to regular cholesterol-free chow diet containing 4.3% (w/w) fat (RM3, Special Diet Services, Witham, UK) for 3 weeks, with or without supplementation of LXR agonist T0901317 (10 mg/kg/day; MSD Oss, The Netherlands). After euthanization, mice were bled via orbital exsanguination, and perfused *in situ* through the left cardiac ventricle with ice-cold PBS (pH 7.4) for 20 minutes. Tissues were dissected and snap-frozen in liquid nitrogen. Heart and one lobe of the liver were dissected free of fat and stored in 3.7% neutral-buffered formalin (Formal-fixx, Shandon Scientific Ltd., UK) for histological analysis. Animal care and procedures were performed in accordance with the national guidelines for animal experimentation. All protocols were approved by the Ethics Committee for Animal Experiments of Leiden University.

Plasma lipid analysis
Plasma lipid analysis was performed at different time points throughout the experiments. At the endpoint, mice were not fasted prior to euthanization. Plasma concentrations of total cholesterol (TC) and triglycerides (TG) were measured using the enzymatic colorimetric assay (Roche Diagnostics, Mannheim, Germany). The distribution of cholesterol over different lipoproteins in plasma was determined by fast protein liquid chromatography (FPLC) through a Superose 6 column (3.2 x 30 mm; Smart-System, Pharmacia, Uppsala, Sweden). Cholesterol content of the lipoprotein fractions was determined as described above.

Hepatic lipid analysis
Lipids were extracted from the liver using the Folch method. Briefly, 100 mg of tissue was homogenized with chloroform/methanol (1:2). The homogenate was centrifuged to recover the upper phase, which was further washed with chloroform-0.9% NaCl (1:1, pH 1.0). After centrifugation, the lower chloroform phase containing lipids was evaporated and the retained lipids were resolubilized in 2% Triton X-100 by sonification. Protein contents were analyzed by BCA assay (Pierce Biotechnology, Thermo Fisher Scientific BV, IL, USA). Cholesterol content of lipid extracts was determined as described above. Data were expressed as milligrams of lipid per milligram of protein.

RNA isolation and gene expression analysis
Total RNA from the liver was isolated using acid guanidinium thiocyanate (GTC)-phenol-chloroform extraction. Briefly, 500 µL of GTC solution (4 M guanidine

isothiocyanate, 25 mM sodium citrate, 0.5% N-lauroylsarcosine) was added to each sample, followed by acid phenol:chloroform extraction. The RNA in aqueous phase was precipitated with isopropanol. The quantity and purity of the isolated RNA were examined using ND-1000 Spectrophotometer (Nanodrop, Wilmington, DE, USA). One microgram of the isolated RNA from each sample was converted into cDNA by reverse transcription with RevertAid™ M-MuLV Reverse Transcriptase (Promega, Madison, WI, USA). Negative controls without addition of reverse transcriptase were prepared for each sample. Quantitative real-time PCR was carried out using ABI Prism 7700 Sequence Detection system (Applied Biosystems, Foster City, CA, USA) according to the manufacturer's instructions. 36B4, Beta-actin, and GAPDH were used as internal housekeeping genes. The gene-specific primer sequences used are listed in Table 1. Amplification curves were analyzed using 7500 Fast System SDS software V1.4 (Applied Biosystems, Foster City, CA, USA). The relative expression of each gene was expressed as fold changes $2^{-(\Delta\Delta CT)}$ compared to baseline group. Standard error of the mean (SEM) and statistical significance were calculated using ΔΔCt formula.

Table 1. Murine primers for quantitative real-time PCR analysis

Gene	Forward primer	Reverse Primer
36B4	GGACCCGAGAAGACCTCCTT	GCACATCACTCAGAATTTCAATGG
Beta-actin	AACCGTGAAAAGATGACCCAGAT	CACAGCCTGGATGGCTACGTA
GAPDH	TCCATGACAACTTTGGCATTG	TCACGCCACAGCTTTCCA
ABCA1	GGAGTTCTTTGCCCTCCTGAG	AGTTTGCGAATTGCCCATTC
ABCG1	AGGTCTCAGCCTTCTAAAGTTCCTC	TCTCTCGAAGTGAATGAAATTTATCG
ABCG5	TGGCCCTGCTCAGCATCT	ATTTTTAAAGGAATGGGCATCTCTT
ABCG8	CCGTCGTCAGATTTCCAATGA	GGCTTCCGACCCATGAATG
SR-BI	GGCTGCTGTTTGCTGCG	GCTGCTTGATGAGGGAGGG
LPL	CCAGCAACATTATCCAGTGCTAG	CAGTTGATGAATCTGGCCACA
FAS	GGCATCATTGGGCACTCCTT	GCTGCAAGCACAGCCTCTCT
CYP7A1	CTGTCATACCACAAAGTCTTATGTCA	ATGCTTCTGTGTCCAAATGCC
SREBP-1c	GGAGCCATGGATTGCACATT	CCTGTCTCACCCCCAGCATA
CD68	CCTCCACCCTCGCCTAGTC	TTGGGTATAGGATTCGGATTTGA

Histological analysis

Accumulation of lipids in the liver and the atherosclerotic plaques at the aortic root in the heart was analyzed. The liver and heart was cut latitudinally and embedded in O.C.T™ Compound (Tissue-Tek, Sakura finetek, Tokyo, Japan), and subsequently sectioned using a Leica CM 3050S cryostat at 10 μm intervals. Cryostat sections were stained with Oil-red O (Sigma-Aldrich) to identify lipids, and counterstained with hematoxylin (Sigma-Aldrich) to assist in tissue visualization. Quantitative analysis of the atherosclerotic lesion area at the aortic root was performed in a blinded fashion. Mean lesion area (in μm^2 per aortic root per mouse) was calculated from ten Oil-red O stained cryostat sections, starting at the appearance of the tricuspid valves.

Statistical analysis

Statistical analyses were performed by the unpaired Student's t-test for independent samples (Instat GraphPad software, San Diego, USA). Statistical significance was defined as $p<0.05$. Data are expressed as means ± SEM.

RESULTS

LXR activation does not induce atherosclerotic plaque regression in LDLr$^{-/-}$ mice

LDLr$^{-/-}$ mice are an established mouse model to study atherogenesis[21,22]. To evaluate the potential of LXR agonists to regress pre-existing atherosclerotic lesions, we fed the LDLr$^{-/-}$ mice with high-fat high-cholesterol Western-type diet (WTD) for 6 weeks to develop atherosclerotic plaques. Subsequently, a group of mice was sacrificed to obtain baseline data, whilst the remainder of the mice was switched to a low-fat cholesterol-free chow diet without or with LXR agonist T0901317 supplementation for 3 weeks.

WTD markedly increased plasma total cholesterol from basal level 235 mg/dL to 1220 mg/dL. Subsequently, when the atherogenic WTD was switched back to cholesterol-free chow diet alone, plasma total cholesterol concentration decreased significantly within one week, and after 3 weeks dropped back to almost basal level (400 mg/dL; Figure 1A). In contrast, T0901317 treatment supplemented in chow diet further increased plasma total cholesterol level up to approximately 2000 mg/dL, which was 1.6-fold higher than baseline ($p<0.001$) and 5-fold higher than the group fed with chow diet alone ($p<0.001$) (Figure 1A). As determined by FPLC lipoprotein separation, the largely enhanced plasma total cholesterol concentration after T0901317 treatment was due to markedly elevated plasma VLDL-cholesterol (23-fold; $p=0.001$) and LDL-cholesterol levels (3-fold; $p=0.04$) (Figure 1B).

6 weeks of atherogenic WTD-feeding induced atherosclerotic lesion development to approximately $60x10^3$ μm^2 at aortic root as baseline, visualized by oil Red-O staining of cryosections (Figure 1C). After the diet was switched to regular chow diet alone, lesion size surprisingly progressed (3-fold; $p<0.001$) despite of the significantly normalized plasma lipoprotein profile in this group (Figure 1C). In the mice treated with T0901317, lesion size also increased 3-fold ($p<0.01$) compared to baseline. However, despite its 5-fold higher plasma total cholesterol level compared to mice fed with chow diet alone, the increase in the lesion size from T0901317-treated mice was not larger than the chow group (Figure 1C). It is interesting that the atherosclerotic lesion progression in LDLr$^{-/-}$ mice was not concomitant with the changes in plasma lipoprotein profiles. We thus measured the ratio between the increase in lesion size and the plasma total cholesterol concentration. T0901317 induced 7-fold less lesion progression per unit of plasma cholesterol concentration compared to mice fed with chow diet alone ($p<0.001$) (Figure 1D).

Taken together, switching atherogenic WTD to cholesterol-free chow diet rapidly normalized plasma lipoprotein profiles, but this measure alone was not enough to attenuate atherosclerotic lesion progression or induce lesion regression in LDLr$^{-/-}$ mice. LXR agonist treatment in LDLr$^{-/-}$ mice failed to normalize plasma lipoprotein profiles, and thus failed to induce regression of pre-existing aterhosclerotic lesion. This may be due to the absence of hepatic LDL receptors, thus LDLr$^{-/-}$ mice exhibit prolonged half lives of plasma VLDL and LDL[23]. Furthermore, the absence of LDL receptor-mediated uptake leads to increased (V)LDL synthesis, which is further enhanced by LXR activation[24,25]. However, T0901317 significantly attenuated the lesion progression per increase of plasma cholesterol concentration.

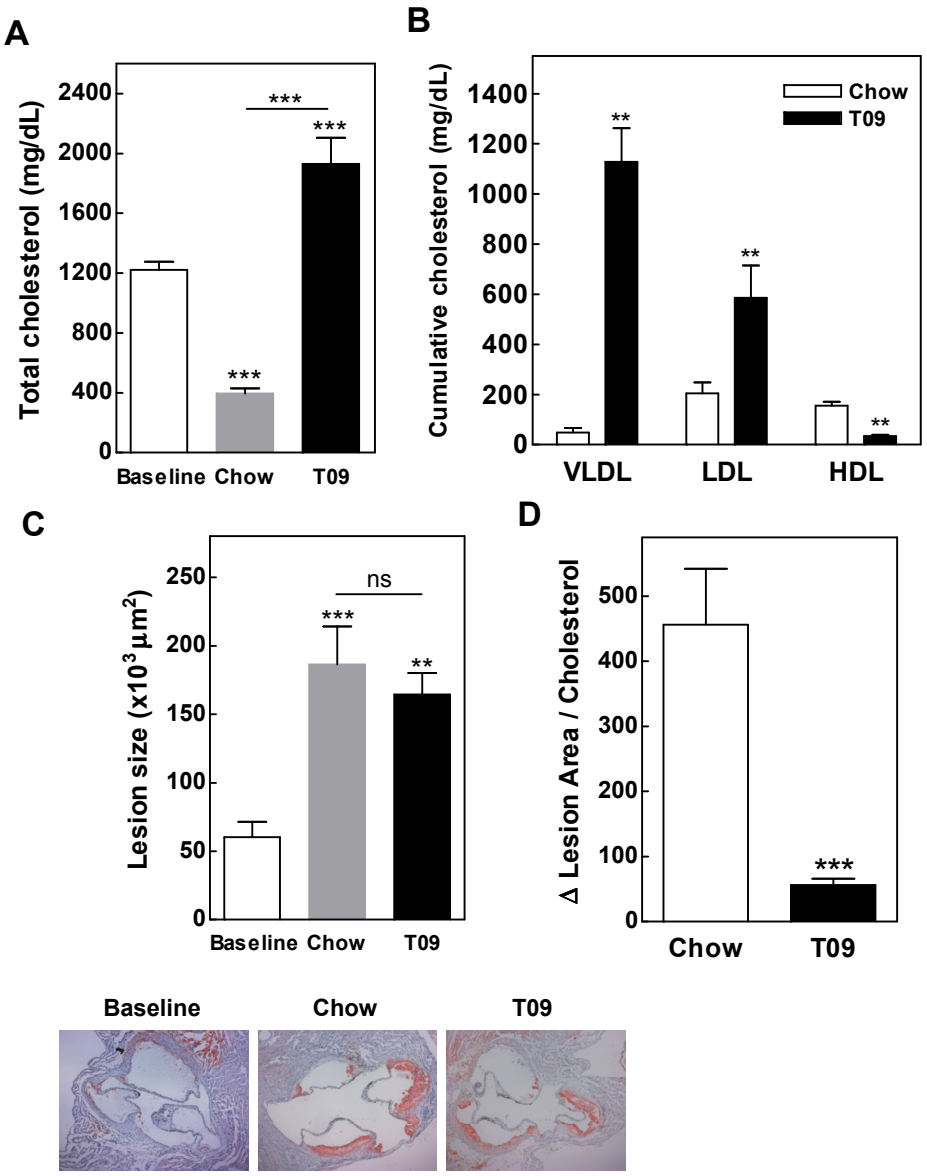

Figure 1. Effects of LXR agonist in LDLr$^{-/-}$ mice. LDLr$^{-/-}$ mice were fed WTD for 6 weeks, after which a group of mice was sacrificed (Baseline), whilst the remainder of the mice was switched to regular chow diet without (Chow) or with LXR agonist T0901317 supplementation (T09) for 3 weeks. Plasma total cholesterol concentration was measured (A). Plasma lipoproteins were separated by FPLC and cholesterol level was measured in each fraction. VLDL represents the sum of cholesterol concentrations from fraction 2 to 7 (VLDL fractions); LDL represents the sum of cholesterol concentrations from fraction 8 to 14 (LDL fractions); HDL represents the sum of cholesterol concentrations from fraction 15 to 22 (HDL fractions) (B). Cryostat sections of the aortic root in heart were stained with oil-red O to identify lipids, and the lesion size was quantified (C). The ratio between the change in lesion size and the plasma total cholesterol concentration was calculated (D). Values are means ± SEM (8 mice per group). **P<0.01; ***P<0.001.

LXR agonist dramatically improved plasma lipoprotein profile in C57BL/6 mice

Because the plasma basal level of (V)LDL-cholesterol in C57BL/6 mice is lower than in LDLr$^{-/-}$ mice, we set out to evaluate the effects of LXR agonist on plaque regression in C57BL/6 mice. The C57BL/6 mouse model has been used to study diet-induced atherosclerosis[26,27,28]. This murine model of atherogenesis represents an alternative to the use of genetically modified mice with impaired lipoprotein clearance, i.e. LDLr$^{-/-}$ mice, for the evaluation of anti-hyperlipidemic agents, including LXR agonists[29]. Here we fed C57BL/6 mice with cholate-containing cholesterol-enriched atherogenic diet for 16 weeks to induce atherosclerotic plaque development. Subsequently, a group of mice were sacrificed to obtain baseline data, whilst the remainder of the mice was switched to low-fat cholesterol-free chow diet without or with LXR agonist T0901317 supplementation for 3 weeks.

Atherogenic diet markedly increased plasma total cholesterol level from basal 30 mg/dL to approximately 300 mg/dL (10-fold; $p<0.001$). When diet was switched to chow diet alone, plasma total cholesterol level decreased significantly within one week, and after 3 weeks dropped back to 65 mg/dL (-80%, $p<0.001$), close to its basal level (Figure 2A). In this mouse model, the presence of T0901317 in chow diet did not elevate the cholesterol levels, and actually a similar 3-fold reduction in plasma total cholesterol concentration was noticed as compared to chow group ($p<0.001$) (Figure 2A). T0901317 did not significantly increase plasma triglycerides levels as compared to chow group (Figure 2B). As determined by FPLC lipoprotein separation, the largely reduced plasma total cholesterol concentration was majorly due to markedly decreased plasma VLDL- and LDL-cholesterol levels. Switching to regular chow diet alone significantly reduced plasma (V)LDL-cholesterol concentration (4-fold, $P < 0.001$). T0901317 treatment in C57BL/6 mice did not induce elevated (V)LDL-cholesterol levels, and actually reduced plasma (V)LDL-cholesterol concentration dramatically (28-fold compared to baseline, $P < 0.001$) (Figure 2C).

In contrast to a decreased plasma HDL-cholesterol level in C57BL/6 mice fed with chow diet alone, T0901317 significantly increased the plasma HDL-cholesterol concentration (+30%; $p<0.05$), which was 2-fold higher ($p<0.01$) than group with chow diet alone (Figure 2C). The ratio between HDL- and non-HDL-cholesterol concentration was dramatically increased by T0901317 treatment (13-fold; $p<0.001$) (Figure 2C).

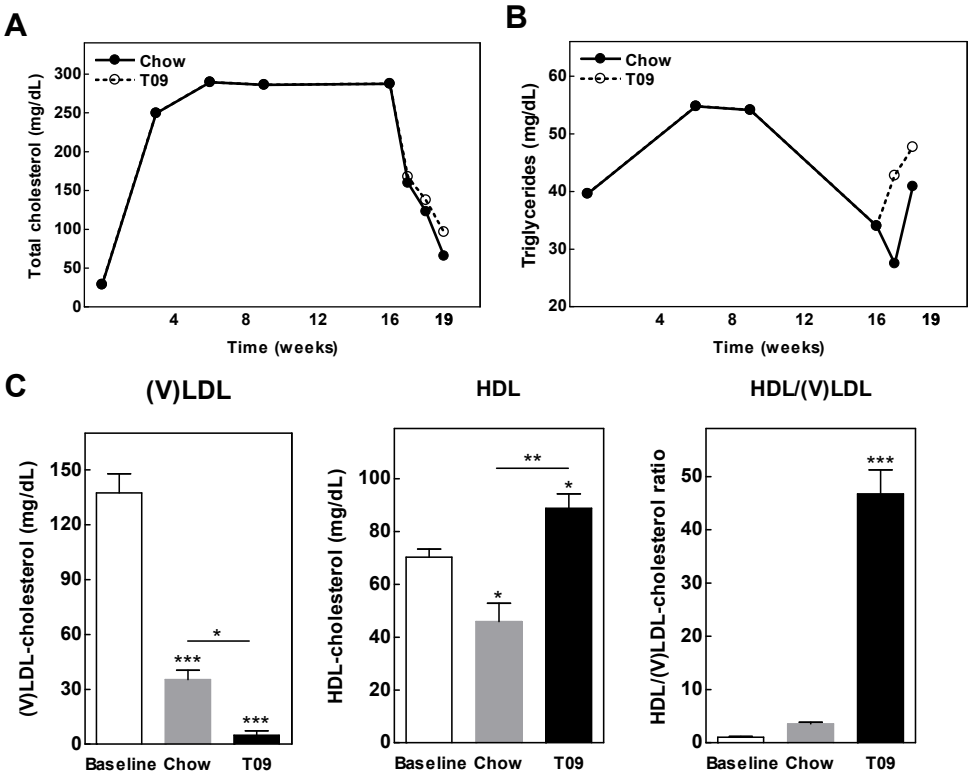

Figure 2. Effects of LXR agonist on plasma lipids in C57BL/6 mice. C57BL/6 mice were fed atherogenic diet for 16 weeks, after which a group of mice was sacrificed (Baseline), whilst the remainder of the mice was switched to regular chow diet without (Chow) or with LXR agonist T0901317 supplementation (T09) for 3 weeks. Plasma total cholesterol (A) and triglycerides (B) concentration were measured. Plasma lipoproteins were separated by FPLC and cholesterol level was measured in each fraction. VLDL represents the sum of cholesterol concentrations from fraction 2 to 7 (VLDL fractions); LDL represents the sum of cholesterol concentrations from fraction 8 to 14 (LDL fractions); HDL represents the sum of cholesterol concentrations from fraction 15 to 22 (HDL fractions) (B). The ratio between HDL- and non-HDL-cholesterol concentration was calculated (C). Values are means ± SEM (8 mice per group). *P<0.05; **P<0.01; ***P<0.001.

LXR agonist dramatically reduced hepatic cholesterol concentration in C57BL/6 mice

Atherogenic diet feeding induced severe liver steatosis in C57BL/6 mice, indicated by enlarged liver size (figure not shown) and intensive accumulation of lipids shown by oil-Red O staining (Figure 3B). However, switching to regular chow diet rapidly reduced liver steatosis. Chow diet alone reduced the hepatic cholesterol content significantly (-27%, P<0.05), while T0901317 supplemented in chow further reduced hepatic cholesterol content (-63%, P<0.001 compared to baseline; -50%, P<0.01 compared to chow group) (Figure 3A). The reduction of cholesterol content was visualized as attenuated neutral lipid staining in liver cryosections (Figure 3B). In addition to the reduced hepatic cholesterol content, hepatic gene expression of macrophage marker CD68 also decreased (-70%, P<0.001) compared to baseline (Figure 3C), indicating largely attenuated hepatic macrophage content and inflammation under chow diet conditions[30,31,32].

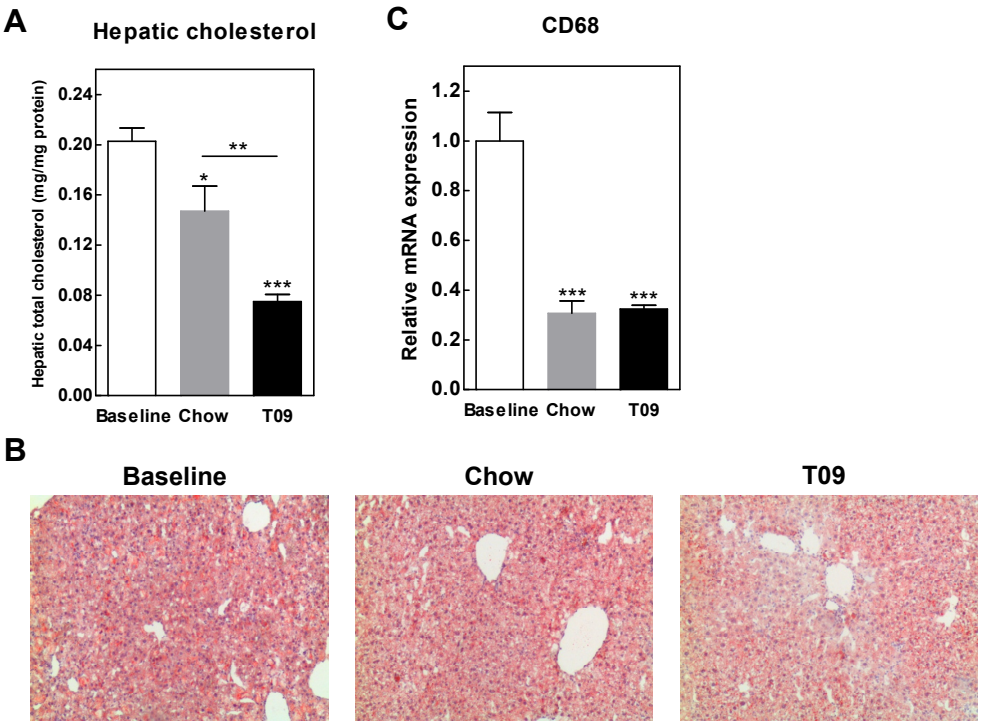

Figure 3. Effects of LXR agonist on hepatic lipids in C57BL/6 mice. Lipids were extracted from liver and hepatic cholesterol concentration was measured (A). Cryostat sections of the liver were stained with oil-red O to identify lipids, and counterstained with hematoxylin to assist in tissue visualization (original magnification: x4) (B). Total RNA was extracted from liver and relative mRNA expression of CD68 was assessed by quantitative PCR and presented as fold-change relative to baseline group (C). Values are means ± SEM (8 mice per group). *P<0.05; **P<0.01; ***P<0.001.

LXR agonist regulated hepatic gene expression in C57BL/6 mice

As expected, T0901317 treatment strongly up-regulated the hepatic expression of the LXR target genes FAS (p<0.001), SREBP-1c (p<0.001) (Figure 4A), and the hepatic triglyceride level (data now shown). This LXR agonist-induced hepatic lipogenesis has been well established as a positive control for LXR activation in mice[33,34].

T0901317 significantly up-regulated the hepatic expression of LDL-receptor compared to group fed chow diet alone (1.7-fold, *P*<0.05) (Figure 4B), suggesting enhanced LDL uptake by the liver in C57BL/6 mice. In addition, T0901317 significantly up-regulated the hepatic expression of ABCG5 (4-fold, *P*<0.05), ABCG8 (2.6-fold, *P*<0.01), and CYP7A1 (1.7-fold, *P*<0.01) compared to group with chow diet alone (Figure 4B), suggesting promoted biliary cholesterol secretion after LXR activation.

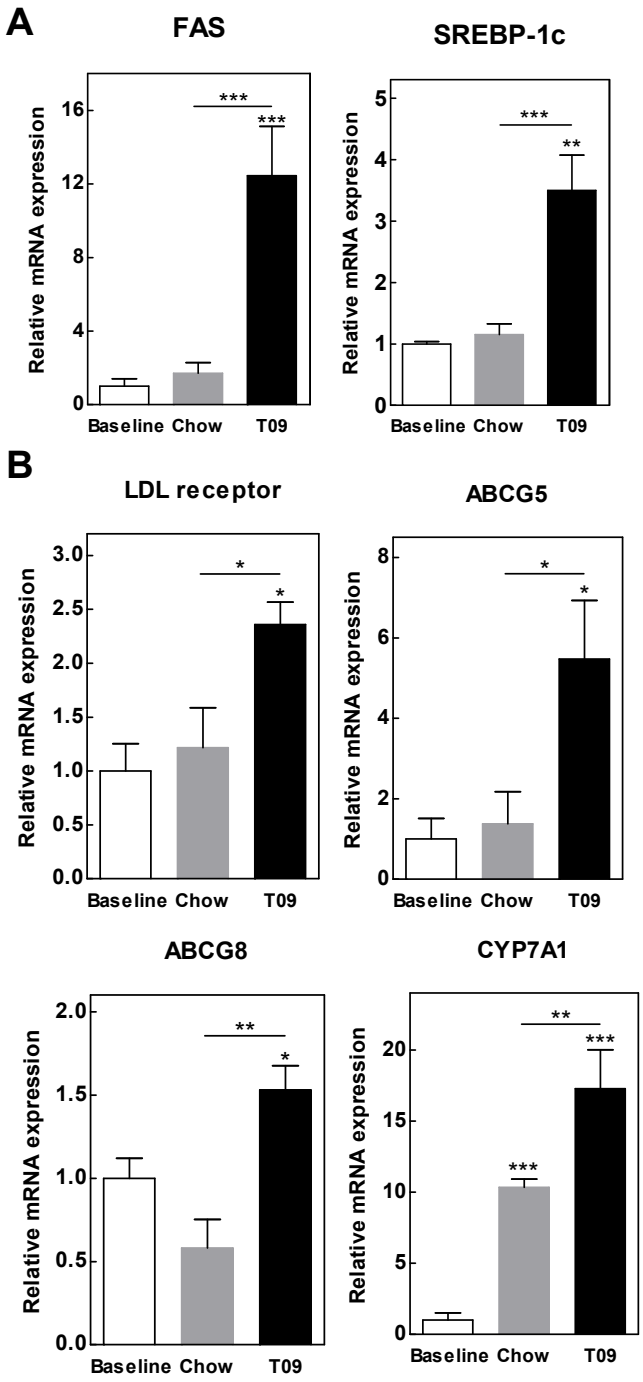

Figure 4. Effects of LXR agonist on hepatic gene expression profiles in C57BL/6 mice. Total RNA was extracted from liver, and relative mRNA expression of FAS, SREBP-1c (A), LDL receptor, ABCG5, ABCG8, and CYP7A1 (B) were determined by quantitative PCR and presented as fold-change relative to baseline group (C). Values are means ± SEM (8 mice per group). *P<0.05; **P<0.01; ***P<0.001.

In line with the elevated plasma HDL-cholesterol level, T0901317 significantly increased the hepatic expression of ABCA1 (+75%, *P*<0.05), ABCG1 (2.3-fold, *P*<0.01), and SR-BI (+70%, *P*<0.05) compared to chow group (Figure 5), suggesting that LXR activation promoted cholesterol efflux and reverse cholesterol transport. T0901317 also significantly increased the hepatic expression of lipoprotein lipase (LPL) (4.5-fold, *P*<0.001) (Figure 5), indicating an enhanced hydrolysis capacity of triacylglycerol component of circulating chylomicrons and VLDL.

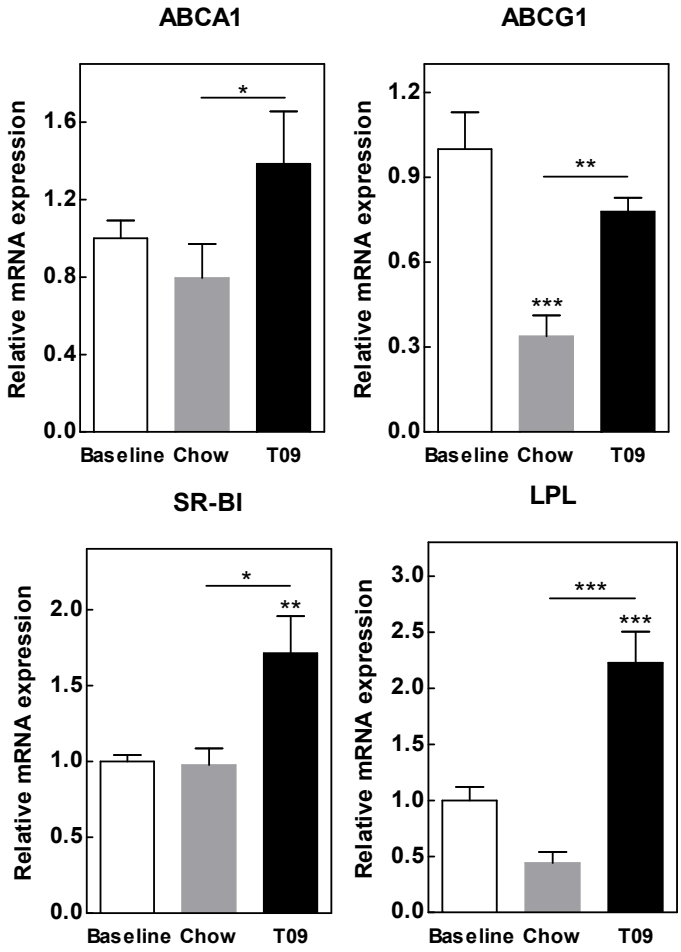

Figure 5. Effects of LXR agonist on hepatic expression of reverse cholesterol transport-related genes in C57BL/6 mice. Total RNA was extracted from liver, and relative mRNA expression of ABCA1, ABCG1, SR-BI, and LPL were determined by quantitative PCR and presented as fold-change relative to baseline group (C). Values are means ± SEM (8 mice per group). *P<0.05; **P<0.01; ***P<0.001.

LXR agonist induced atherosclerotic plaque regression in C57BL/6 mice

After atherogenic diet feeding, C57BL/6 mice developed initial atherosclerotic lesion of approximately $43x10^3$ μm^2 at aortic root as baseline (Figure 6). Three weeks after the diet was switched to chow diet alone, the lesion size stayed

unchanged at approximately $50x10^3$ μm^2, despite of a significantly normalized plasma lipoprotein profile. In contrast, T0901317 treatment supplemented in chow diet significantly reduced the pre-existing atherosclerotic plaque to approximately $25x10^3$ μm^2 (-43%, $P<0.05$), indicating that LXR agonist treatment successfully induced atherosclerotic lesion regression in C57BL/6 mice.

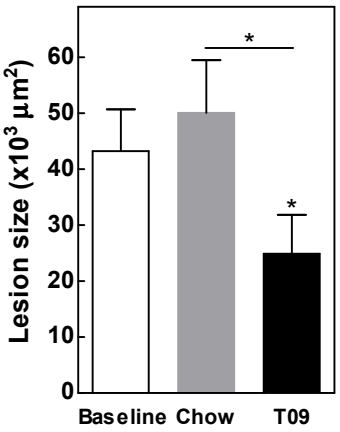

Figure 6. Effects of LXR agonist on atherosclerotic lesion development in C57BL/6 mice. Cryostat sections of the aortic root in heart were stained with oil-red O to identify lipids, and the lesion size was quantified. Values are means ± SEM (8 mice per group). *P<0.05.

DISCUSSION

In the current study, we evaluated the potential of LXR agonist T0901317 to regress diet-induced pre-existing atherosclerotic plaque in $LDLr^{-/-}$ and C57BL/6 mouse models. Our results show that LXR activation is crucial for atherosclerotic lesion regression. In C57BL/6 mouse with diet-induced lesion, LXR agonist supplemented in chow diet rapidly optimized plasma lipoprotein profiles and promoted reverse cholesterol transport, and subsequently induced regression of pre-existing atherosclerotic plaques.

The LXR agonist exhibited opposite effects on plasma lipoprotein and atherosclerotic lesion development in $LDLr^{-/-}$ and C57BL/6 mice. The unfavorable lipoprotein profile induced by LXR agonist in $LDLr^{-/-}$ mice prevented its beneficial effects on atherosclerotic lesion formation. The absence of the LDL receptor and thus impaired LDL clearance and increased VLDL secretion in $LDLr^{-/-}$ mice hampered the LXR agonist-induced lowering of plasma (V)LDL-cholesterol. The LDL receptor-mediated cholesterol uptake and feedback regulation are crucial when evaluating LDL-lowering effects of compounds[35]. Recent studies have shown that when LDL receptor gene was transferred back into hypercholesterolemic $LDLr^{-/-}$ mice to restore sustained expression of LDL-receptor protein in the liver, there was a drastic reduction in plasma cholesterol and non-HDL cholesterol levels and a pronounced regression of advanced atherosclerotic lesions[36,37]. Thus, it is proposed that intact LDL receptor is crucial for creating a lipoprotein profile which permits the regression of atherosclerotic lesions.

Cholesterol-enriched diets are often used to induce or accelerate atherosclerotic lesion progression in murine models. It appears that the induction of persistent hypercholesterolemia to levels higher than approximately 300 mg/dL is required for the development of experimental atherosclerosis in mouse[38]. In the current study, atherogenic diet feeding induced persistent hypercholesterolemia and initial atherosclerotic plaque development. After switching atherogenic diet to regular chow diet, there was a rapid and dramatic reduction in plasma total cholesterol level in both LDLr$^{-/-}$ and C57BL/6 mice, indicating that, with dietary cholesterol being the major proatherogenic component, low-fat cholesterol-free chow diet can largely improve plasma lipoprotein profile to achieve a regressive environment. However, despite the improved plasma lipoprotein profile, chow diet alone did not induce lesion regression in C57BL/6 mice, while in LDLr$^{-/-}$ mice the lesion size even increased. Similar observations were reported in literature where switching high-fat atherogenic diet to a standard chow diet led to markedly reduced plasma (V)LDL-cholesterol without significant reduction in lesion size[39], or with even significantly increased lesion size[40]. Taken together, our data further confirmed that improved plasma lipoprotein profile induced by chow diet alone is not enough to trigger atherosclerotic plaque regression.

The LXR agonist induced plaque regression is due to multiple metabolic effects. The LXR agonist T0901317 not only reduced plasma (V)LDL-cholesterol levels, but also significantly increased HDL-cholesterol level, leading to a 10-fold increased ratio between anti-atherogenic HDL and pro-atherogenic (V)LDL-cholesterol. This indicates that LXR agonist, supplemented in chow diet, rapidly optimizes the plasma lipoprotein profile and achieves a regressive plasma environment in C57BL/6 mice. In addition, the LXR agonist increased the hepatic expression of ABCG5, ABCG8, and CYP7A1, indicating down-regulated cholesterol absorption and up-regulated biliary sterol secretion[41]. Furthermore, the LXR agonist increased the hepatic expression of ABCA1, SRBI, and ABCG1, suggesting increased HDL synthesis, promoted reverse cholesterol transport, and diminished macrophage foam cell formation[42,43].

In conclusion, the current study shows that 1) intact LDL receptor function is crucial to overcome LXR-induced hyperlipidemia; and 2) rapidly optimized plasma lipoprotein profiles combined with LXR agonist induced favorable gene expression profiles can induce regression of pre-existing atherosclerotic plaques in C57BL/6 mice. In addition, our study shows that C57BL/6 mice with diet-induced atherosclerotic lesions may provide an alternative model to investigate plaque regression without robust surgical measures. Further investigations in more humanized animal models may similarly show the potential beneficial effects of LXR activation in the reversal of pre-existing atherosclerotic lesions.

ACKNOWLEDGEMENTS

This work was supported by TIPharma (Grant T2-110 to Z.L., T.J.C.V.B., M.H.) and the Netherlands Heart Foundation (Grant 2008T070 to M.H.).

REFERENCES

1. Aikawa M, Libby P. Lipid lowering therapy in atherosclerosis. Semin Vasc Med. 2004;4:357-366.
2. Paras C, Hussain MM, Rosenson RS. Emerging drugs for hyperlipidemia. Expert Opin Emerg Drugs. 2010;15:433-451.
3. Toutouzas K, Drakopoulou M, Skoumas I, Stefanadis C. Advancing therapy for hypercholesterolemia. Expert Opin Pharmacother. 2010;11:1659-1672.
4. Lee JM, Choudhury RP. Atherosclerosis regression and high-density lipoproteins. Expert Rev Cardiovasc Ther. 2010;8:1325-1334.
5. Ragbir S, Farmer JA. Dysfunctional high-density lipoprotein and atherosclerosis. Curr Atheroscler Rep. 2010;12:343-348.
6. Ye D, Lammers B, Zhao Y, Meurs I, Van Berkel T, Van Eck M. ATP-Binding Cassette Transporters A1 and G1, HDL Metabolism, Cholesterol Efflux, and Inflammation: Important Targets for the Treatment of Atherosclerosis. Curr Drug Targets. 2010. [Epub ahead of print]
7. Lund-Katz S, Phillips MC. High density lipoprotein structure-function and role in reverse cholesterol transport. Subcell Biochem. 2010;51:183-227.
8. Meurs I, Van Eck M, Van Berkel TJ. High-density lipoprotein: key molecule in cholesterol efflux and the prevention of atherosclerosis. Curr Pharm Des. 2010;16:1445-1467.
9. Spillmann F, Schultheiss HP, Tschöpe C, Van Linthout S. High-density lipoprotein-raising strategies: update 2010. Curr Pharm Des. 2010;16:1517-1530.
10. Repa JJ, Mangelsdorf DJ. The liver X receptor gene team: potential new players in atherosclerosis. Nat Med. 2002;8:1243-1248.
11. Repa JJ, Turley SD, Lobaccaro JA, Medina J, Li L, Lustig K, Shan B, Heyman RA, Dietschy JM, Mangelsdorf DJ. Regulation of absorption and ABC1-mediated efflux of cholesterol by RXR heterodimers. Science. 2000;289:1524-1529.
12. Venkateswaran A, Laffitte BA, Joseph SB, Mak PA, Wilpitz DC, Edwards PA, Tontonoz P. Control of cellular cholesterol efflux by the nuclear oxysterol receptor LXR alpha. Proc Natl Acad Sci U S A. 2000;97:12097-12102.
13. Yu L, York J, von Bergmann K, Lutjohann D, Cohen JC, Hobbs HH. Stimulation of cholesterol excretion by the liver X receptor agonist requires ATP-binding cassette transporters G5 and G8. J Biol Chem. 2003;278:15565-15570.
14. Calpe-Berdiel L, Rotllan N, Fiévet C, Roig R, Blanco-Vaca F, Escolà-Gil JC. Liver X receptor-mediated activation of reverse cholesterol transport from macrophages to feces in vivo requires ABCG5/G8. J Lipid Res. 2008;49:1904-1911.
15. Terasaka N, Hiroshima A, Koieyama T, Ubukata N, Morikawa Y, Nakai D, Inaba T. T-0901317, a synthetic liver X receptor ligand, inhibits development of atherosclerosis in LDL receptor-deficient mice. FEBS Lett. 2003;536:6-11.
16. Tontonoz P, Mangelsdorf DJ. Liver X receptor signaling pathways in cardiovascular disease. Mol Endocrinol. 2003;17:985-993.
17. Trogan E, Feig JE, Dogan S, Rothblat GH, Angeli V, Tacke F, Randolph GJ, Fisher EA. Gene expression changes in foam cells and the role of chemokine receptor CCR7 during atherosclerosis regression in ApoE-deficient mice. Proc Natl Acad Sci U S A. 2006;103:3781-3786.
18. Feig JE, Pineda-Torra I, Sanson M, Bradley MN, Vengrenyuk Y, Bogunovic D, Gautier EL, Rubinstein D, Hong C, Liu J, Wu C, van Rooijen N, Bhardwaj N, Garabedian M, Tontonoz P, Fisher EA. LXR promotes the maximal egress of monocyte-derived cells from mouse aortic plaques during atherosclerosis regression. J Clin Invest. 2010;120:4415-4424.
19. Joseph SB, McKilligin E, Pei L, Watson MA, Collins AR, Laffitte BA, Chen M, Noh G, Goodman J, Hagger GN, Tran J, Tippin TK, Wang X, Lusis AJ, Hsueh WA, Law RE, Collins JL, Willson TM, Tontonoz P. Synthetic LXR ligand inhibits the development of atherosclerosis in mice. Proc Natl Acad Sci U S A. 2002;99:7604-7609.
20. Peng D, Hiipakka RA, Xie JT, Dai Q, Kokontis JM, Reardon CA, Getz GS, Liao S. A novel potent synthetic steroidal liver X receptor agonist lowers plasma cholesterol and triglycerides and reduces atherosclerosis in LDLR–/– mice. Br J Pharmacol. 2011. [Epub ahead of print]
21. Kowala MC, Recce R, Beyer S, Gu C, Valentine M. Characterization of atherosclerosis in LDL receptor knockout mice: macrophage accumulation correlates with rapid and sustained expression of aortic MCP-1/JE. Atherosclerosis. 2000;149:323-330.
22 . Knowles JW, Maeda N. Genetic modifiers of atherosclerosis in mice. Arterioscler Thromb Vasc Biol. 2000;20:2336–2345.

23. Ishibashi S, Brown MS, Goldstein JL, Gerard RD, Hammer RE, Herz J. Hypercholesterolemia in low density lipoprotein receptor knockout mice and its reversal by adenovirus-mediated gene delivery. J Clin Invest. 1993;92:883-893.
24. Joyce CW, Wagner EM, Basso F, Amar MJ, Freeman LA, Shamburek RD, Knapper CL, Syed J, Wu J, Vaisman BL, Fruchart-Najib J, Billings EM, Paigen B, Remaley AT, Santamarina-Fojo S, Brewer HB Jr. ABCA1 overexpression in the liver of LDLr-KO mice leads to accumulation of pro-atherogenic lipoproteins and enhanced atherosclerosis. J Biol Chem. 2006;281:33053-33065.
25. Basciano H, Miller A, Baker C, Naples M, Adeli K. LXRalpha activation perturbs hepatic insulin signaling and stimulates production of apolipoprotein B-containing lipoproteins. Am J Physiol Gastrointest Liver Physiol. 2009;297:G323-G332.
26. Schreyer SA, Wilson DL, LeBoeuf RC. C57BL/6 mice fed high fat diets as models for diabetes-accelerated atherosclerosis. Atherosclerosis. 1998;136:17-24.
27. Paigen B, Mitchell D, Reue K, Morrow A, Lusis AJ, LeBoeuf RC. Ath-1, a gene determining atherosclerosis susceptibility and high density lipoprotein levels in mice. Proc Natl Acad Sci U S A. 1987;84:3763-3767.
28. Liao F, Andalibi A, deBeer FC, Fogelman AM, Lusis AJ. Genetic control of inflammatory gene induction and NF-kappa B-like transcription factor activation in response to an atherogenic diet in mice. J Clin Invest. 1993;91:2572-2579.
29. Johnston TP. The P-407-induced murine model of dose-controlled hyperlipidemia and atherosclerosis: a review of findings to date. J Cardiovasc Pharmacol. 2004;43:595-606.
30. Lanthier N, Molendi-Coste O, Horsmans Y, van Rooijen N, Cani PD, Leclercq IA. Kupffer cell activation is a causal factor for hepatic insulin resistance. Am J Physiol Gastrointest Liver Physiol. 2010;298:G107-G116.
31. Wouters K, van Gorp PJ, Bieghs V, Gijbels MJ, Duimel H, Lütjohann D, Kerksiek A, van Kruchten R, Maeda N, Staels B, van Bilsen M, Shiri-Sverdlov R, Hofker MH. Dietary cholesterol, rather than liver steatosis, leads to hepatic inflammation in hyperlipidemic mouse models of nonalcoholic steatohepatitis. Hepatology. 2008;48:474-486.
32. Park JW, Jeong G, Kim SJ, Kim MK, Park SM. Predictors reflecting the pathological severity of non-alcoholic fatty liver disease: comprehensive study of clinical and immunohistochemical findings in younger Asian patients. J Gastroenterol Hepatol. 2007;22:491-497.
33. Cha JY, Repa JJ. The liver X receptor (LXR) and hepatic lipogenesis. The carbohydrate-response element-binding protein is a target gene of LXR. J Biol Chem. 2007;282:743-751.
34. van Straten E, van Meer H, Huijkman N, van Dijk TH, Baller JF, Verkade HJ, Kuipers F, Plosch T. Fetal Liver X Receptor activation acutely induces lipogenesis, but does not affect plasma lipid response to a high-fat diet in adult mice. Am J Physiol Endocrinol Metab. 2009;297: E1171–E1178.
35. Goldstein JL, Brown MS. The LDL receptor. Arterioscler Thromb Vasc Biol. 2009;29:431-438.
36. Van Craeyveld E, Gordts SC, Nefyodova E, Jacobs F, De Geest B. Regression and stabilization of advanced murine atherosclerotic lesions: a comparison of LDL lowering and HDL raising gene transfer strategies. J Mol Med. 2011. [Epub ahead of print]
37. Kassim SH, Li H, Vandenberghe LH, Hinderer C, Bell P, Marchadier D, Wilson A, Cromley D, Redon V, Yu H, Wilson JM, Rader DJ. Gene therapy in a humanized mouse model of familial hypercholesterolemia leads to marked regression of atherosclerosis. PLoS One. 2010;5:e13424.
38. Getz GS, Reardon CA. Diet and murine atherosclerosis. Arterioscler Thromb Vasc Biol. 2006;26:242-249.
39. Raffai RL, Loeb SM, Weisgraber KH. Apolipoprotein E promotes the regression of atherosclerosis independently of lowering plasma cholesterol levels. Arterioscler Thromb Vasc Biol. 2005;25:436-441.
40. Rong JX, Li J, Reis ED, Choudhury RP, Dansky HM, Elmalem VI, Fallon JT, Breslow JL, Fisher EA. Elevating high-density lipoprotein cholesterol in apolipoprotein E-deficient mice remodels advanced atherosclerotic lesions by decreasing macrophage and increasing smooth muscle cell content. Circulation. 2001;104:2447-2452.
41. Yu L, Li-Hawkins J, Hammer RE, Berge KE, Horton JD, Cohen JC, Hobbs HH. Overexpression of ABCG5 and ABCG8 promotes biliary cholesterol secretion and reduces fractional absorption of dietary cholesterol. J Clin Invest. 2002;110:671-680.
42. Out R, Hoekstra M, Habets K, Meurs I, de Waard V, Hildebrand RB, Wang Y, Chimini G, Kuiper J, Van Berkel TJ, Van Eck M. Combined deletion of macrophage ABCA1 and ABCG1 leads to massive lipid accumulation in tissue macrophages and distinct atherosclerosis at relatively low plasma cholesterol levels. Arterioscler Thromb Vasc Biol. 2008;28:258-264.
43. Hoekstra M, Van Berkel TJ, Van Eck M. Scavenger receptor BI: a multi-purpose player in cholesterol and steroid metabolism. World J Gastroenterol. 2010;16:5916-5924.

Chapter 7

Bone marrow reconstitution in ApoE$^{-/-}$ mice: a novel model to induce atherosclerotic plaque regression

Zhaosha Li[1*], Laura Calpe-Berdiel[1*], Peshtiwan Saleh[1], Ronald J. van der Sluis[1], Sanne Remmerswaal[1], Heather J. McKinnon[2], Martin J. Smit[3], Miranda Van Eck[1], Theo J.C. Van Berkel[1], Menno Hoekstra[1]

[1]Division of Biopharmaceutics, Leiden/Amsterdam Center for Drug Research, Leiden University, The Netherlands.
[2]Schering-Plough (Part of the MSD Organisation), Newhouse, UK.
[3]Merck Research Laboratories, MSD Oss, The Netherlands.
[*]These authors contributed equally to this work.

Manuscript in preparation

ABSTRACT

Background & Aims: While numerous studies have been dedicated to inhibit the development and progression of atherosclerosis, recent attention has been drawn to the goal of reversing atherosclerosis, meaning regressing of pre-existing atherosclerotic plaques. The aim of this study is to investigate the potential of combined macrophage-specific apoE production and LXR agonist treatment to induce atherosclerotic plaque regression.
Methods and Results: ApoE$^{-/-}$ mice were fed with regular chow diet for 16 weeks and then switched to an atherogenic diet for another 3 days or 3 weeks to develop initial or advanced atherosclerotic lesions. We used bone marrow transplantation technique, reconstituting ApoE$^{-/-}$ mice with bone marrow from C57BL/6 mice, to restore apoE function in macrophages and normalize plasma lipoprotein profiles. Combined with LXR agonist T0901317, we evaluated the potential of LXR activation to regress diet-induced pre-existing atherosclerotic plaques.
Conclusions: Our study shows that 1) ApoE$^{-/-}$ mice reconstituted with bone marrow from C57BL/6 mice represents a promising mouse model with chow diet feeding to study atherosclerosis regression, providing an alternative model to investigate plaque regression; and 2) rapidly optimized plasma lipoprotein profiles, combined with LXR agonist treatment, induced favorable gene expression profiles that can induce significant regression of both initial and more advanced atherosclerotic plaques.
Keywords: LXR, T0901317, bone marrow transplantation, apoE, lipoprotein, atherosclerosis, regression

INTRODUCTION

Hypercholesterolemia plays a key role in the development of atherosclerosis and is a causative factor for coronary artery disease[1]. Hyperlipidemia is a metabolic disorder defined by elevated levels of plasma low-density lipoprotein (LDL)-cholesterol and triglycerides concentrations, and/or decreased levels of the athero-protective high-density lipoprotein (HDL)-cholesterol and its major protein component apolipoprotein AI (apoA-I)[2]. Lowering of very-low-density lipoprotein (VLDL)- and low-density lipoprotein (LDL)-cholesterol levels leads to a reduction in cardiovascular morbidity and mortality2. In contrast, high levels of HDL-cholesterol are associated with a decreased risk of cardiovascular disease[3]. HDL serves anti-atherogenic functions because of its ability to mediate reverse cholesterol transport (RCT)[4]. RCT involves the HDL mediated removal of cholesterol from the periphery, allowing it to be cleared by the liver and then excreted into bile[5]. Modulation of major macrophage mediators in RCT, such as ATP-binding cassette transporter A1 (ABCA1), ATP-binding cassette transporter G1 (ABCG1), and scavenger receptor class BI (SR-BI) has been considered as promising strategies for the prevention of atherosclerosis[6,7,8].

Hematopoietic cells, in particular monocytes and macrophages, play integral roles at all stages of atherosclerosis. The lipid-laden macrophage-derived foam cells are present from the earliest discernable fatty-streak lesions to advanced plaques, and are key factors in the pathology of plaques[9]. Much of the work exploring the role of macrophages in atherosclerosis has been carried out using the murine bone marrow transplantation model in which recipient mice prone to atherosclerosis development are reconstituted with donor bone marrow cells from transgenic or knockout mice to over express or delete genes in macrophages in a relevant pathway[10].

ApoE-deficient ($ApoE^{-/-}$) mice are one of the most common animal models to study atherogenesis. $ApoE^{-/-}$ mice show impaired clearance of plasma lipoproteins[11]. The most obvious phenotype of $ApoE^{-/-}$ mice is the spontaneous development of atherosclerotic lesions, even on a regular chow diet which is low in fat content and does not contain added cholesterol. Lesions of $ApoE^{-/-}$ mice develop over time from initial fatty streaks to complex lesions, and this process can be strongly accelerated by a high-fat, high-cholesterol diet[12].

ApoE is a major component of several classes of plasma lipoproteins[13]. Increasing evidence from both animal and human studies suggests that apoE is able to protect not only against hyperlipidemia, but also against atherosclerosis via a variety of mechanisms, including promoting efficient uptake of triglyceride-rich lipoproteins from the circulation by peripheral tissues for utilization or by liver for excretion, maintaining normal macrophage lipid homeostasis, and enhancing RCT from macrophage foam cells in the atherosclerotic lesion[14,15,16]. Although the majority of apoE in plasma originates from the liver, apoE is synthesized by a variety of peripheral tissues and cell types, including macrophages[17]. Previous studies have shown that reconstruction of macrophage-specific expression of apoE reduces atherosclerosis in $ApoE^{-/-}$ mice, whereas reconstitution of C57BL/6 mice with macrophages from $ApoE^{-/-}$ mice increases atherosclerosis, suggesting that apoE produced by macrophages was sufficient to induce changes in atherosclerotic development[18,19].

While numerous studies have been dedicated to inhibit the development and

progression of atherosclerosis, recent attention has been drawn to the goal of reversing atherosclerosis, meaning regressing of pre-existing atherosclerotic plaques. The first evidence of dramatic atherosclerotic regression in mice was achieved via robust surgical measures to rapidly improve the plaque environment[20]. This study suggested that the essential prerequisite for promoting regression of atherosclerotic lesions is robust improvement of plasma lipoprotein profiles and plaque milieu, including large plasma reductions in atherogenic apoB-lipoproteins and brisk enhancements in efflux of cholesterol from plaques to the liver. Recently, Feig *et al* showed that the LXR agonist T0901317 promotes egress of monocyte-derived cells from mouse aortic plaques, indicating that LXR is required for maximal effects on plaque macrophage egression during atherosclerosis regression in mice[21]. Liver X receptors (LXRs) are sterol-responsive transcription factors which regulate expression of genes involved in cholesterol metabolism and homeostasis [22]. LXRs act as cholesterol sensors. When cellular oxysterols accumulate as a result of increasing concentrations of cholesterol, LXR induces the transcription of genes that protect cells from cholesterol overload[23]. LXR activation has been shown to significantly promote biliary sterol secretion and reduce cholesterol absorption[24,25], up-regulate cholesterol efflux to HDL particles[26,27], and inhibit development of atherosclerosis, providing direct evidence for an anti-atherogenic effect of LXR agonists[28,29,30]. However, in those studies, LXR agonists are only shown to attenuate the progression of atherosclerosis in mouse models, while their potential to abrogate pre-existing cardiovascular disease and to stabilize established atherosclerotic lesions has not been widely addressed. It is thus clinically interesting to examine whether rapidly improved plasma lipoprotein profiles combined with therapeutic LXR agonist could induce atherosclerotic lesion regression.

In the current study, we used bone marrow transplantation technique, reconstituting ApoE$^{-/-}$ mice with bone marrow from C57BL/6 mice, to restore apoE function in macrophages and normalize plasma lipoprotein profiles. Combined with LXR agonist T0901317, we evaluated the potential of LXR activation to regress diet-induced pre-existing atherosclerotic plaques.

MATERIALS AND METHODS

Animals

Female homozygous ApoE-deficient (ApoE$^{-/-}$; C57BL/6 background) mice of 12 weeks old were used. To study the effects on initial atherosclerotic plaques, mice were fed with semi-synthetic Western-type diet (WTD) containing 15% (w/w) fat and 0.25% (w/w) cholesterol (Diet W, Special Diet Services, Witham, UK) for 3 days to induce the development of initial atherosclerotic lesions. To study the effects on advanced atherosclerotic plaques, the animals were fed with WTD for 3 weeks to induce the further development of advanced atherosclerotic lesions. After the formation of atherosclerotic plaques, in both studies, bone marrow transplantation was performed and the diet was switched to regular cholesterol-free chow diet containing 4.3% (w/w) fat (RM3, Special Diet Services, Witham, UK) for 6 weeks, with or without supplementation of the LXR agonist T0901317 (10 mg/kg/day; MSD Oss, The Netherlands). After euthanization, mice were bled via orbital exsanguination, and perfused *in situ* through the left cardiac ventricle with

ice-cold PBS (pH 7.4) for 20 minutes. Tissues were dissected and snap-frozen in liquid nitrogen. Heart was dissected free of fat and stored in 3.7% neutral-buffered formalin (Formal-fixx, Shandon Scientific Ltd., UK) for histological analysis. Animal care and procedures were performed in accordance with the national guidelines for animal experimentation. All protocols were approved by the Ethics Committee for Animal Experiments of Leiden University.

Bone marrow transplantation

From one week before bone marrow transplantation, recipient female ApoE$^{-/-}$ mice were kept on antibiotics-containing drinking water (83 mg/L ciprofloxacin, 67 mg/L polymyxin B sulfate, 6.5 g/L sucrose). To induce bone marrow aplasia, recipient ApoE$^{-/-}$ mice were exposed to a single dose of 9 Gy (0.19 Gy/min, 200 kV, 4 mA) total body X-ray irradiation, using an Andrex Smart 225 Röntgen source (YXLON International, Copenhagen, Denmark) with a 6-mm aluminum filter. Bone marrow from donor female C57BL/6 mice was harvested by flushing the femurs and tibias with PBS (pH 7.4). Single-cell suspensions were prepared by passing the cells through a 70 µm cell strainer (BD, Breda, The Netherlands). 0.5 x 10^7 donor bone marrow cells were injected intravenously into the lateral tail vein of each irradiated recipient mouse. All transplanted mice were housed in sterilized filter-top cages with drinking water containing antibiotics throughout the whole experiment. After the mice were euthanized at 6 weeks of regular chow diet feeding, the hematological chimerism of the transplanted mouse was assessed by polymerase chain reaction (PCR) analysis of DNA harvested from bone marrow to detect the presence of the apoE allele.

Plasma lipid analysis

Plasma lipid analysis was performed at different time points throughout the experiments. At the endpoint, mice were not fasted prior to euthanization. Plasma concentrations of total cholesterol (TC) and triglycerides (TG) were measured using the enzymatic colorimetric assay (Roche Diagnostics, Mannheim, Germany). The distribution of cholesterol over different lipoproteins in plasma was determined by fast protein liquid chromatography (FPLC) through a Superose 6 column (3.2 x 30 mm; Smart-System, Pharmacia, Uppsala, Sweden). Cholesterol content of the lipoprotein fractions was determined as described above.

RNA isolation and gene expression analysis

Total RNA from the liver was isolated using acid guanidinium thiocyanate (GTC)-phenol-chloroform extraction. Briefly, 500 µL of GTC solution (4 M guanidine isothiocyanate, 25 mM sodium citrate, 0.5% N-lauroylsarcosine) was added to each sample, followed by acid phenol:chloroform extraction. The RNA in the aqueous phase was precipitated with isopropanol. The quantity and purity of the isolated RNA were examined using an ND-1000 Spectrophotometer (Nanodrop, Wilmington, DE, USA). One microgram of the isolated RNA from each sample was converted into cDNA by reverse transcription with RevertAid™ M-MuLV Reverse Transcriptase (Promega, Madison, WI, USA). Negative controls without addition of reverse transcriptase were prepared for each sample. Quantitative real-time PCR was carried out using ABI Prism 7700 Sequence Detection system (Applied Biosystems, Foster City, CA, USA) according to the manufacturer's instructions. 36B4, Beta-actin, and GAPDH were used as internal housekeeping genes. The

gene-specific primer sequences used are listed in Table 1. Amplification curves were analyzed using 7500 Fast System SDS software V1.4 (Applied Biosystems, Foster City, CA, USA). The relative expression of each gene was expressed as fold changes compared to baseline group.

Table 1. Primers for quantitative real-time PCR analysis

Gene	Forward primer	Reverse Primer
36B4	GGACCCGAGAAGACCTCCTT	GCACATCACTCAGAATTTCAATGG
Beta-actin	AACCGTGAAAAGATGACCCAGAT	CACAGCCTGGATGGCTACGTA
GAPDH	TCCATGACAACTTTGGCATTG	TCACGCCACAGCTTTCCA
ABCA1	GGAGTTCTTTGCCCTCCTGAG	AGTTTGCGAATTGCCCATTC
ABCG1	AGGTCTCAGCCTTCTAAAGTTCCTC	TCTCTCGAAGTGAATGAAATTTATCG
ABCG5	TGGCCCTGCTCAGCATCT	ATTTTTAAAGGAATGGGCATCTCTT
ABCG8	CCGTCGTCAGATTTCCAATGA	GGCTTCCGACCCATGAATG
ApoA-I	ACTCTGGGTTCAACCGTTAGTCA	TCCCAGAAGTCCCGAGTCA
ApoE	AGCCAATAGTGGAAGACATGCA	GCAGGACAGGAGAAGGATACTCAT
SR-BI	GGCTGCTGTTTGCTGCG	GCTGCTTGATGAGGGAGGG
LPL	CCAGCAACATTATCCAGTGCTAG	CAGTTGATGAATCTGGCCACA
FAS	GGCATCATTGGGCACTCCTT	GCTGCAAGCACAGCCTCTCT
CYP7A1	CTGTCATACCACAAAGTCTTATGTCA	ATGCTTCTGTGTCCAAATGCC
SREBP-1c	GGAGCCATGGATTGCACATT	CCTGTCTCACCCCCAGCATA
CD68	CCTCCACCCTCGCCTAGTC	TTGGGTATAGGATTCGGATTTGA

Histological analysis

Accumulation of lipids in the atherosclerotic plaques at the aortic root in the heart was analyzed. The heart was cut latitudinally and embedded in O.C.T™ Compound (Tissue-Tek, Sakura finetek, Tokyo, Japan), and subsequently sectioned using a Leica CM 3050S cryostat at 10 μm intervals. Cryostat sections were stained with Oil-red O (Sigma-Aldrich) to identify lipids, and counterstained with hematoxylin (Sigma-Aldrich) to assist in tissue visualization. Quantitative analysis of the atherosclerotic lesion area at the aortic root was performed in a blinded fashion. Mean lesion area (in μm^2 per aortic root per mouse) was calculated from 10 Oil-red O stained cryostat sections, starting at the appearance of the tricuspid valves.

Immunohistochemistry

Ten-micrometer cryosections of the aortic root were obtained as described above. After incubation with blocking solution (5% goat serum), macrophages were detected using MOMA-2 antibody (rat antibody directed against murine monocytes/macrophages, Serotec, Oxford, UK). A rabbit anti rat IgG/HRP was used as second antibody (Dako, Heverlee, Belgium). Sections were developed using NovaRED Peroxidase Substrate Kit (VECTOR LABORATORIES, Peterborough, UK) according to kit instructions. Slides were counterstained with hematoxylin (Sigma-Aldrich) to assist in tissue visualization.

Masson's Trichrome Staining

Tissue sections were prepared as described above and subjected to Masson's trichrome staining using the Masson's Trichrome Stain kit (Sigma-Aldrich) and counterstained with hematoxylin, to assess the extent of collagen deposition and the structural integrity of fibrillar collagen in the plaque.

Statistical analysis

Mean values between two groups were analyzed with the unpaired Student's t-test;

data sets containing multiple groups were analyzed by ANOVA (Instat GraphPad software, San Diego, USA). Statistical significance was defined as $p<0.05$. Data are expressed as means ± SEM.

RESULTS

To investigate the potential of combined macrophage-specific apoE production and LXR agonist treatment to induce atherosclerotic plaque regression, bone marrow transplantation was performed to selectively express apoE in bone marrow-derived hematopoietic cells, including macrophages. We started our investigation with initial atherosclerotic lesions, which was thought to form an easier target for regression. Hereto we fed female ApoE$^{-/-}$ mice with regular chow diet for 16 weeks and then switched to an atherogenic WTD for another 3 days to develop initial atherosclerotic lesions. In addition, we also evaluated the regression of advanced atherosclerotic lesions in the same model. Here we fed female ApoE$^{-/-}$ mice with regular chow diet for 16 weeks and then switched to an atherogenic WTD for another 3 weeks to develop more advanced atherosclerotic lesions. A group of mice were sacrificed to obtain baseline data, whilst the remainder of the mice received bone marrow from either C57BL/6 mice, or from original ApoE$^{-/-}$ mice as a control group for the BMT procedure. After bone marrow transplantation, mice were fed low-fat cholesterol-free chow diet with or without LXR agonist supplementation for 6 weeks, during which the plasma lipid concentrations were monitored over regression period.

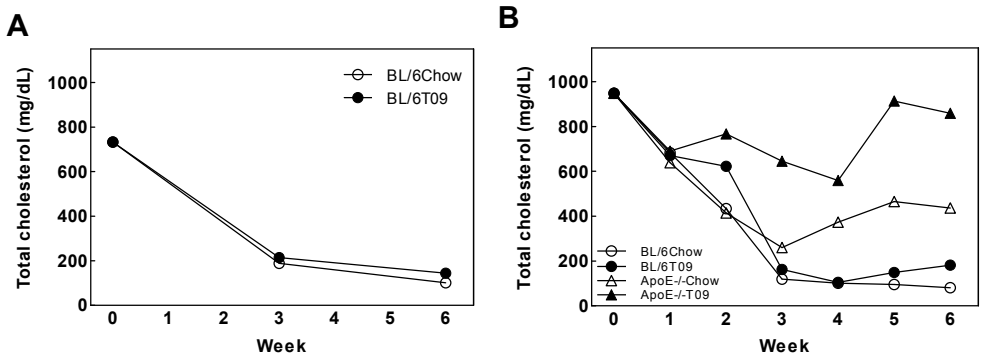

Figure 1. Overview of changes in plasma total cholesterol level during regression studies in initial lesions (A) and advanced lesions (B). We fed female ApoE$^{-/-}$ mice with regular chow diet for 16 weeks and then switched to an atherogenic WTD for 3 days (A) or 3 weeks (B) to develop initial and advanced atherosclerotic lesions, respectively. A group of mice were then sacrificed to obtain baseline data, whilst the remainder of the mice received bone marrow from either C57BL/6 mice, or from original ApoE$^{-/-}$ mice as a control group for the BMT procedure. After bone marrow transplantation, mice were fed low-fat cholesterol-free chow diet with or without LXR agonist T0901317 supplementation for 6 weeks, during which the plasma lipid concentrations were monitored. Values are means ± SEM (10 mice per group). BL/6: Bone marrow from wildtype C57BL/6 mice. ApoE$^{-/-}$: Bone marrow from ApoE$^{-/-}$ mice. T09: LXR agonist T0901317 supplementation.

Reconstitution of macrophage apoE dramatically normalized plasma lipoprotein profile in ApoE$^{-/-}$ mice

In ApoE$^{-/-}$ mice, WTD markedly increased plasma total cholesterol level to approximately 730 mg/dL in the initial lesion study (Figure 1A) and 950 mg/dL in advanced lesion study (Figure 1B). Bone marrow from apoE containing donor C57BL/6 mice was transplanted into ApoE$^{-/-}$ mice and a diet switch to low-fat chow diet led to a sharp drop in plasma total cholesterol level within 3 weeks to 188 mg/dL (-74%) in the initial lesion study and 120 mg/dL (-87%) in advanced lesion study, and these levels remained low until 6 weeks after BMT (Figure 1A, 1B). The presence of LXR agonist in chow diet did not change the cholesterol levels, and actually a similar persistent reduction in plasma total cholesterol concentration was noticed (Figure 1A, 1B). In contrast, the cholesterol levels in the control group where ApoE$^{-/-}$ mice received bone marrow from original ApoE$^{-/-}$ mice started to rise again after an initial drop and displayed a significantly higher plasma total cholesterol level compared to ApoE$^{-/-}$ mice with bone marrow from C57BL/6 mice (Figure 1B). At 6 weeks after BMT, in both initial and advanced lesion studies, ApoE$^{-/-}$ mice with bone marrow from C57BL/6 mice showed approximately 90% reduction in plasma cholesterol level compared to baseline and there was no significant difference between mice fed chow diet alone or with LXR agonist treatment; Control ApoE$^{-/-}$ mice with bone marrow from ApoE$^{-/-}$ mice showed significantly higher plasma cholesterol level compared to mice with wildetype C57BL/6 bone marrow, especially when treated with LXR agonist (Figure 2A, 2C). As expected, LXR agonist significantly increased plasma triglycerides levels as compared to mice fed with chow diet alone in both the initial lesion study (1.4-fold, Figure 2B) and advanced lesion study (2.3-fold, Figure 2D).

As determined by FPLC lipoprotein separation, the largely reduced plasma total cholesterol concentration in ApoE$^{-/-}$ mice with C57BL/6 bone marrow was primarily due to markedly reduced plasma VLDL- (-94%, $P < 0.001$ in initial lesions; -97%, $P < 0.001$ in advanced lesions) and LDL- (-82%, $P < 0.001$ in initial lesions; -91%, $P < 0.001$ in advanced lesions) cholesterol level (Figure 3A, 3C). LXR agonist treatment increased the plasma HDL-cholesterol concentration in ApoE$^{-/-}$ mice with C57BL/6 bone marrow compared to baseline (1.6-fold in initial lesions; 1.7-fold, $P < 0.05$ in advanced lesions; Figure 3B, 3D). In conclusion, after transplanting bone marrow from C57BL/6 mice into ApoE$^{-/-}$ mice, combined with a switch to chow diet with or without LXR agonist, successfully normalized the plasma cholesterol profile.

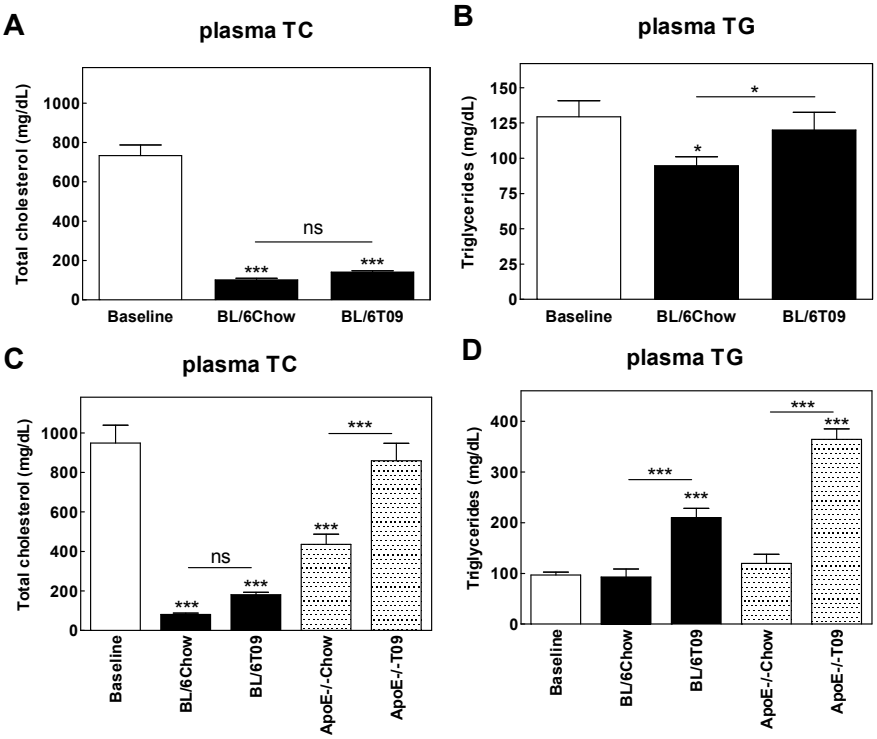

Figure 2. Plasma concentration of total cholesterol and triglycerides from initial lesion study (A, B) and advanced lesion study (C, D) at endpoint of experiments were measured. Values are means ± SEM (10 mice per group). *P<0.05; ***P<0.001; ns, not significant.

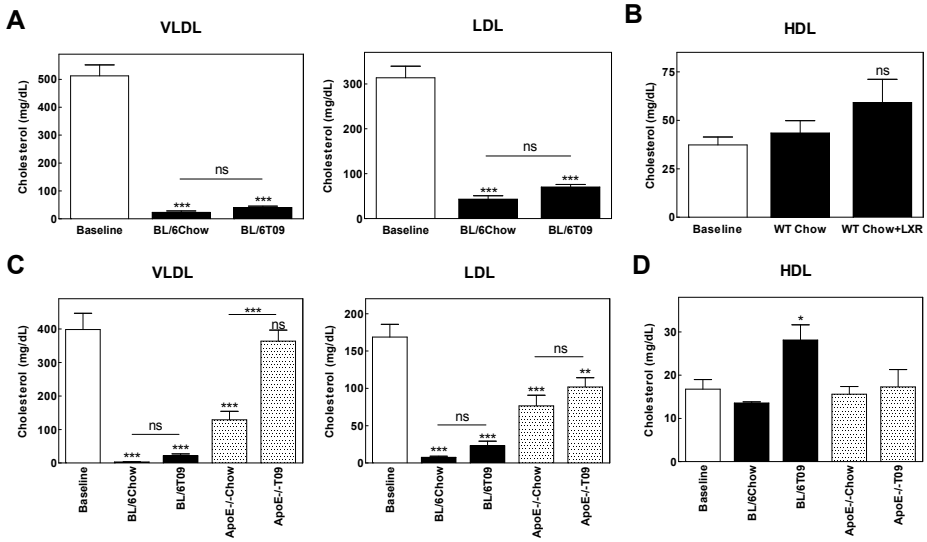

Figure 3. Plasma lipoproteins profile in initial lesion study (A, B) and advanced lesion study (C, D) at endpoint of experiments. Plasma lipoproteins were separated by FPLC and cholesterol level was measured in each fraction. VLDL represents the sum of cholesterol concentrations from fraction 2 to 7 (VLDL fractions); LDL represents the sum of cholesterol concentrations from fraction 8 to 14 (LDL fractions); HDL represents the sum of cholesterol concentrations from fraction 15 to 22 (HDL fractions) (B). Values are means ± SEM (10 mice per group). *P<0.05; **P<0.01; ***P<0.001; ns, not significant.

LXR agonist regulated hepatic gene expression in ApoE$^{-/-}$ mice reconstituted with C57BL/6 bone marrow

As expected, LXR agonist treatment increased the liver weight (data not shown) and strongly up-regulated the hepatic expression of LXR target genes SREBP-1c, FAS, and LPL compared to mice fed chow diet alone (Figure 4A, 4B). This LXR agonist-induced hepatic lipogenesis has been well established as a positive control for LXR activation in mice[31,32].

After transplanting C57BL/6 bone marrow into ApoE$^{-/-}$ mice, the mRNA expression of apoE showed up in the liver. LXR agonist treatment further up-regulated the hepatic gene expression of apoE compared to group fed chow diet alone (2-fold, P<0.001 in initial lesions; 1.7-fold, P<0.001 in advanced lesions) (Figure 5A, 5D). In addition, LXR agonist treatment significantly up-regulated the hepatic expression of ABCG5 and ABCG8 compared to group fed chow diet alone (Figure 5B, 5E), suggesting promoted biliary cholesterol secretion upon LXR activation.

In line with the significantly elevated plasma HDL-cholesterol level in ApoE-/- mice reconstituted with C57BL/6 bone marrow, LXR agonist treatment significantly increased the hepatic expression of ABCG1 (1.4-fold, P<0.05 in initial lesions; 2.3-fold, P<0.001 in advanced lesions) and ApoA-I (1.6-fold, P<0.001 in advanced lesions) compared to the chow group (Figure 5C, 5F), suggesting that LXR activation promoted the cholesterol efflux capacity.

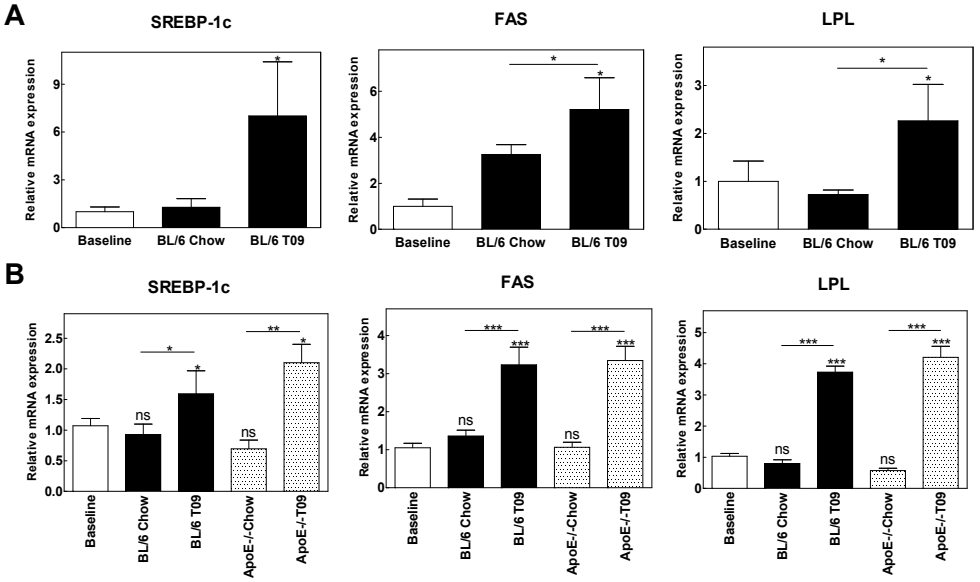

Figure 4. Changes in hepatic gene expression profiles during regression studies in initial lesions (A) and advanced lesions (B). Total RNA was extracted from liver, and relative mRNA expression of SREBP-1c, FAS, CYP7A1, and LPL were determined by quantitative PCR and presented as fold-change relative to baseline group (C). Values are means ± SEM (10 mice per group). *P<0.05; **P<0.01; ***P<0.001; ns, not significant.

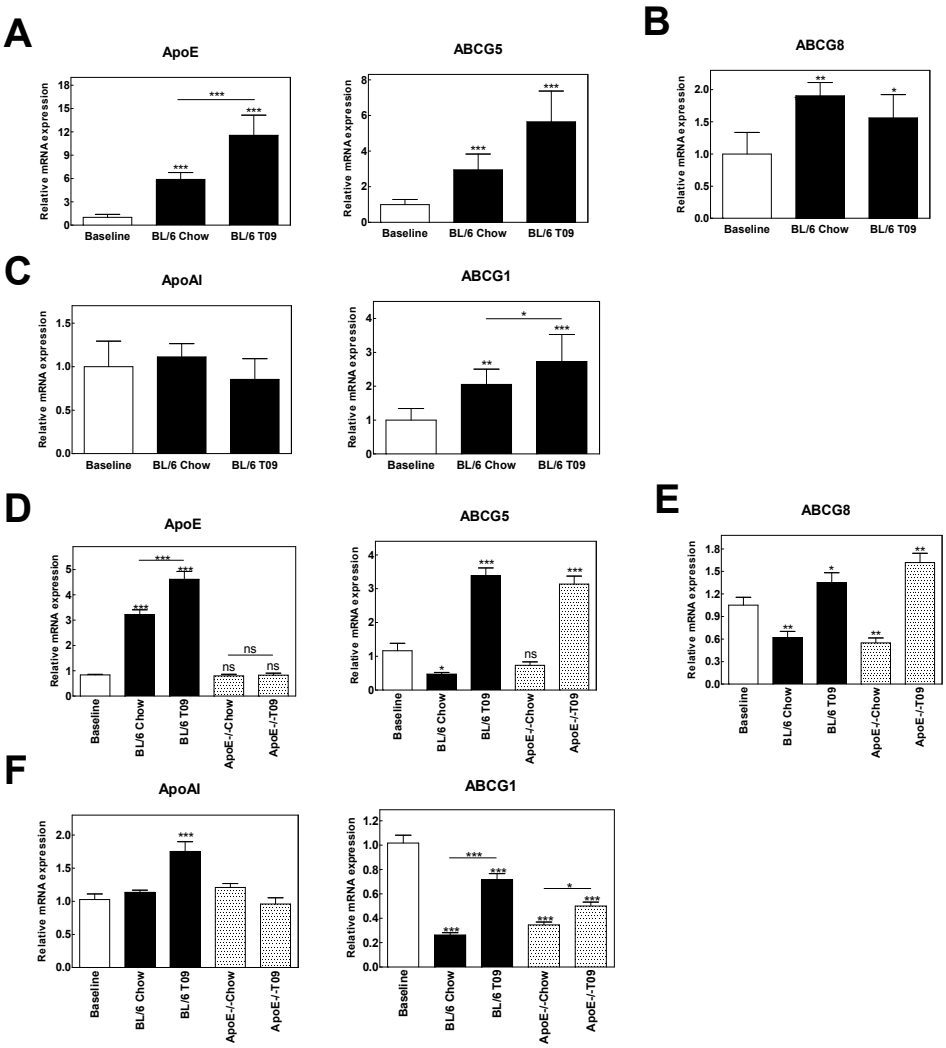

Figure 5. Changes in hepatic gene expression profiles during regression studies in initial lesions (A, B, C) and advanced lesions (D, E, F). Total RNA was extracted from liver, and relative mRNA expression of ApoE, ABCG5, ABCG8, ApoA-I, and ABCG1 were determined by quantitative PCR and presented as fold-change relative to baseline group (C). Values are means ± SEM (10 mice per group). *P<0.05; **P<0.01; ***P<0.001; ns, not significant.

Atherosclerotic plaque regression after transplanting wild-type C57BL/6 bone marrow into ApoE$^{-/-}$ mice

With WTD feeding, ApoE$^{-/-}$ mice developed atherosclerotic lesions of ± 70x10^3 µm^2 at the aortic root in initial lesion study (Figure 6A) and ± 550x10^3 µm^2 in advanced lesion study at baseline (Figure 6B). In control mice reconstituted with ApoE$^{-/-}$ bone marrow, plaque size did not decrease after 6 weeks of chow diet feeding, with or without LXR agonist supplementation (Figure 6B). In contrast, six weeks after transplanting wildtype C57BL/6 bone marrow into ApoE$^{-/-}$ mice, with chow diet feeding alone, the lesion size decreased significantly to ± 39x10^3 µm^2 (-45%,

P<0.001) in initial lesions (Figure 6A), and to ± 420x10^3 µm^2 (-23%, *P*<0.01) in advanced lesions (Figure 6B). LXR agonist treatment further reduced lesion size significantly to ± 20x10^3 µm^2 in initial lesions (-71%, *P*<0.001 compared to Baseline; -48%, *P*<0.01 compared to chow group; Figure 6A) and to ± 350x10^3 µm^2 in advanced lesions (-36%, *P*<0.001 compared to Baseline; -17%, *P*=0.06 compared to chow group; Figure 6B). The results indicated that this ApoE-/- mice model reconstituted with wildetype C57BL/6 bone marrow is an interesting new model to successfully induce atherosclerotic lesion regression.

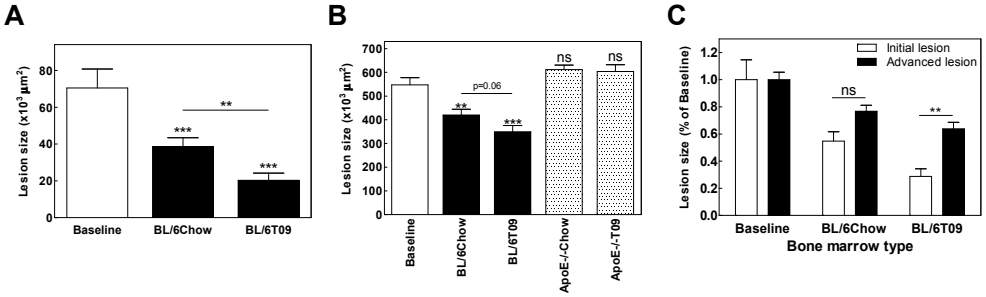

Figure 6. Changes in atherosclerotic lesion size during regression studies in initial lesions (A) and advanced lesions (B), and comparison of lesion size from both studies expressed as percentage of baseline lesion (C). Cryostat sections of the aortic root in heart were stained with oil-red O to identify lipids, and the lesion size was quantified. Values are means ± SEM (10 mice per group). **P<0.01; ***P<0.001; ns, not significant.

LXR agonist reduced plaque macrophage content during atherosclerosis regression

Further analysis of atherosclerotic lesion composition showed that the collagen content of the plaque in initial lesions decreased after bone marrow reconstitution with chow diet alone (-66%, *P*<0.001), and LXR agonists further reduced the collagen amount in initial plaques (-81%, *P*<0.001 compared to Baseline; -45%, *P*<0.01 compared to chow group (Figure 7A). However, in advanced plaques, despite the significant reduction of plaque size after BMT, the collagen content of plaque in ApoE$^{-/-}$ mice with wildtype C57BL/6 bone marropw remained the same, with or without treatment of LXR agonist (Figure 7B). In contrast, the absolute macrophage-positive area and percentile of area of the lesion occupied by macrophages decreased dramatically in accordance to the reduction of total lesion size. In the initial lesion induced by 3 days of WTD feeding, the size of macrophage-positive area was 63x10^3 µm^2 at aortic root as baseline (Figure 8A). In the advanced lesion induced by 6 weeks of WTD feeding, the size of macrophage-positive area was 125x10^3 µm^2 at aortic root as baseline (Figure 8B). Six weeks after transplanting wildtype C57BL/6 bone marrow into ApoE$^{-/-}$ mice, the macrophage-positive area decreased significantly in both studies with chow diet alone (-43%, *P*<0.05 in initial lesions; -96%, *P*<0.01 in advanced lesions; Figure 8A, 8B). LXR agonist treatment further reduced the plaque macrophage content significantly in both initial lesions (-70%, *P*<0.001 compared to Baseline; -50%, *P*<0.01 compared to chow group) and in advanced lesions (-100%, *P*<0.01 compared to Baseline; -100%, *P*<0.01 compared to chow group) (Figure 8A, 8B) that no positive macrophage-staining was visible anymore. The results indicated that the reduction in plaque size observed in this mouse model was primarily due to the decreased macrophage content in the plaques.

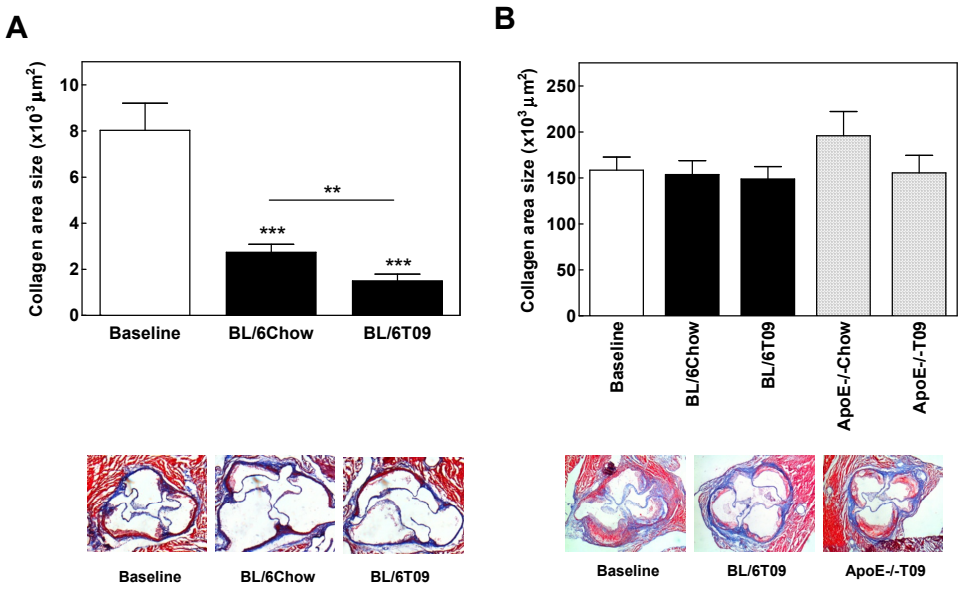

Figure 7. Changes in size of collagen area in atherosclerotic plaques during regression studies in initial lesions (A) and advanced lesions (B) were measured. Cryostat sections of the aortic root in heart were stained with Masson's Trichrome Stain kit and counterstained with hematoxylin to assess the extent of collagen deposition and the structural integrity of fibrillar collagen in the plaque. Size of collagen area in plaques was quantified. Values are means ± SEM (10 mice per group). **P<0.01; ***P<0.001.

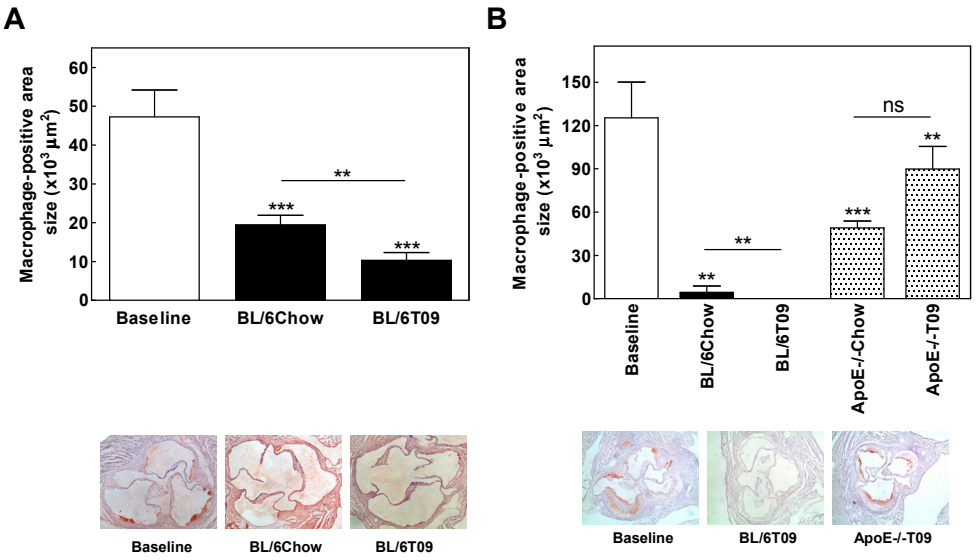

Figure 8. Changes in size of macrophage-positive area in atherosclerotic plaques during regression studies in initial lesions (A) and advanced lesions (B) were measured. Cryostat sections of the aortic root in heart were stained with MOMA-2 antibody (rat antibody directed against murine monocytes/macrophages) and rabbit anti rat IgG/HRP to identify macrophage-positive area. Sections were developed using NovaRED Peroxidase Substrate Kit, and the size of macrophage-positive area was quantified. Values are means ± SEM (10 mice per group). *P<0.05; **P<0.01; ***P<0.001; ns, not significant.

DISCUSSION

In the current study, we set up a new mouse model to study atherosclerotic lesion regression. Our results show that ApoE$^{-/-}$ mice reconstituted with bone marrow from wildtype C57BL/6 mice form a promising model to induce rapidly normalized plasma lipoprotein profiles and the regression of pre-existing atherosclerotic plaques.

In previous studies where dramatic regression of large advanced lesions was achieved with or without LXR agonist[20,21], surgical aorta transplantation into wildtype mice was performed to rapidly improve the atherosclerotic plaque milieu. In our study, we used the BMT procedure to induce plaque regression, which raises the opportunity to analyze the relative importance of individual genes in hematopoietic cells for plaque regression, by using specific knockout mice as bone marrow donors.

Bone marrow transplantation leads to the replacement of bone marrow-derived cells, including recipient tissue macrophages by cells of donor origin. After transplantation of bone marrow from mice with wildtype apoE expression into ApoE$^{-/-}$ mice, we observed rapid improvement and normalization of the plasma cholesterol profile. This cholesterol lowering effect of macrophage-derived apoE was reported in previous studies, where apoE of donor origin was present in the recipient peripheral circulation as early as 2 weeks after transplantation, and by 4 weeks, apoE production by bone marrow-derived cells was sufficient to normalize plasma lipid levels of ApoE$^{-/-}$ recipient mice[33,34]. The apoE level in circulation after BMT was only 12.5% of those in wildtype mice but nevertheless sufficient to reduce the severe hypercholesterolemia of ApoE$^{-/-}$ mice, due to accelerated hepatic clearance of plasma cholesterol and promoted cholesterol efflux[19,35,36].

Raffai *et al* for the first time addressed the apoE-mediated mechanisms of atherosclerosis regression[37]. They demonstrate that apoE promotes the regression of atherosclerosis independently of lowering plasma cholesterol levels. In contrast, a study from Shi *et al* concluded differently. They demonstrated that regression of atherosclerotic lesions is a slow process and macrophage-derived apoE was insufficient to induce significant regression of established atherosclerotic lesions in ApoE$^{-/-}$ mice, although it was sufficient to eliminate hypercholesterolemia and prevent progression of aortic lesions34. The difference in conclusions between their study and our current observations may come from the differences in experimental set-up.

Study from Zhao *et al* showed that in both LDLr$^{-/-}$ and C57BL/6 mice, switch of an atherogenic diet to regular chow diet could not trigger lesion regression despite a rapid and dramatic reduction in plasma total cholesterol levels. In LDLr$^{-/-}$ mice, lesion sizes even increased despite the cholesterol lowering[38]. Similar observations were reported where switching high-fat atherogenic diet to a standard chow diet led to markedly reduced plasma (V)LDL-cholesterol without significant reduction in lesion size37, or with even significantly increased lesion size[39]. In the current study with BMT procedure, chow diet alone induced a significant regression of both initial and advanced plaques, which was in accordance with study from Bengtsson *et al* where ApoE$^{-/-}$ mice were transplanted with wildtype bone marrow and a 35% plaque regression was observed[40]. Taken together, our data confirmed that ApoE$^{-/-}$ mice reconstituted with wildtype C57BL/6 bone marrow is a valid regression mouse model.

We performed this regression study in parallel on initial and advanced lesions. The atherosclerotic plaque is a dynamic tissue, where increases in cell number (driven by cell proliferation and migration) and decreases in cell number (driven by cell death and possibly emigration) are continuous processes [41]. Initial atherosclerotic lesions are primarily composed of lipid-loaded macrophages. Stable advanced lesion contains a macrophage core, a small necrotic core, if present at all, extracellular matrix and a firm fibrous cap of smooth muscle cells (SMCs)[42]. Instable advanced atherosclerotic lesions are characterized by a thin fibrous cap containing few SMCs and overlying a large necrotic core composed of dead cells, lipid deposits, and cellular debris[43]. For long it has been thought that advanced lesion could not regress since they contain thick fibrous cap, large amount of necrotic material, extracellular lipids and extracellular matrix. In the current study, we showed that via the bone marrow transplantation technique, successful plaque regression can be induced in both initial and advanced lesion. The current mouse model is thus a good model to study atherosclerosis regression in different stages of the disease.

LXR agonists have potent anti-atherogenic effects in different hyperlipidemic mouse models. Several studies have demonstrated that activation of LXR significantly up-regulated cholesterol efflux activity and inhibited the development of atherosclerosis29,30. However, the ability of LXR agonists to abrogate pre-existing cardiovascular disease by inducing regression and stabilization of established atherosclerotic lesions has not been widely addressed. We used LXR agonist treatment in our mouse model to assess the potential of LXR activation to induce atherosclerosis regression. The LXR agonist T0901317 not only reduced plasma (V)LDL-cholesterol levels, but also significantly increased HDL-cholesterol. This indicates that LXR agonist, supplemented in chow diet, rapidly optimizes the plasma lipoprotein profile and achieves a regressive plasma environment in this mouse model. In addition, compared to group fed with chow diet alone, LXR agonist treatment in this study induced further 48% reduction in initial lesion size, 17% reduction in advanced lesion size, and also a further 50% reduction in the macrophage-positive area size in initial lesions. In advanced lesions, there was merely visible macrophage-positive staining observed in LXR agonists treated group, indicating the diminishing of macrophages during atherosclerotic regression in our mouse model. Combined, our results were in line with findings from Feig *et al*21 that LXR activation is necessary for maximal effects on plaque macrophage content reduction during atherosclerosis regression in mice.

To further analyze the dynamics and the cellular cause of the rapid reduction of total plaque size, we examined the lesion composition in detail. The atherosclerotic plaque is a complicated structure. In addition to cholesterol-filled macrophage core, it contains large numbers of immune cells, SMCs, vascular endothelial cells, and a large amount of extracellular matrix products that includes sulfated glycosaminoglycans, collagen, fibrin, and extracellular lipids[44]. The complexity of atherosclerosis is highlighted by the multifaceted effects that apoptosis and proliferation of specific cell types can have on vessels at different stages of the disease[45]. In initial lesions, a 45% reduction in lesion size was observed with chow diet alone, and even a 71% reduction with LXR agonist treatment, whilst in advanced lesions there was only a 23% reduction with chow diet alone, and a 36% reduction with LXR activation. This can be explained by the difference in plaque composition and characteristics between initial and advanced lesion. Initial lesions

contain primarily cholesterol-filled macrophages, while in advanced lesion, SMCs and extracellular matrix products comprise the major structural components of the atherosclerotic plaques[46]. SMCs and extracellular matrix products remained unchanged and are more difficult to be modulated during the regression process. Therefore, the extent of lesion size reduction was smaller in advanced lesions compared to initial lesions.

Interestingly, our lesion composition analysis showed that the reduction of total lesion size during regression was primarily due to the reduction and diminishing of macrophage content in the plaque. The fate of the macrophages during lesion regression is currently under debate. It has been proposed that regression is not merely a rewinding of progression, but instead involves induction of CCR7 expression, a mediator of leukocyte emigration, in foam cells and emigration of the maladaptive macrophage infiltrate, followed by the initiation of influx of healthy phagocytes that mobilize necrotic debris and all other components of advanced plaques[47]. Interestingly, Ye *et al* showed that macrophage infiltration into pre-existing advanced lesions was limited, likely because of the formation of fibrous caps[48]. In contrast, Potteaux *et al* also showed that regression of atherosclerosis after apoE complementation in $ApoE^{-/-}$ mice did not involve migratory egress of macrophages from plaques or induction of CCR7. Instead, marked suppression of monocyte recruitment coupled with a stable rate of apoptosis accounted for loss of plaque macrophages, suggesting that therapies to inhibit monocyte recruitment to plaques may constitute a viable strategy to reduce plaque macrophage burden than attempts to promote migratory egress[49]. Further research is necessary to establish the processes and mechanisms underlying the diminished macrophage content during regression in our experimental mouse model.

In conclusion, our current study shows that 1) $ApoE^{-/-}$ mice reconstituted with bone marrow from C57BL/6 mice represents a promising mouse model with chow diet feeding to study atherosclerosis regression, providing an alternative model to investigate plaque regression; and 2) rapidly optimized plasma lipoprotein profiles, combined with LXR agonist treatment, induced favorable gene expression profiles that can induce significant regression of both initial and more advanced atherosclerotic plaques.

ACKNOWLEDGEMENTS

This work was supported by TIPharma (Grant T2-110 to Z.L., T.J.C.V.B., M.H.) and the Netherlands Heart Foundation (Grant 2008T070 to M.H.).

REFERENCES

1. Toutouzas K, Drakopoulou M, Skoumas I, Stefanadis C. Advancing therapy for hypercholesterolemia. Expert Opin Pharmacother. 2010;11:1659-1672.
2. Paras C, Hussain MM, Rosenson RS. Emerging drugs for hyperlipidemia. Expert Opin Emerg Drugs. 2010;15:433-451.
3. Lee JM, Choudhury RP. Atherosclerosis regression and high-density lipoproteins. Expert Rev Cardiovasc Ther. 2010;8:1325-1334.
4. Rothblat GH, Phillips MC. High-density lipoprotein heterogeneity and function in reverse cholesterol transport. Curr Opin Lipidol. 2010;21:229-238.
5. Ragbir S, Farmer JA. Dysfunctional high-density lipoprotein and atherosclerosis. Curr Atheroscler Rep. 2010;12:343-348.
6. Van Der Velde AE. Reverse cholesterol transport: from classical view to new insights. World J Gastroenterol. 2010;16:5908-5915.
7. Lund-Katz S, Phillips MC. High density lipoprotein structure-function and role in reverse cholesterol transport. Subcell Biochem. 2010;51:183-227.
8. Meurs I, Van Eck M, Van Berkel TJ. High-density lipoprotein: key molecule in cholesterol efflux and the prevention of atherosclerosis. Curr Pharm Des. 2010;16:1445-1467.
9. Webb NR, Moore KJ. Macrophage-derived foam cells in atherosclerosis: lessons from murine models and implications for therapy. Curr Drug Targets. 2007;8:1249-1263.
10. Aparicio-Vergara M, Shiri-Sverdlov R, De Haan G, Hofker MH. Bone marrow transplantation in mice as a tool for studying the role of hematopoietic cells in metabolic and cardiovascular diseases. Atherosclerosis. 2010;213:335-344.
11. Kolovou G, Anagnostopoulou K, Mikhailidis DP, Cokkinos DV. Apolipoprotein E knockout models. Curr Pharm Des. 2008;14:338-351.
12. Zadelaar S, Kleemann R, Verschuren L, De Vries-Van Der Weij J, Van Der Hoorn J, Princen HM, Kooistra T. Mouse models for atherosclerosis and pharmaceutical modifiers. Arterioscler Thromb Vasc Biol. 2007;27:1706-1721.
13. Greenow K, Pearce NJ, Ramji DP. The key role of apolipoprotein E in atherosclerosis. J Mol Med. 2005;83:329-342.
14. Mahley RW. Apolipoprotein E: cholesterol transport protein with expanding role in cell biology. Science. 1988;240:622-630.
15. Shimano H, Ohsuga J, Shimada M, Namba Y, Gotoda T, Harada K, Katsuki M, Yazaki Y, Yamada N. Inhibition of diet-induced atheroma formation in transgenic mice expressing apolipoprotein E in the arterial wall. J Clin Invest. 1995;95:469-476.
16. Davignon J, Cohn JS, Mabile L, Bernier L. Apolipoprotein E and atherosclerosis: insight from animal and human studies. Clin Chim Acta. 1999;286:115-143.
17. Basu SK, Brown MS, Ho YK, Havel RJ, Goldstein JL. Mouse macrophages synthesize and secrete a protein resembling apolipoprotein E. Proc Natl Acad Sci U S A. 1981;78:7545-7549.
18. Fazio S, Babaev VR, Murray AB, Hasty AH, Carter KJ, Gleaves LA, Atkinson JB, Linton MF. Increased atherosclerosis in mice reconstituted with apolipoprotein E null macrophages. Proc Natl Acad Sci U S A. 1997;94:4647-52.
19. Boisvert WA, Spangenberg J, Curtiss LK. Treatment of severe hypercholesterolemia in apolipoprotein E-deficient mice by bone marrow transplantation. J Clin Invest. 1995;96:1118-1124.
20. Trogan E, Feig JE, Dogan S, Rothblat GH, Angeli V, Tacke F, Randolph GJ, Fisher EA. Gene expression changes in foam cells and the role of chemokine receptor CCR7 during atherosclerosis regression in ApoE-deficient mice. Proc Natl Acad Sci U S A. 2006;103:3781-3786.
21. Feig JE, Pineda-Torra I, Sanson M, Bradley MN, Vengrenyuk Y, Bogunovic D, Gautier EL, Rubinstein D, Hong C, Liu J, Wu C, van Rooijen N, Bhardwaj N, Garabedian M, Tontonoz P, Fisher EA. LXR promotes the maximal egress of monocyte-derived cells from mouse aortic plaques during atherosclerosis regression. J Clin Invest. 2010;120:4415-4424.
22. Repa JJ, Mangelsdorf DJ. The liver X receptor gene team: potential new players in atherosclerosis. Nat Med. 2002;8:1243-1248.
23. Zhao C, Dahlman-Wright K. Liver X receptor in cholesterol metabolism. J Endocrinol. 2010;204:233-240.
24. Yu L, York J, Von Bergmann K, Lutjohann D, Cohen JC, Hobbs HH. Stimulation of cholesterol excretion by the liver X receptor agonist requires ATP-binding cassette transporters G5 and G8. J Biol Chem. 2003;278:15565-15570.

25. Calpe-Berdiel L, Rotllan N, Fiévet C, Roig R, Blanco-Vaca F, Escolà-Gil JC. Liver X receptor-mediated activation of reverse cholesterol transport from macrophages to feces in vivo requires ABCG5/G8. J Lipid Res. 2008;49:1904-1911.
26. Tontonoz P, Mangelsdorf DJ. Liver X receptor signaling pathways in cardiovascular disease. Mol Endocrinol. 2003;17:985-993.
27. Tall AR, Costet P, Wang N. Regulation and mechanisms of macrophage cholesterol efflux. J Clin Invest. 2002;110:899-904.
28. Oosterveer MH, Grefhorst A, Groen AK, Kuipers F. The liver X receptor: control of cellular lipid homeostasis and beyond Implications for drug design. Prog Lipid Res. 2010;49:343-352.
29. Joseph SB, McKilligin E, Pei L, Watson MA, Collins AR, Laffitte BA, Chen M, Noh G, Goodman J, Hagger GN, Tran J, Tippin TK, Wang X, Lusis AJ, Hsueh WA, Law RE, Collins JL, Willson TM, Tontonoz P. Synthetic LXR ligand inhibits the development of atherosclerosis in mice. Proc Natl Acad Sci U S A. 2002;99:7604-7609.
30. Peng D, Hiipakka RA, Xie JT, Dai Q, Kokontis JM, Reardon CA, Getz GS, Liao S. A novel potent synthetic steroidal liver X receptor agonist lowers plasma cholesterol and triglycerides and reduces atherosclerosis in LDLR–/– mice. Br J Pharmacol. 2011;162:1792-1804.
31. Cha JY, Repa JJ. The liver X receptor (LXR) and hepatic lipogenesis. The carbohydrate-response element-binding protein is a target gene of LXR. J Biol Chem. 2007;282:743-751.
32. Van Straten E, Van Meer H, Huijkman N, Van Dijk TH, Baller JF, Verkade HJ, Kuipers F, Plosch T. Fetal Liver X Receptor activation acutely induces lipogenesis, but does not affect plasma lipid response to a high-fat diet in adult mice. Am J Physiol Endocrinol Metab. 2009;297: E1171-E1178.
33. Van Eck M, Herijgers N, Yates J, Pearce NJ, Hoogerbrugge PM, Groot PH, Van Berkel TJ. Bone marrow transplantation in apolipoprotein E-deficient mice. Effect of ApoE gene dosage on serum lipid concentrations, (beta)VLDL catabolism, and atherosclerosis. Arterioscler Thromb Vasc Biol. 1997;17:3117-3126.
34. Shi W, Wang X, Wang NJ, McBride WH, Lusis AJ. Effect of macrophage-derived apolipoprotein E on established atherosclerosis in apolipoprotein E-deficient mice. Arterioscler Thromb Vasc Biol. 2000;20:2261-2266.
35. Linton MF, Atkinson JB, Fazio S. Prevention of atherosclerosis in apolipoprotein E-deficient mice by bone marrow transplantation. Science. 1995;267:1034-1037.
36. Bellosta S, Mahley RW, Sanan DA, Murata J, Newland DL, Taylor JM, Pitas RE. Macrophage-specific expression of human apolipoprotein E reduces atherosclerosis in hypercholesterolemic apolipoprotein E-null mice. J Clin Invest. 1995;96:2170-2179.
37. Raffai RL, Loeb SM, Weisgraber KH. Apolipoprotein E promotes the regression of atherosclerosis independently of lowering plasma cholesterol levels. Arterioscler Thromb Vasc Biol. 2005;25:436-441.
38. Zhao Y, Ye D, Wang J, Calpe-Berdiel L, Azzis SB, Van Berkel TJ, Van Eck M. Stage-Specific Remodeling of Atherosclerotic Lesions on Cholesterol Lowering in LDL Receptor Knockout Mice. Am J Pathol. 2011 Jul 8 Epub ahead of print.
39. Rong JX, Li J, Reis ED, Choudhury RP, Dansky HM, Elmalem VI, Fallon JT, Breslow JL, Fisher EA. Elevating high-density lipoprotein cholesterol in apolipoprotein E-deficient mice remodels advanced atherosclerotic lesions by decreasing macrophage and increasing smooth muscle cell content. Circulation. 2001;104:2447-2452.
40. Bengtsson E, To F, Grubb A, Håkansson K, Wittgren L, Nilsson J, Jovinge S. Absence of the protease inhibitor cystatin C in inflammatory cells results in larger plaque area in plaque regression of apoE-deficient mice. Atherosclerosis. 2005;180:45-53.
41. Bennett MR. Life and death in the atherosclerotic plaque. Curr Opin Lipidol. 2010;21:422-426.
42. Schrijvers DM, De Meyer GR, Herman AG, Martinet W. Phagocytosis in atherosclerosis: Molecular mechanisms and implications for plaque progression and stability. Cardiovasc Res. 2007;73:470-480.
43. Zhang T, Zhai Y, Chen Y, Zhou Z, Yang J, Liu H. Effects of emotional and physiological stress on plaque instability in apolipoprotein E knockout mice. J Physiol Biochem. 2011, Epub ahead of print.
44. Brown MS, Goldstein JL. Lipoprotein metabolism in the macrophage: implications for cholesterol deposition in atherosclerosis. Annu Rev Biochem. 1983;52:223-261.
45. Kavurma MM, Tan NY, Bennett MR. Death receptors and their ligands in atherosclerosis. Ateriosclerosis Thromb Vasc Biol. 2008;28:1694-1702.
46. Yu H, Stoneman V, Clarke M, Figg N, Xin HB, Kotlikoff M, Littlewood T, Bennett M. Bone marrow-derived smooth muscle-like cells are infrequent in advanced primary atherosclerotic plaques but promote atherosclerosis. Arterioscler Thromb Vasc Biol. 2011;31:1291-1299.

47. Williams KJ, Feig JE, Fisher EA. Rapid regression of atherosclerosis: insights from the clinical and experimental literature. Nat Clin Pract Cardiovasc Med. 2008;5:91-102.
48. Ye D, Zhao Y, Hildebrand RB, Singaraja RR, Hayden MR, Van Berkel TJ, Van Eck M. The dynamics of macrophage infiltration into the arterial wall during atherosclerotic lesion development in low-density lipoprotein receptor knockout mice. Am J Pathol. 2011;178:413-422.
49. Potteaux S, Gautier EL, Hutchison SB, Van Rooijen N, Rader DJ, Thomas MJ, Sorci-Thomas MG, Randolph GJ. Suppressed monocyte recruitment drives macrophage removal from atherosclerotic plaques of ApoE-/- mice during disease regression. J Clin Invest. 2011;121:2025-2036.

Chapter 8

General discussion and perspectives

Zhaosha Li

Division of Biopharmaceutics, Leiden/Amsterdam Center for Drug Research, Leiden University, The Netherlands

GENERAL DISCUSSION AND PERSPECTIVES

Atherosclerosis is the underlying cause of most cardiovascular diseases [1]. Hypercholesterolemia holds a key role in the development of atherosclerosis and is a causative factor for coronary artery disease[2]. Lowering of VLDL- and LDL-cholesterol levels leads to a reduction in cardiovascular morbidity and mortality[3]. In contrast, high levels of HDL-cholesterol are associated with a decreased risk of cardiovascular disease[4]. This dissertation is dedicated to the regulation of lipid metabolism pathways and its subsequent effects on atherosclerotic lesion progression and regression.

1. Hepatic lipid metabolism and pharmaceutical interventions in the liver

Atherosclerosis is a liver disease of the heart[5]. Liver is considered as the major organ with significant therapeutic importance for the maintenance of metabolic homeostasis[6]. The first part of the thesis focuses on the hepatic lipid metabolism and the pharmaceutical interventions in the liver.

1.1 Nuclear receptors in the liver: potential targets for pharmaceutical interventions

Nuclear receptors (NRs) are ligand-activated transcription factors that act as sensors for a broad range of natural and synthetic ligands. A growing number of NRs have been identified as regulators in lipid metabolism and energy utilization[7]. Moreover, NRs control hepatic inflammation, regeneration, fibrosis, and tumor formation. Therefore, NRs are crucial for understanding the pathogenesis and pathophysiology of a wide range of hepatic disorders. Targeting NRs and their regulations in the liver offers new perspectives for the treatment of metabolic diseases[8].

In **Chapter 2**, we have composed the hepatic cell type-specific expression profile of NRs to provide the most complete quantitative assessment of NRs distribution in the liver reported to date. We have identified several liver-enriched orphan NRs as potential novel targets for pharmaceutical interventions. Specifically, members of the orphan receptor family COUP-TFs showed distinguished distributions in liver. COUP-TF3 was abundantly and exclusively expressed in liver parenchymal cells, while the other two members, COUP-TF1 and COUP-TF2, were expressed exclusively in non-parenchymal cells. Despite the moderate to high expression level in the liver, the physiological functions of COUP-TFs have not been fully exploited, and the ligand for COUP-TFs has not been identified. Our study suggests a physiologic important role of COUP-TF3 in hepatocytes, and that of COUP-TF2 in endothelial cells and macrophages. Previous studies have shown that the activity of COUP-TFs is associated with the transcriptional regulation of a number of genes expressed mainly in the liver[9]. COUP-TF2 and COUP-TF3 have been generally considered to be repressors or regulators for transcription of NRs such as RARs, TRs, PPARs, and HNF4alpha[10]. The cellular distribution pattern from the present study suggests that COUP-TF3, given its high expression in liver parenchymal cells, may have a potential role in hepatic lipid and xenobiotic metabolism regulation via cross-talking with other liver-enriched NRs. Our study identifies COUP-TF2 as highly expressed in endothelial cells, which is in

accordance with published data upon the role of COUP-TF2 in angiogenesis and generation of haematopoietic cell clusters[11]. In addition, COUP-TF2 was shown to have a potential role in regulation of cholesterol homeostasis[12]. The observation from our current study that the expression of COUP-TF2 is as high as NGFIB in Kupffer cells raises interest to further investigate whether COUP-TF2 is involved, similarly as NGFIB, in lipid metabolism in macrophages.

We used real-time quantitative PCR to gain the expression profiles of NRs. It is a standardized method in the NR field to characterize the expression pattern of individual receptors in tissue or cells. It provides a simple but powerful way to obtain comprehensive understanding of the distribution and biological functions of NRs[13]. Real-time quantitative PCR has been applied in numerous studies to profile the expression pattern of NRs in tissues representing diverse anatomical systems under various pharmacological conditions and genotypes[14,15]. However, because NRs are transcription factors, the regulation of NRs are not only at the mRNA level, but also on the protein activity level. Therefore, it is important to further extend the gene expression profiles of NRs into their protein expression and/or functionality profiles by using immunohistochemical staining or flow cytometry. Furthermore, in addition to the hepatic endothelial cells and Kupffer cells, which were investigated in the current study, hepatic stellate cells are also major repositories for lipids, being activated during chronic liver injury and mediating the fibrotic response[16,17]. It is thus interesting to include in future studies the hepatic stellate cells when investigating gene expression profiles of NRs in the liver.

1.2 Niacin regulates hepatic lipid metabolism and CETP expression

The use of statins in patients with high risk for cardiovascular disease (CVD) has resulted in a 30-40% decrease in clinical events in the last couple of decades. However, despite of a marked reduction (up to 60%) in LDL-C, about 30% of patients continue to have CVD events[18]. Therefore, HDL has become the next promising therapeutic target. The anti-dyslipidemic drug niacin, also known as nicotinic acid, not only lowers plasma levels of pro-atherogenic lipids/lipoproteins[19], but also is the most effective agent available to increase HDL-cholesterol[20,21]. Several clinical trials have shown that niacin reduces cardiovascular disease and myocardial infarction incidence, providing an emerging rationale for the use of niacin in the treatment of atherosclerosis[22,23]. Only recently, it has been shown that niacin also reduces the hepatic expression and plasma levels of the pro-atherogenic CETP[24]. In **Chapter 4** we investigated the mechanism underlying the CETP-lowering effect of niacin. We propose that the primarily reduced hepatic cholesterol accumulation via the lipid-lowering effect of niacin leads to attenuated hepatic inflammation, and thus less macrophage infiltration into and/or increased macrophage emigration out of the liver. The decreased amount of hepatic macrophages, which are significant contributors of CETP, leads to an overall reduction in hepatic CETP expression and a lower plasma CETP level. In conclusion, we have shown that niacin does not directly alter macrophage CETP expression, but attenuates the liver inflammation and macrophage content in response to its primary lipid-lowering effect, which leads to a decrease in hepatic CETP expression and the plasma CETP mass. Our study sheds a new light on the mechanism underlying the CETP-lowering effect of niacin in CETP transgenic mice.

Niacin receptor GPR109A is highly expressed in adipose tissue. Interestingly, adipose tissue appears to be a highly conserved site of CETP expression across

species. Adipose tissue CETP makes a major contribution to CETP in the circulation, reduces HDL, and increases non-HDL cholesterol levels. Adipose tissue CETP plays a local role in adipocyte cholesteryl ester accumulation from HDL, indicating a novel role of CETP in modulating adiposity. It is thus of interest to further investigate the potential regulation effects of niacin on adipose tissue CETP expression.

Hernandez *et al*[25] demonstrated for the first time the critical role of CETP in niacin-mediated HDL-elevation by using CETP tg mice and suggested that transgenic mice expressing the human CETP could be a useful animal model for studying the established HDL-regulating effect of niacin. However, in the current study we did not observe the HDL-raising effect of niacin in CETP Tg mice. This might be due to diet differences. Hernandez *et al* used regular chow diet supplemented with niacin, while we used WTD diet which contains more fat and 0.25% cholesterol that has been shown to upregulate CETP expression. Furthermore, although niacin significantly increased hepatic apoA-I expression in our study, the hepatic expression of ABCA1, which is involved in apoA-I-mediated cholesterol efflux, significantly decreased by 45% at the same time upon niacin treatment, which can ultimately result in unchanged HDL formation in plasma. Interestingly, our observations corroborate recent data from Li *et al*[26]*,* who showed that niacin-mediated activation of GPR109A in liver led to reduced hepatocyte ABCA1 expression and thus an unexpectedly reduced plasma HDL-C level in C57BL/6J mice. The current study was set out to investigate the mechanism underlying the hepatic and plasma CETP-lowering effect of niacin in mice, instead of determining the mechanism of HDL-C elevation by niacin. This mechanistic approach in a mouse model thus differs from a clinical investigation.

Recent unexpected termination of AIM-HIGH Clinical Trial on niacin and HDL hypothesis has drawn much attention. AIM-HIGH is the first large randomized trial to evaluate the effect of niacin on cardiovascular events among statin-treated patients with established atherosclerotic cardiovascular disease who are at the desired level for LDL-C but who have residual abnormalities in HDL-C and triglycerides. It was meant to test whether adding high dose, extended-release niacin to a statin (simvastatin) is better than a statin alone in reducing long-term cardiovascular events in participants[27]. The trial was started in September 2005, but was stopped early due to the lack of incremental benefit on cardiovascular risk reduction in the extended-release niacin plus simvastatin treatment group over simvastatin alone. At this time, the FDA has made no new conclusions or recommendations regarding the use of extended-release niacin alone or in combination with simvastatin or other statins[28]. The lack of additional effect of niacin on cardiovascular events is unexpected and a striking contrast to the results of previous trials and observational studies, despite that niacin in this trial produced the predicted effects on all lipid parameters measured including increasing HDL levels by 20% and reducing triglycerides by around 25%[29]. The early termination of this trial raised questions about the suggested beneficial effects of the HDL-elevation hypothesis[30]. However, the AIM-HIGH study population was not a very high-risk population because the patients were already on statin-treatment and their LDL-cholesterol level was already well controlled. The study population in this trial does not represent all patient populations in whom the importance of treating low HDL and lowering triglycerides with Niaspan may be significant. Therefore, the relevance of these results to patients outside the AIM-HIGH study population is

currently unknown and it would be premature to extrapolate these results with Niaspan to a broader patient population at this time[31].

The clinical use of niacin has been limited due to the cutaneous flushing effect, which is mediated by the niacin receptor GPR109A in the skin. Therefore, in **Chapter 5**, we assessed the properties of two partial agonists for GPR109A and compared them to niacin. We show that these two GPR109A partial agonists of the pyrazole class are promising drug candidates to achieve the beneficial lipid-lowering effects while they successfully avoid the unwanted flushing side effect. Interestingly, our flushing results are somewhat complicated due to the unexpected skin temperature increase observed in the C57BL/6 mice treated with the vehicle DMSO. DMSO is one of the most common solvents used for *in vivo* administration of water-insoluble substances. In literatures, a wide range of pharmacological effects of DMSO has been documented in both animal and human experimental models, including membrane penetration and vasodilation[32,33,34]. It is proposed that DMSO provokes a histamine-like response, possesses potent histamine-liberating properties, and increases blood flow[35]. Despite being frequently used as a solvent in biological studies and as a vehicle for drug therapy, the undesirable side-effects of DMSO both *in vivo* and *in vitro* should be taken into consideration[36].

2. Atherosclerotic lesion regression and mouse models

The second part of the thesis focuses on the concept of atherosclerotic lesion regression, shedding insights in the role of LXR activation and application of mouse models in regression studies.

While numerous studies have been dedicated to inhibit the progression of atherosclerosis, recent attention has been focused on reversing atherosclerosis, which is the regression of existing atherosclerotic plaque. In previous studies, a dramatic regression of large advanced lesion was achieved with or without LXR agonist[37,38] by utilizing surgical aorta transplantation into wildtype mice. This procedure leads to a rapidly improved milieu for the atherosclerotic lesions. In another mouse model, apoE*3Leiden mice, LXR agonist were also shown to promote regression of moderate lesions[39]. In both **Chapter 6** and **Chapter 7** we investigated other different mouse models to explore technically easier and more efficient approaches for plaque regression.

In **Chapter 6** we first fed LDLr$^{-/-}$ mice with high-fat high-cholesterol Western-type diet (WTD) for 6 weeks to develop atherosclerotic plaques. Subsequently, a group of mice was sacrificed to obtain baseline data, whilst the rest of the mice were switched to a low-fat cholesterol-free chow diet without or with LXR agonist T0901317 supplementation for 3 weeks. Unexpectedly, T-0901317 supplemented in regular chow diet largely elevated plasma cholesterol level, and thus the atherosclerotic plaque continued its progression. Therefore, we set out to evaluate the effects of LXR agonist on plaque regression in C57BL/6 mice. The C57BL/6 mouse model has been used to study diet-induced atherosclerosis[40,41,42]. This murine model of atherogenesis represents an alternative to the use of genetically modified mice with impaired lipoprotein clearance, i.e. LDLr$^{-/-}$ mice, for the evaluation of anti-hyperlipidemic agents, including LXR agonists[43]. Here we fed C57BL/6 mice with cholate-containing cholesterol-enriched atherogenic diet for 16 weeks to induce atherosclerotic plaque development. Subsequently, a group of mice were sacrificed to obtain baseline data, whilst the remainder of the mice was

switched to low-fat cholesterol-free chow diet without or with LXR agonist T0901317 supplementation for 3 weeks. In contrast to data from $LDL^{-/-}$ mice, in C57BL/6 mice LXR agonist supplemented in regular chow diet successfully reduced the diet-induced hypercholesterolemia rapidly. LXR agonist not only reduced plasma (V)LDL cholesterol levels, but also significantly increased HDL level, leading to a 10-fold increased ratio between antiatherogenic HDL and proatherogenic (V)LDL level. This indicates that LXR agonist, together with chow diet, rapidly improved the plasma lipoprotein profile and induced a regression environment in C57BL/6 mice.

LXR agonist exhibited opposite effects on plasma lipoprotein and lesion progression in $LDLr^{-/-}$ and C57BL/6 mice, and we propose that this is due to the absence of LDL receptor and thus impaired LDL clearance in $LDLr^{-/-}$ mice. The LDL receptor-mediated cholesterol uptake and feedback regulation are crucial when evaluating LDL-lowering effects of compounds[44]. Studies have show that when LDL receptor gene was transferred back into hypercholesterolemic $LDLr^{-/-}$ mice to restore sustained expression of the LDLr protein in the liver, there was drastic reduction of plasma cholesterol and non-HDL cholesterol levels persistently and pronounced regression of advanced atherosclerotic[45,46]. Thus, it is proposed that C57BL/6 mice is a better model than $LDLr^{-/-}$ to evaluate (V)LDL-lowering induced atherosclerotic regression.

However, the limitation of the C57BL/6 mouse model is that the atherosclerotic plaque induced by an atherogenic diet was relatively small (~50 x 10^3 μm^2 in the aortic root), and there was hardly any lesion developed in the aortic arch or the descending aorta yet. Thus, the effect of LXR-agonist in this study was limited to diminishing early atheromatous lesion with small size and less complexity. It is thus important to further investigate the potential of LXR activation on diminishing larger advanced atherosclerotic plaque in both the aortic root and descending aorta.

In **Chapter 7** we used bone marrow transplantation technique, reconstituting $ApoE^{-/-}$ mice with bone marrow from wildtype mice, to restore apoE function in macrophages and normalize plasma lipoprotein profiles. This is a novel mouse model with chow diet feeding, providing an alternative model to investigate atherosclerotic plaque regression without robust surgical measures. We performed this regression study in parallel on initial and advanced lesions. We show that the bone marrow transplantation technique leads to successful plaque regression of both initial and advanced lesions. The current mouse model is thus a good model to study atherosclerosis regression in different stages of the disease. However, in initial lesions, a 45% reduction in lesion size was observed with chow diet alone, and even a 71% reduction with LXR agonist treatment, whilst in advanced lesions there was a more limited 23% reduction with chow diet alone, and a 36% reduction with LXR activation. This can be explained by the difference in plaque composition and characteristics between initial and advanced lesion. Initial lesions contain primarily cholesterol-filled macrophages covered by a thin cap, while in advanced lesion, SMCs and extracellular matrix products comprise the major structural components of the atherosclerotic plaques, covered by a thick fibrous cap[47], which make the advanced lesions more difficult to be modulated during the regression process.

Interestingly, our lesion composition analysis showed that the reduction of total lesion size during regression was primarily due to a reduction of the macrophage content in the plaque. However, the fate of the macrophages during lesion

regression is currently still under debate. It has been proposed that regression is not merely a rewinding of progression, but instead involves induction of CCR7 expression, a mediator of leukocyte emigration, leading to the emigration of the lipid-loaded macrophages, followed by the initiation of influx of healthy phagocytes that mobilize necrotic debris and all other components of advanced plaques[48]. Interestingly, Ye *et al* showed that macrophage infiltration into pre-existing advanced lesions was limited, likely because of the formation of fibrous caps[49]. In contrast, Potteaux *et al* also showed that regression of atherosclerosis after apoE complementation in ApoE$^{-/-}$ mice did not involve migratory egress of macrophages from plaques or induction of CCR7. Instead, marked suppression of monocyte recruitment coupled with a stable rate of apoptosis accounted for loss of plaque macrophages, suggesting that therapies to inhibit monocyte recruitment to plaques may constitute a viable strategy to reduce plaque macrophage burden than attempts to promote migratory egress[50]. Further research is necessary to establish the processes and mechanisms underlying the diminished macrophage content during regression in our experimental mouse model.

In conclusion, the second part of this thesis, focusing on novel mouse models to induce atherosclerotic lesion regression, shows that 1) intact LDL receptor function is crucial to overcome LXR-induced hyperlipidemia as to achieve plaque regression; 2) ApoE$^{-/-}$ mice reconstituted with bone marrow from C57BL/6 mice represents a promising mouse model with chow diet feeding to study the regression of atherosclerosis, providing an alternative model to investigate plaque regression without robust surgical measures; and 3) rapidly optimized plasma lipoprotein profiles, combined with LXR agonist treatment, induced favorable gene expression profiles, leading to regression of both initial and more advanced atherosclerotic plaques.

REFERENCES

1. Boehm M, Nabel EG. The cell cycle and cardiovascular diseases. Prog Cell Cycle Res. 2003;5:19-30.
2. Toutouzas K, Drakopoulou M, Skoumas I, Stefanadis C. Advancing therapy for hypercholesterolemia. Expert Opin Pharmacother. 2010;11:1659-1672.
3. Paras C, Hussain MM, Rosenson RS. Emerging drugs for hyperlipidemia. Expert Opin Emerg Drugs. 2010;15:433-451.
4. Lee JM, Choudhury RP. Atherosclerosis regression and high-density lipoproteins. Expert Rev Cardiovasc Ther. 2010;8:1325-1334.
5. Davis RA, Hui TY. George Lyman Duff Memorial Lecture: atherosclerosis is a liver disease of the heart. Arterioscler Thromb Vasc Biol. 2001;21:887-898.
6. Marchesini G, Moscatiello S, Di Domizio S, Forlani G. Obesity-associated liver disease. J Clin Endocrinol Metab. 2008;93:S74-S80.
7. Schulman IG. Nuclear receptors as drug targets for metabolic disease. Adv Drug Deliv Rev. 2010;62:1307-1315.
8. Trauner M, Halilbasic E. Nuclear receptors as new perspective for the management of liver diseases. Gastroenterology. 2011;140:1120-1125.
9. Lazennec G, Kern L, Valotaire Y, Salbert G. The nuclear orphan receptors COUP-TF and ARP-1 positively regulate the trout estrogen receptor gene through enhancing autoregulation. Mol Cell Biol. 1997;17:5053-5066.
10. Park JI, Tsai SY, Tsai MJ. Molecular mechanism of chicken ovalbumin upstream promoter-transcription factor (COUP-TF) actions. Keio J Med. 2003;52:174-181.
11. You LR, Lin FJ, Lee CT, DeMayo FJ, Tsai MJ, Tsai SY. Suppression of Notch signaling. by the COUP-TFII transcription factor regulates vein identity. Nature. 2005;435:98-104.
12. Myers SA, Wang SC, Muscat EO. The chicken ovalbumin upstream promoter-transcription factors modulate genes and pathways involved in skeletal muscle cell metabolism. J Biol Chem. 2006;281:24149-24160.
13. Bookout AL, Mangelsdorf DJ. Quantitative real-time PCR protocol for analysis of nuclear receptor signaling pathways. Nucl Recept Signal. 2003;1:12.
14. Bookout AL, Jeong Y, Downes M, Yu RT, Evans RM, Mangelsdorf DJ. Anatomical profiling of nuclear receptor expression reveals a hierarchical transcriptional network. Cell. 2006;126:789-799.
15. Yang X, Downes M, Yu RT, Bookout AL, He W, Straume M, Mangelsdorf DJ, Evans RM. Nuclear receptor expression links the circadian clock to metabolism. Cell. 2006;126:801-810.
16. Mallat A, Lotersztajn S. The liver x receptor in hepatic stellate cells: a novel antifibrogenic target ? J Hepatol. 2011; Epub ahead of print.
17. Anty R, Lemoine M. Liver fibrogenesis and metabolic factors. Clin Res Hepatol Gastroenterol. 2011;35 Suppl 1:S10-20.
18. Asztalos BF. High-density lipoprotein particles, coronary heart disease, and niacin. J Clin Lipidol. 2010;4:405-410.
19. Carlson LA. Niaspan, the prolonged release preparation of nicotinic acid (niacin), the broad-spectrum lipid drug. Int J Clin Pract. 2004;58:706-713.
20. Brooks EL, Kuvin JT, Karas RH. Niacin's role in the statin era. Expert Opin Pharmacother. 2010;11:2291-2300.
21. Al-Mohaissen MA, Pun SC, Frohlich JJ. Niacin: from mechanisms of action to therapeutic uses. Mini Rev Med Chem. 2010;10:204-217.
22. Lee JM, Robson MD, Yu LM, Shirodaria CC, Cunnington C, Kylintireas I, Digby JE, Bannister T, Handa A, Wiesmann F, Durrington PN, Channon KM, Neubauer S, Choudhury RP. Effects of high-dose modified-release nicotinic acid on atherosclerosis and vascular function: a randomized, placebo-controlled, magnetic resonance imaging study. J Am Coll Cardiol. 2009;54:1787-1794.
23. Taylor AJ, Villines TC, Stanek EJ, Devine PJ, Griffen L, Miller M, Weissman NJ, Turco M. Extended-release niacin or ezetimibe and carotid intima-media thickness. N Engl J Med. 2009;361:2113-2122.
24. Van Der Hoorn JW, De Haan W, Berbée JF, Havekes LM, Jukema JW, Rensen PC, Princen HM. Niacin increases HDL by reducing hepatic expression and plasma levels of cholesteryl ester transfer protein in APOE*3Leiden.CETP mice. Arterioscler Thromb Vasc Biol. 2008;28:2016-2022.
25. Hernandez M, Wright SD, Cai TQ. Critical role of cholesterol ester transfer protein in nicotinic acid-mediated HDL elevation in mice. Biochem Biophys Res Commun. 2007;355:1075-1080.
26. Li X, Millar JS, Brownell N, Briand F, Rader DJ. Modulation of HDL metabolism by the niacin receptor GPR109A in mouse hepatocytes. Biochem Pharmacol. 2010;80:1450-1457.

27. AIM-HIGH Investigators. The role of niacin in raising high-density lipoprotein cholesterol to reduce cardiovascular events in patients with atherosclerotic cardiovascular disease and optimally treated low-density lipoprotein cholesterol: baseline characteristics of study participants. The Atherothrombosis Intervention in Metabolic syndrome with low HDL/high triglycerides: impact on Global Health outcomes (AIM-HIGH) trial. Am Heart J. 2011;161:538-43.
28. Food and Drug Administration. FDA statement on the AIM-HIGH trial. May 26, 2011.
29. National Institutes of Health. NIH stops clinical trial on combination cholesterol treatment [press release]. May 26, 2011.
30. AIM-HIGH Investigators. The role of niacin in raising high-density lipoprotein cholesterol to reduce cardiovascular events in patients with atherosclerotic cardiovascular disease and optimally treated low-density lipoprotein cholesterol Rationale and study design. The Atherothrombosis Intervention in Metabolic syndrome with low HDL/high triglycerides: Impact on Global Health outcomes (AIM-HIGH). Am Heart J. 2011;161:471-477.
31. Wise J. Trial of niacin alongside statin is stopped early. BMJ. 2011; 342:d3400 doi: 10.1136/bmj.d3400
32. Colucci M, Maione F, Bonito MC, Piscopo A, Di Giannuario A, Pieretti S. New insights of dimethyl sulphoxide effects (DMSO) on experimental in vivo models of nociception and inflammation. Pharmacol Res. 2008;57:419-425.
33. Jacob SW, Herschler R. Pharmacology of DMSO. Cryobiology. 1986;23:14-27.
34. Adamson JE, Crawford HH, Horton CE. The action of dimethyl sulfoxide on the experimental pedicle flap. Surg Forum. 1966;17:491-492.
35. Kligman AM. Topical pharmacology and toxicology of dimethyl sulfoxide. JAMA. 1965;193:796-804.
36. Santos NC, Figueira-Coelho J, Martins-Silva J, Saldanha C. Multidisciplinary utilization of dimethyl sulfoxide: pharmacological, cellular, and molecular aspects. Biochem Pharmacol. 2003;65:1035-1041.
37. Trogan E, Feig JE, Dogan S, Rothblat GH, Angeli V, Tacke F, Randolph GJ, Fisher EA. Gene expression changes in foam cells and the role of chemokine receptor CCR7 during atherosclerosis regression in ApoE-deficient mice. Proc Natl Acad Sci U S A. 2006;103:3781-3786.
38 . Feig JE, Pineda-Torra I, Sanson M, Bradley MN, Vengrenyuk Y, Bogunovic D, Gautier EL, Rubinstein D, Hong C, Liu J, Wu C, van Rooijen N, Bhardwaj N, Garabedian M, Tontonoz P, Fisher EA. LXR promotes the maximal egress of monocyte-derived cells from mouse aortic plaques during atherosclerosis regression. J Clin Invest. 2010;120:4415-4424.
39. Verschuren L, De Vries-Van Der Weij J, Zadelaar S, Kleemann R, Kooistra T. LXR agonist suppresses atherosclerotic lesion growth and promotes lesion regression in apoE*3Leiden mice: time course and mechanisms. J Lipid Res. 2009;50:301-311.
40. Schreyer SA, Wilson DL, LeBoeuf RC. C57BL/6 mice fed high fat diets as models for diabetes-accelerated atherosclerosis. Atherosclerosis. 1998;136:17-24.
41. Paigen B, Mitchell D, Reue K, Morrow A, Lusis AJ, LeBoeuf RC. Ath-1, a gene determining atherosclerosis susceptibility and high density lipoprotein levels in mice. Proc Natl Acad Sci U S A. 1987;84:3763-3767.
42. Liao F, Andalibi A, deBeer FC, Fogelman AM, Lusis AJ. Genetic control of inflammatory gene induction and NF-kappa B-like transcription factor activation in response to an atherogenic diet in mice. J Clin Invest. 1993;91:2572-2579.
43. Johnston TP. The P-407-induced murine model of dose-controlled hyperlipidemia and atherosclerosis: a review of findings to date. J Cardiovasc Pharmacol. 2004;43:595-606.
44. Goldstein JL, Brown MS. The LDL receptor. Arterioscler Thromb Vasc Biol. 2009;29:431-438.
45. Van Craeyveld E, Gordts SC, Nefyodova E, Jacobs F, De Geest B. Regression and stabilization of advanced murine atherosclerotic lesions: a comparison of LDL lowering and HDL raising gene transfer strategies. J Mol Med. 2011; Epub ahead of print.
46. Kassim SH, Li H, Vandenberghe LH, Hinderer C, Bell P, Marchadier D, Wilson A, Cromley D, Redon V, Yu H, Wilson JM, Rader DJ. Gene therapy in a humanized mouse model of familial hypercholesterolemia leads to marked regression of atherosclerosis. PLoS One. 2010;5:e13424.
47. Yu H, Stoneman V, Clarke M, Figg N, Xin HB, Kotlikoff M, Littlewood T, Bennett M. Bone marrow-derived smooth muscle-like cells are infrequent in advanced primary atherosclerotic plaques but promote atherosclerosis. Arterioscler Thromb Vasc Biol. 2011;31:1291-1299.
48. Williams KJ, Feig JE, Fisher EA. Rapid regression of atherosclerosis: insights from the clinical and experimental literature. Nat Clin Pract Cardiovasc Med. 2008;5:91-102.
49. Ye D, Zhao Y, Hildebrand RB, Singaraja RR, Hayden MR, Van Berkel TJ, Van Eck M. The dynamics of macrophage infiltration into the arterial wall during atherosclerotic lesion development in low-density lipoprotein receptor knockout mice. Am J Pathol. 2011;178:413-422.

50. Potteaux S, Gautier EL, Hutchison SB, van Rooijen N, Rader DJ, Thomas MJ, Sorci-Thomas MG, Randolph GJ. Suppressed monocyte recruitment drives macrophage removal from atherosclerotic plaques of ApoE-/- mice during disease regression. J Clin Invest. 2011;121:2025-2036.

Chapter 9

English summary
Nederlandse samenvatting
List of abbreviations
List of publications
Curriculum Vitae

Zhaosha Li

Division of Biopharmaceutics, Leiden/Amsterdam Center for Drug Research, Leiden University, The Netherlands

ENGLISH SUMMARY

Atherosclerosis is the underlying cause of most cardiovascular diseases. It is a progressive inflammatory disease which has a clinical onset by vascular obstruction from the deposits of plaque, subsequently developing into athero-thrombosis and abnormal blood flow. The evidence to support a cholesterol-atherosclerosis link has been revealed in the past three decades. There is a growing consensus that therapeutic lowering of plasma VLDL- and LDL-cholesterol levels and raising of HDL-cholesterol level will reduce the risk of cardiovascular incidence. This dissertation is dedicated to the regulation of lipid metabolism pathways, both in plasma and liver, and its subsequent effects on atherosclerotic lesion progression and regression. In **Chapter 1**, established mechanisms underlying lipid metabolism and atherosclerotic pathology are reviewed, including the important players involved in plasma and hepatic lipoprotein metabolism pathways and the atherosclerotic plaque progression / regression process.

1. Hepatic lipid metabolism and pharmaceutical interventions in the liver

The first part of the thesis focuses on the hepatic lipid metabolism and the pharmaceutical interventions in the liver.

In **Chapter 2**, we used real-time quantitative PCR to compose the hepatic cell type-specific expression profile of nuclear receptors (NRs), providing the most complete quantitative assessment of NRs distribution in liver reported to date. We have identified several liver-enriched orphan NRs as potential novel targets for pharmaceutical interventions. Specifically, members of the orphan receptor family COUP-TFs showed distinguished distributions in liver. COUP-TF3 was abundantly and exclusively expressed in liver parenchymal cells, while the other two members, COUP-TF1 and COUP-TF2, were expressed exclusively in non-parenchymal cells. Despite the moderate to high expression level in the liver, the physiological functions of COUP-TFs have not been fully exploited, and the ligand for COUP-TFs has not been identified. Our study suggests a physiologic important role of COUP-TF3 in hepatocytes, and that of COUP-TF2 in endothelial cells and macrophages.

In **Chapter 3**, we have determined the hepatic expression profile of NAFLD-related gene PNPLA3. To gain insight into the potential function of PNPLA3 in liver, we have determined the effect of diet change on the hepatic expression profile of PNPLA3 in mice, using microarray and real-time PCR analysis. Cellular distribution analysis revealed that PNPLA3 is expressed in hepatocytes but not in liver endothelial or Kupffer cells. Microarray-based gene profiling showed that the expression level of PNPLA3 is highly influenced by the intra-hepatic lipid status. Furthermore, our study suggests an essential function of PNPLA3 in hepatic lipogenesis.

In addition to lipid-lowering therapies, HDL has become the next promising therapeutic target. The anti-dyslipidemic drug niacin, also known as nicotinic acid, not only lowers plasma levels of pro-atherogenic lipids/lipoproteins, but also is the most effective agent available to increase HDL-cholesterol. Recently, it has been shown that niacin also reduces the hepatic expression and plasma levels of the pro-atherogenic CETP. In **Chapter 4** we investigated the mechanism underlying the CETP-lowering effect of niacin. We propose that the primarily reduced hepatic

cholesterol accumulation via the lipid-lowering effect of niacin leads to attenuated hepatic inflammation, and thus less macrophage infiltration into and/or increased macrophage emigration out of the liver. The decreased amount of hepatic macrophages, which are significant contributors of CETP, leads to an overall reduction in hepatic CETP expression and a lower plasma CETP level. In conclusion, we have shown that niacin does not directly alter macrophage CETP expression, but attenuates the liver inflammation and macrophage content in response to its primary lipid-lowering effect, which leads to a decrease in hepatic CETP expression and the plasma CETP mass.

The clinical use of niacin has been limited due to the cutaneous flushing effect, which is mediated by the niacin receptor GPR109A in the skin. Therefore, in **Chapter 5**, we assessed the properties of two partial agonists for GPR109A and compared them to niacin. We show that these two GPR109A partial agonists of the pyrazole class are promising drug candidates to achieve the beneficial lipid-lowering effects while they successfully avoid the unwanted flushing side effect.

2. Atherosclerotic lesion regression and mouse models

The second part of the thesis focuses on the concept of atherosclerotic lesion regression, shedding insights in the role of LXR activation and application of mouse models in regression studies.

While numerous studies have been dedicated to inhibit the progression of atherosclerosis, recent attention has been focused on reversing atherosclerosis, which is the regression of existing atherosclerotic plaque. In previous studies, a dramatic regression of large advanced lesion was achieved with or without LXR agonist by utilizing surgical aorta transplantation into wildtype mice. This procedure leads to a rapidly improved milieu for the atherosclerotic lesions. In both **Chapter 6** and **Chapter 7** we investigated other mouse models to explore technically easier and more efficient approaches for plaque regression.

In **Chapter 6** we first used LDLr$^{-/-}$ mice with high-fat high-cholesterol Western-type diet (WTD) for 6 weeks to develop atherosclerotic plaques. Subsequently, a group of mice was sacrificed to obtain baseline data, whilst the rest of the mice were switched to a low-fat cholesterol-free chow diet without or with LXR agonist T0901317 supplementation for 3 weeks. In addition, we fed C57BL/6 mice with cholate-containing cholesterol-enriched atherogenic diet for 16 weeks to induce atherosclerotic plaque development and perform regression study with LXR agonist T0901317. In **Chapter** 7 we used bone marrow transplantation technique, reconstituting ApoE$^{-/-}$ mice with bone marrow from wildtype mice, to restore apoE function in macrophages and normalize plasma lipoprotein profiles. This is a novel mouse model with chow diet feeding, providing an alternative model to investigate atherosclerotic plaque regression without robust surgical measures. We performed this regression study in parallel on initial and advanced lesions. In conclusion, both of these two chapters, focusing on novel mouse models to induce atherosclerotic lesion regression, demonstrate that 1) intact LDL receptor function is crucial to overcome LXR-induced hyperlipidemia and to achieve plaque regression; 2) ApoE$^{-/-}$ mice reconstituted with bone marrow from C57BL/6 mice represents a promising mouse model with chow diet feeding to study the regression of atherosclerosis, providing an alternative model to investigate plaque regression without robust surgical measures; and 3) rapidly optimized plasma lipoprotein profiles, combined

with LXR agonist treatment, induced favorable gene expression profiles, leading to regression of both initial and more advanced atherosclerotic plaques.

In **Chapter 8**, the results obtained from all the experiments mentioned above are summarized and discussed with respect to the implications of these studies for future investigations.

NEDERLANDSE SAMENVATTING

Atherosclerose is de onderliggende oorzaak van de meeste hart- en vaatziekten. Het is een progressieve aandoening die vernauwing van de bloedvaten veroorzaakt door de afzetting van vetten (lipiden) in de vaatwand. De afgelopen drie decennia is het bewijs geleverd voor een verband tussen cholesterol in bloedplasma en atherosclerose. Er is een groeiende consensus dat de therapeutische verlaging van VLDL- en LDL-cholesterolwaarden en verhoging van de HDL-cholesterol in het plasma het risico op hartinfarcten kan verminderen. Dit proefschrift is gewijd aan studies naar de regulatie van het lipidenmetabolisme, zowel in plasma als de lever, en de effecten daarvan op de progressie en regressie van de vernauwingen van het bloedvat, de zogenaamde atherosclerotische plaques. In **hoofdstuk 1** wordt een overzicht gegeven van de mechanismen die ten grondslag liggen aan het lipidenmetabolisme en de pathologie van atherosclerose, inclusief de belangrijke factoren die een rol spelen bij de regulatie van lipoproteïnen in plasma en lever en de progressie en regressie van atherosclerotische plaques.

1. Lipidenmetabolisme in de lever en farmaceutische interventies

Het eerste deel van dit proefschrift richt zich op het lipidenmetabolisme en de farmaceutische interventies in de lever.

In **hoofdstuk 2** gebruikten we kwantitatieve PCR (polymerase-kettingreactie) in real-time om het levercelspecifieke expressieprofiel van nucleaire receptoren (NRs) samen te stellen, wat heeft geresulteerd in de meest complete kwantitatieve analyse van de distributie van NRs in de lever die tot op heden is gepubliceerd. We hebben een aantal wees-NRs, die veelvuldig voorkomen in de lever, geïdentificeerd als mogelijk nieuwe targets voor farmaceutische interventies. In het bijzonder vertoonden de leden van de weesreceptorfamilie COUP-TFs een specifieke distributie in de lever. COUP-TF3 kwam in grote mate en exclusief tot expressie in de leverparenchymcellen, terwijl COUP-TF1 en COUP-TF2 uitsluitend tot expressie kwamen in niet-parenchymcellen. Ondanks de matige tot hoge expressieniveaus in de lever, zijn de fysiologische functies van COUP-TFs nog niet volledig onderzocht en is het ligand voor de verschillende COUP-TFs nog niet geïdentificeerd. Onze studie suggereert een fysiologisch belangrijke rol van de COUP-TF3 in levercellen (hepatocyten), en voor COUP-TF2 in endotheelcellen en macrofagen.

Hoofdstuk 3 beschrijft het expressieprofiel van PNPLA3 in de lever, een gen dat gerelateerd is aan niet-alcoholische leververvetting (NAFLD). Om inzicht te krijgen in de mogelijke functie van PNPLA3 in de lever, hebben wij het effect van dieetverandering op de expressie van PNPLA3 in de lever van muizen onderzocht, met behulp van microarray en real-time PCR. Uit analyse van de cellulaire distributie is gebleken dat PNPLA3 vooral tot expressie komt in hepatocyten, maar niet in leverendotheelcellen of Kupffercellen. Genprofilering gebaseerd op microarray toont aan dat de expressie van PNPLA3 in hoge mate beïnvloed wordt door lipiden in de lever. Bovendien suggereert onze studie een essentiële functie van PNPLA3 in hepatische lipidensynthese.

Naast lipidenverlagende therapieën is het verhogen van de concentratie HDL in

het bloed uitgegroeid tot een belangrijk therapeutisch doel. Niacine of nicotinezuur, een geneesmiddel tegen dyslipidemie, verlaagt niet alleen plasmaspiegels van proatherogene lipiden en lipoproteïnen, maar is momenteel ook het meest effectieve middel om HDL-cholesterol te verhogen. Onlangs is aangetoond dat niacine ook de expressie van het proatherogene eiwit CETP (choleseryl ester transfer protein) in de lever en de plasmaspiegels daarvan verlaagt. In **hoofdstuk 4** onderzochten we het onderliggende mechanisme van het CETP-verlagende effect van niacine. Wij suggereren dat het lipidenverlagende effect van niacine leidt tot minder ophoping van cholesterol in de lever, waardoor het ontstekingsproces in de lever wordt afgeremd en er minder macrofagen infiltreren in de lever en/of er meer macrofagen emigreren uit de lever. De vermindering van de hoeveelheid macrofagen in de lever, die een belangrijke bron zijn van CETP, leidt tot een algemene daling van de CETP-expressie in de lever en een lager CETP-gehalte in het plasma.

De klinische toepassing van niacine is beperkt vanwege de plotselinge roodheid van de huid, de zogenaamde flushing, die het kan veroorzaken via activatie van de niacinereceptor GPR109A in de huid. In **hoofdstuk 5** zijn de eigenschappen van twee partiële agonisten voor GPR109A vergeleken met niacine. Deze twee partiële GPR109A-agonisten uit de klasse van pyrazolen blijken veelbelovende kandidaatgeneesmiddelen te zijn omdat ze een verlaging van het lipidengehalte kunnen bewerkstelligen zonder de ongewenste flushing.

2. Regressie van de atherosclerotische laesie en muismodellen

Het tweede deel van het proefschrift draait om regressie van de atherosclerotische plaque.en geeft inzicht in de rol van de lever X receptor (LXR) en de toepassing van muismodellen in regressiestudies.

Terwijl vele studies zijn gewijd aan het afremmen van de progressie van atherosclerose is recentelijk de aandacht gericht op de mogelijkheid om via regressietherapie bestaande atherosclerotische plaques te verkleinen. In eerdere studies werd een dramatische vermindering van grote geavanceerde laesies bereikt door middel van aortatransplantatie in wild-type muizen, al dan niet in combinatie met LXR-agonisten. Dit leidt tot zeer snelle verbetering van de omgeving rondom de plaque. In zowel **hoofdstuk 6** en **hoofdstuk 7** onderzochten we alternatieve muismodellen waarin gemakkelijker en efficiënter plaqueregressie is te bewerkstelligen

In **hoofdstuk 6** werd gebruik gemaakt van LDL-receptordeficiënte muizen die een vet- en cholesterolrijk westers dieet kregen om atherosclerotische plaques te ontwikkelen. Vervolgens werd een groep muizen opgeofferd om plaques te analyseren; de rest van de muizen werd gedurende 3 weken overgezet op een vet- en cholesterolarm dieet dat al dan niet verrijkt was met de LXR-agonist T0901317. Daarnaast zijn in C57BL/6 muizen door middel van een cholaatbevattend cholesterolrijk dieet atherosclerotische plaques ontwikkeld gedurende 16 weken, waarna een regressiestudie werd uitgevoerd met de LXR-agonist T0901317. In **hoofdstuk 7** werd beenmergtransplantatie toegepast om de functie van apoE in macrofagen van apoE-deficiënte muizen te herstellen en de plasmaspiegels van lipoproteïnen te normaliseren. Deze techniek levert een alternatief muismodel voor plaqueregressie zonder intensieve chirurgische ingrepen. Deze regressiestudie werd uitgevoerd met zowel initiële als geavanceerde laesies. De data beschreven

in beide hoofdstukken ondersteunen de conclusies dat 1) normale LDL-receptorfunctie cruciaal is om LXR-geïnduceerde hyperlipidemie te verminderen en plaqueregressie te bereiken, 2) apoE-deficiënte muizen gereconstitueerd met beenmerg van C57BL/6 muizen een veelbelovend muismodel vormen voor studies naar het mechanisme van de regressie van atherosclerose zonder intensieve chirurgische ingrepen, en 3) een snel geoptimaliseerd lipoproteïnenprofiel in plasma in combinatie met een LXR-agonist leidt tot regressie van zowel initiële als meer geavanceerde atherosclerotische plaques.

In **hoofdstuk 8** worden de resultaten van alle experimenten samengevat en worden de consequenties van deze studies voor de toekomstige behandeling van hart- en vaatziekten besproken.

LIST OF ABBREVIATIONS

ABCA1	ATP binding cassette transporter A1
ABCG1	ATP binding cassette transporter G1
ACAT	acyl-cholesterol acyl transferase
AD	atherogenic diet
ADPN	adiponutrin
ApoA-I	apolipoprotein A-I
ApoB	apolipoprotein B
$ApoE^{-/-}$	apoE-deficient
ATGL	adipose triglyceride lipase
BMT	bone marrow transplantation
CCR	C-C chemokine receptor
CE	cholesteryl ester
CETP	cholesterol ester transfer protein
COUP-TF	chicken ovalbumin upstream promoter-transcription factor
CVD	cardiovascular disease
CYP7A1	cholesterol 7 alpha-hydroxylase
DGAT1	acyl-coenzyme A:diacylglycerol transferase 1
DMSO	dimethyl sulphoxide
EC	endothelial cell
FAS	fatty acid synthase
FC	free cholesterol
FCS	fetal calf serum
FFA	free fatty acids
FPLC	fast protein liquid chromatography
FXR	farnesoid X receptor
GAPDH	glyceraldehyde-3-phosphate dehydrogenase
GTC	guanidinium thiocyanate
HCA_2	hydroxy-carboxylic acid receptor 2
HDL	high-density lipoprotein
HEK	human embryonic kidney
HFD	high-fat Diet
HPRT	hypoxanthine-guanine phosphoribosyltransferase
ICAM	intercellular adhesion molecule
IDL	intermediate-density lipoprotein
IL	interleukin
KC	Kupffer cell
KO	knockout
LCAT	lecithin-cholesterol acyltransferase
LDL	low-density lipoprotein
LDLr	LDL receptor
$LDLr^{-/-}$	LDL receptor-deficient
LPL	lipoprotein lipase
LRP	LDLr-related protein
LXR	liver X receptor
MCP	monocyte chemoattractant protein
MTP	microsomal transfer protein

NAFLD	non-alcoholic fatty liver disease
NASH	non-alcoholic steatohepatitis
NR	nuclear receptor
Ox-LDL	oxidized LDL
PBS	phosphate buffered saline
PC	parenchymal cell
PCR	polymerase chain reaction
PGD_2	prostaglandin D_2
PGE_2	prostaglandin E_2
PL	phospholipids
PNPLA3	patatin-like phospholipase domain-containing protein 3
PPAR	peroxosimal proliferator activating receptor
RCT	reverse cholesterol transport
ROR	retinoid-related orphan receptor
RXR	retinoid X receptor
SMC	smooth muscle cell
SR-BI	scavenger receptor class B, type I
SREBP	sterol regulatory element binding protein
TC	total cholesterol
TG	triglycerides
Tg	transgenic
TNF	tumor necrosis factor
TRL	triglyceride-rich lipoproteins
VCAM	vascular cell adhesion molecule
VLDL	very-low-density lipoprotein
WT	wild-type
WTD	Western-type diet

LIST OF PUBLICATIONS

Full papers

Li Z, Calpe-Berdiel L, Saleh P, Van der Sluis RJ, Remmerswaal S, McKinnon HJ, Smit MJ, Van Eck M, Van Berkel TJC, Hoekstra M. Bone marrow reconstitution in $ApoE^{-/-}$ mice: a novel model to induce atherosclerotic plaque regression. *Manuscript in preparation*.

Li Z, Van der Stoep M, Van der Sluis RJ, McKinnon HJ, Smit MJ, Van Eck M, Van Berkel TJC, Hoekstra M. LXR activation is essential to induce atherosclerotic plaque regression in C57BL/6 mice. *Submitted for publication*.

Li Z, Blad CC, Van der Sluis RJ, De Vries H, Van Berkel TJC, IJzerman AP, Hoekstra M. Effects of pyrazole partial agonists on HCA_2-mediated flushing and hepatic VLDL production in mice. *Submitted for publication*.

Li Z, Wang Y, Hildebrand RB, Van der Hoorn JWA, Princen HMG, Van Eck M, Van Berkel TJC, Rensen PCN, Hoekstra M. Niacin reduces plasma CETP levels by diminishing liver macrophage content in CETP transgenic mice. *Submitted for publication*.

Li Z, Kruijt JK, Van Berkel TJC, Hoekstra M. Gene Expression Profiling of Nuclear Receptors in Mouse Liver Parenchymal, Endothelial, and Kupffer Cells. *Submitted for publication*.

Hoekstra M, Van der Sluis RJ, **Li Z**, Van Berkel TJC. Profiling of the adrenal stress signature reveals candidate steroidogenic nuclear receptor targets. *Submitted for publication*.

Reuwer AQ, Van der Sluis RJ, **Li Z**, Goffin V, Twickler MTB, Kastelein J, Van Berkel TJC, Hoekstra M. Hyperprolactinemia in LDL receptor knockout mice is associated with a pro-atherogenic metabolic phenotype, but not with increased atherosclerosis. *Submitted for publication*.

Hoekstra M, Van der Sluis RJ, **Li Z**, Oosterveer MH, Groen AK, Van Berkel TJC. The farnesoid X receptor (FXR) stimulates adrenal steroidogenesis in mice. *Submitted for publication*.

Hoekstra M, Korporaal SJ, **Li Z**, Zhao Y, Van Eck M, Van Berkel TJ. Plasma lipoproteins are required for both basal and stress-induced adrenal glucocorticoid synthesis and protection against endotoxemia in mice. *Am J Physiol Endocrinol Metab*. 2010;299:E1038-E1043.

Hoekstra M, **Li Z**, Kruijt JK, Van Eck M, Van Berkel TJ, Kuiper J. The expression level of non-alcoholic fatty liver disease-related gene PNPLA3 in hepatocytes is highly influenced by hepatic lipid status. *J Hepatol*. 2010;52:244-251.

Hoekstra M, Lammers B, Out R, **Li Z**, Van Eck M, Van Berkel TJ. Activation of the nuclear receptor PXR decreases plasma LDL-cholesterol levels and induces hepatic steatosis in LDL receptor knockout mice. *Mol Pharm*. 2009;6:182-189.

Out R, Hoekstra M, Hildebrand RB, Kruit JK, Meurs I, **Li Z**, Kuipers F, Van Berkel TJ, Van Eck M. Macrophage ABCG1 deletion disrupts lipid homeostasis in alveolar macrophages and moderately influences atherosclerotic lesion development in LDL receptor-deficient mice. *Arterioscler Thromb Vasc Biol*. 2006;26:2295-2300.

Peer reviewed abstracts

Li Z, Wang Y, Hildebrand RB, Van der Hoorn JWA, Princen HMG, Van Eck M, Van Berkel TJC, Rensen PCN, Hoekstra M. Niacin reduces plasma CETP levels by diminishing liver macrophage content in CETP transgenic mice. *Gordon Conference on Atherosclerosis.* 2011.

Hoekstra M, **Li Z**, Van der Sluis RJ, Van Berkel TJ. The Farnesoid X Receptor (FXR) Stimulates Adrenal Steroidogenesis in Mice. *Endocr Rev.* 2010;31:3.

Li Z, Kruijt JK, Van Berkel TJC, Hoekstra M. Gene Expression Profiling of Nuclear Receptors in Mouse Liver Parenchymal, Endothelial, and Kupffer Cells. *Atherosclerosis suppl.* 2009;10:2.

Hoekstra M, Lammers B, Out R, **Li Z**, Van Eck M, Van Berkel TJ. Activation of the nuclear receptor PXR decreases plasma LDL-cholesterol levels and induces hepatic steatosis in LDL receptor knockout mice. *Atherosclerosis suppl.* 2009;10:2.

CURRICULUM VITAE

Zhaosha Li was born on May 26th 1983 in Changsha, China. In 2001, she started her university education at Capital Normal University, Beijing, China, majoring in Biological Sciences. During her study, she did a 5-month internship at Chinese Academy of Agricultural Sciences (CAAS) titled 'Application of amplified ribosomal DNA restriction analysis in characterizing biodiversity of endophytic bacteria in rice'.

In 2005, she graduated with honors and came to The Netherlands to start her master study in Bio-Pharmaceutical Sciences, Faculty of Science, Leiden University, with Leiden University Excellence Scholarship. During this 2-year master program, she did a 9-month internship titled 'Role of macrophage scavenger-receptor BI and CD36 in atherosclerosis', under the supervision of Prof. Dr. Theo J.C. van Berkel and Dr. Ruud Out, at the Division of Biopharmaceutics, Leiden University, and a 6-month internship titled 'Effects of genetic variation in the human organic cation transporter hOCT1 on drug inhibition' with ULLA MSc Grant at Department of Pharmacy, Uppsala University, Sweden, under the supervision of Prof. Dr. Per Artursson and Dr. Gustav Ahlin.

From October 2007 to September 2011, she has been working as a PhD candidate (Assistent in Opleiding) at the Division of Biopharmaceutics, Leiden/Amsterdam Center for Drug Research (LACDR), Leiden University. Her PhD research was financially sponsored by Top Institute Pharma (TI Pharma) project T2-110-1 'Nuclear receptors as targets for anti-atherosclerotic therapies', under the supervision of promotor Prof. Dr. Theo J.C. van Berkel, co- promotor Dr. Menno Hoekstra, and TI Pharma principal investigator Dr. Martin-Jan Smit from MSD, Oss. Her research was mainly focused on the pathology and novel pharmaceutical interventions in hyperlipidemia, hepatic lipid metabolism, and atherosclerotic plaque regression. The results of this program are presented in this thesis.

Stellingen

behorende bij het proefschrift

Intervention in Hepatic Lipid Metabolism: Implications for Atherosclerosis Progression and Regression

1. Their specific cellular activity and localization suggest that the orphan nuclear receptors COUP-TF2, COUP-TF3, and TR4 may be of significant importance as novel targets for pharmaceutical interventions in liver. (*this thesis*)

2. Niacin does not directly alter CETP expression in the macrophage, but attenuates liver inflammation and macrophage content in response to its primary lipid-lowering effect, leading to a decrease in hepatic CETP expression and plasma CETP mass. (*this thesis*)

3. Mouse models are not the most suitable platform to study the mechanism of the HDL-raising effect of niacin. (*this thesis*)

4. ApoE$^{-/-}$ mice, reconstituted with bone marrow from C57BL/6 mice, represent a promising mouse model to study regression of atherosclerosis. (*this thesis*)

5. Improvement in the plasma lipid profile, specifically large reductions in plasma concentrations of apoB-lipoproteins, is crucial to trigger atherosclerotic plaque regression. (*Williams KJ et al., Nat Clin Pract Cardiovasc Med. 2008;5:91-102*)

6. The relevance of the results from the AIM-HIGH trial for patients outside this study population is currently unknown, and it would be premature to extrapolate the current results with Niaspan to a broader patient population at this time. (*Wise J. BMJ. 2011;342:d3400*)

7. Characterizing the tissue expression pattern of nuclear receptors and their gene regulation pathways may identify novel drug targets. (*Chawla A et al., Science. 2001;294:1866-1870*)

8. ‘Inburgeren’ is important, because it feels good when you pass a Dutch billboard and actually know what it’s talking about.

9. We can’t run away from who we are. So, check Careertest.net, a website telling you who you are.

10. In the hope of reaching the moon, we may fail to see the flowers that blossom at our feet.

11. More than often, we are more disappointed by the things that we didn't do than the ones we did do.

Zhaosha Li
27 September 2011

Acknowledgements

This is going to be an emotional moment, because it is time to thank the many people who made this thesis possible. As quoted from Shakespeare, 'I can no other answer make, but, thanks, and thanks'.

First and foremost, it is difficult to overstate my gratitude to my promotor, Professor **Theo**, as how I always call you. You are everything a PhD student can dream of; an insightful advisor, a dedicated supporter, and, more importantly, a sincere friend. Thank you for all the precious opportunities you gave me during my study. You made me realize that true scientists could also be so caring, understanding, and so much fun. What I have learnt from you, as a person, will be precious for my future life. If there is only space to mention one conversation between us that I would never forget, it is when you told me 'You need to feel comfortable. Everyone here in lab needs to be happy. That's what it's about.' (December 2009, a morning, during P&O assessment).

In addition, I am deeply indebted to my daily supervisor **Menno**. With your enthusiasm and great efforts to encourage me, you helped to make science fun for me. Throughout my PhD study, 'goede tijden, slechte tijden', when I couldn't see the land burying any gold, you taught me about belief and persistence in the face of hardship, and you gave me inspiring advice and scientific sparks. What especially touches me is that we are not only 'the boss and the bottom of food chain', but also friends, friends that I would like to share my laughter and tears with. The thing is, there may be two of me, me, and dark me. You were there supporting both of me. Time fades away; move on, let go; but this memory is written in stone, because I am your first PhD student, and you are my only PhD supervisor.

Furthermore, I owe my deep gratitude to **Miranda** and **Johan**. Although we didn't have much direct cooperation, I know, by heart, that you were truly supporting me and caring about me. **Miranda**, you were always laughing so happily whenever I made funky jokes, seems like you can always get my jokes. It was really sweet when we sat on New Port lawn discussing about science & personality. And **Johan**, you approved without hesitation when I had problem with grinding niacin powder food and asked money to buy niacin pellets, and you were taking care of me and encouraging me before my presentation at Gordon conference. Both of you witnessed me grow up in our Biopharmaceutics family.

In addition, I must thank **Ruud**. You are the first Dutch person who literally stepped into my Dutch life when I was still pretty lost. Things could have been more difficult without your guidance and support from the beginning. You witnessed me strive to reach my dream. I would not forget the speech you gave during my master graduation. Time goes by. I don't remember days; I remember moments.

I would like to thank the other colleagues from the '**lipid group**', **Bart**, **Reeni**, **Suzanne**, **Erik**, **Ying**, **Dan**, and **Illiana**. We were a good team. Thank you all for your ideas and support. I framed our funky Volendam group picture on my wall. I framed all of you in my heart.

Now it's turn to give my many thanks to my roomies from **Room 829**. **Ornelia** – my Paranimf – and **Laura**, I thank you, because we had so much fun in our 'deserted corner'. We were together during up and downs. Especially the last months, the hardship upsets me, but you were always there, worried when I had

bad news and cheered for me when I had good news. **Ronald**, I thank you, because we shared happy moments in our 'menNo/menYes team'. You are really kind and warm-hearted, and the golden X'mas tree you gave me will stay on my window day and night. **Martine**, **Anouk**, and **Max**, I thank you, because it's beautiful destiny that we happened to be roomies and you were all warm-hearted and active in organizing our room-gathering.

I would like to thank all the *gezellige* colleagues in Biopharmaceutics, **Ilze**, **Saskia**, **Kim**, **Amanda**, **Vanessa**, **Gijs**, and **Thijs**, who have always laughed with me and provided me with intellectual and technical assistance. It's an honor to work with all of you. Special thanks go to **Sigrid** for being my Personal Assistant (PA) in the final messy two months to finish this 'mission impossible'.

I am especially grateful to **Mariette**, **Peter**, and **Kar**. Although we were not directly working in the same team, you were particularly helpful in techniques and patiently teaching me elutriation or staining methods. And Peter, your funky T-shirts always enlightened me.

I am grateful to **Fred**, **Johan (P)**, and **Ine** for your generous help for animal experiments. You together made my 4 years of experiments run smoothly.

I need to thank **Professor IJzerman**, **Clara**, **Patrick**, **Nancy**, **Jimmy**, and **José**, who gave me enlightening ideas during our cooperation on the niacin project and niacin-derivative project. I also thank **Professor Danhof** and **Professor Staels** for being my PhD committee members and giving suggestions upon my thesis.

I would like to extend my sincere gratitude to **TI-Pharma** for financially funding my PhD study since 2007. Special thanks go to **Martin**, the captain of our 'T2-110-Nuclear receptor' team, together with all the other team members. We have synchronized to build up our TI-Pharma project. Thank you all.

I wish to thank my students, especially **Marco** and **Sanne**, for our amazing cooperation. It's unique experience to guide both of you. I realized how much I could have got inspired by intelligent young people. It's very sweet to see that you got the best from this internship and stepped further.

I am grateful to **Yuwen** & **Professor Schrijver** together with **Lineke** and **Kees**. Hard to believe that it's been 6 years since I met your family. I had much fun with the two lovely kids and learnt a lot from your family. In addition, I want to thank my dear friends **Eri**, **Anne-Lo**, **Alejandro**, **Fang** & **Mai**, **Xinyu** & **Chen**, **Meng** & **Yini**, **Wen** & **Chao**, for your spiritual support through difficult times and for all the information you brought to me, about life, about career, about another different world. You opened my mind. It's not easy for any of us to fight for our own dreams far away from our homes. It's great to have friends like you guys.

Finally, to **my family** I dedicate this thesis. I would like to give my deepest gratitude to **my parents**, who made me who I am. You raised me, taught me, supported me, and loved me. I own my life to you.

Last but not least, I thank my love, **Tristan**. When things were at their worst, having met you during that bloody course became the only reason that made me not regret. There were so-difficult moments for me. But you are there; Always have, always will. When I felt like I was on a running train, couldn't get off, couldn't see where it headed, you were my shining beacon of hope, holding my hands and telling me not to give up. We made it. This is it. I thank, you. I promise you, me.

Zhaosha
27 September 2011